AD_____

GRANT NUMBER DAMD17-93-J-3070

TITLE: Gene Structure and Somatic Mutation Analysis of Neurofibromatosis Type 1

PRINCIPAL INVESTIGATOR: Dr. David H. Viskochil

CONTRACTING ORGANIZATION: University of Utah
Salt Lake City, Utah 84112

REPORT DATE: October 1996

TYPE OF REPORT: Final

PREPARED FOR: Commander
U.S. Army Medical Research and Materiel Command
Fort Detrick, Frederick, Maryland 21702-5012

DISCLAIMER NOTICE

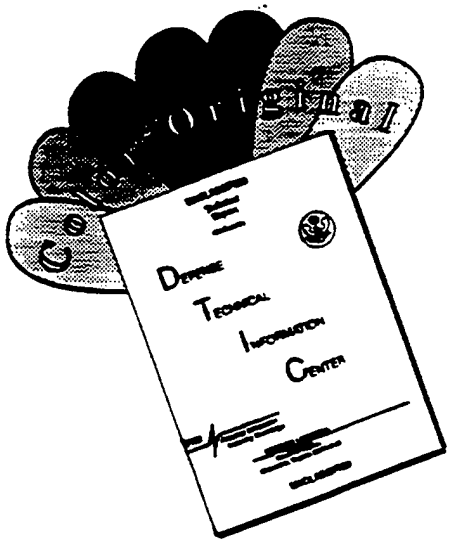

THIS DOCUMENT IS BEST QUALITY AVAILABLE. THE COPY FURNISHED TO DTIC CONTAINED A SIGNIFICANT NUMBER OF COLOR PAGES WHICH DO NOT REPRODUCE LEGIBLY ON BLACK AND WHITE MICROFICHE.

REPORT DOCUMENTATION PAGE

Form Approved
OMB No. 0704-0188

1. AGENCY USE ONLY *(Leave blank)*	2. REPORT DATE	3. REPORT TYPE AND DATES COVERED
	October 1996	Final (22 Sep 93 - 21 Sep 96)

4. TITLE AND SUBTITLE Gene Structure and Somatic Mutation Analysis of Neurofibromatosis Type 1

5. FUNDING NUMBERS
DAMD17-93-J-3070

6. AUTHOR(S)
Dr. David H. Viskochil

7. PERFORMING ORGANIZATION NAME(S) AND ADDRESS(ES)
University of Utah
Salt Lake City, Utah 84112

8. PERFORMING ORGANIZATION REPORT NUMBER

9. SPONSORING/MONITORING AGENCY NAME(S) AND ADDRESS(ES)
U.S. Army Medical Research and Materiel Command
Fort Detrick
Frederick, Maryland 21702-5012

10. SPONSORING/MONITORING AGENCY REPORT NUMBER

11. SUPPLEMENTARY NOTES

12a. DISTRIBUTION / AVAILABILITY STATEMENT
Approved for public release; distribution unlimited

12b. DISTRIBUTION CODE

13. ABSTRACT *(Maximum 200*

This research focuses on the characterization of the human neurofibromatosis 1 (*NF1*) locus. Initially, we determined intron-exon boundaries of exons 1 through 27b. In the process of characterizing genomic clones that harbored *NF1* exons we identified and partially characterized *NF1*-homologous loci distributed throughout the genome. With this information we designed oligonucleotides as primers in the polymerase chain reaction (PCR) to specifically amplify from the *NF1* locus. *NF1* primer sets were adapted to screen DNA for *NF1* mutations by an exon-specific PCR approach. Application of this technique enables us to identify both germ-line and somatic *NF1* mutations. We identified a somatic mutation in the normal *NF1* allele in a dermal neurofibroma from an NF1 individual who is hemizygous at the *NF1* locus. This is the first demonstration of complete inactivation of the gene in a neurofibroma, and it suggests that *NF1* can act as a tumor suppressor in cells that proliferate as benign tumors in NF1. We also developed primer sets and methodology for PCR genotyping of the *NF1* locus, and we identified and adapted *NF1* genomic clones for fluorescence *in situ* hybridization (FISH) analysis. Finally, the *NF1* promoter has been subcloned and approximately 4.4 kilobases upstream of the transcription start site has been sequenced.

14. SUBJECT TERMS	15. NUMBER OF PAGES
Neurofibromatosis, Mutations, Cloning	98
	16. PRICE CODE

17. SECURITY CLASSIFICATION OF REPORT	18. SECURITY CLASSIFICATION OF THIS PAGE	19. SECURITY CLASSIFICATION OF ABSTRACT	20. LIMITATION OF ABSTRACT
Unclassified	Unclassified	Unclassified	Unlimited

FOREWORD

Opinions, interpretations, conclusions and recommendations are those of the author and are not necessarily endorsed by the U.S. Army.

____ Where copyrighted material is quoted, permission has been obtained to use such material.

____ Where material from documents designated for limited distribution is quoted, permission has been obtained to use the material.

DV Citations of commercial organizations and trade names in this report do not constitute an official Department of Army endorsement or approval of the products or services of these organizations.

____ In conducting research using animals, the investigator(s) adhered to the "Guide for the Care and Use of Laboratory Animals," prepared by the Committee on Care and use of Laboratory Animals of the Institute of Laboratory Resources, national Research Council (NIH Publication No. 86-23, Revised 1985).

DV For the protection of human subjects, the investigator(s) adhered to policies of applicable Federal Law 45 CFR 46.

____ In conducting research utilizing recombinant DNA technology, the investigator(s) adhered to current guidelines promulgated by the National Institutes of Health.

____ In the conduct of research utilizing recombinant DNA, the investigator(s) adhered to the NIH Guidelines for Research Involving Recombinant DNA Molecules.

____ In the conduct of research involving hazardous organisms, the investigator(s) adhered to the CDC-NIH Guide for Biosafety in Microbiological and Biomedical Laboratories.

David V. Reed 10/18/96

PI - Signature Date

TABLE OF CONTENTS

INTRODUCTION

Neurofibromatosis 1 (NF1) is an autosomal dominant condition that afflicts 1 in 3500 individuals worldwide. It typically manifests in an age-related fashion with cafe-au-lait spots and cutaneous neurofibromas. Approximately 2/3 of NF1 patients experience only the cutaneous manifestations, whereas 1/3 have disease-related complications that require medical care. Surgical management for abnormal tissue growth and bone dysplasias is the current modality for most complications, and its effectiveness is often suboptimal. The purpose of the present work is to comprehensively characterize the NF1 gene in an effort to better understand the pathophysiology of this condition. A direct application of this work involves both germline and somatic *NF1* mutation screening.

The NF1 gene was partially cloned in 1990 (1,2,3), yet the *NF1* locus has not been fully characterized. The locus spans approximately 335 kilobases of DNA and it is comprised of a core of 57 exons with three additional alternatively spliced exons for a total of 60 (4,43). The cDNA has been completely sequenced, and its open reading frame encodes a peptide of 2818 amino acids (5) which has been named neurofibromin. One domain of neurofibromin, representing approximately 1/5 of the protein, functions as an activator of the intrinsic GTPase in p21ras (6,7,8,9), and other domains share homology to the yeast proteins, IRA1 and IRA2 (10,11). The role of neurofibromin in the Ras signal transduction pathway has not been entirely elucidated, however, through its negative regulation of Ras-signaling *NF1* has been speculated to be

a tumor suppressor gene. Indeed, some malignancies associated with NF1 clearly have mutations that predict complete inactivation of intracellular neurofibromin which supports the hypothesis that neurofibromin functions in some way as a growth inhibitor (12,13,14,15,16,17). However, other genetic events have not been systematically evaluated in the NF1-specific malignant peripheral nerve sheath tumors even though they demonstrate complex cytogenetic abnormalities.

In general, the tumors of NF1 are benign and observations related to genetic alterations in malignancies may not apply to common benign tumors such as neurofibromas. The simplified "two-hit" model of tumor development and progression, as proposed for *FAP* in colon carcinogenesis in familial adenomatous polyposis, may not apply to NF1 tumors. The status of the second *NF1* allele in benign tissue has not been adequately investigated, although multiple studies (18,19,20,21,22,23) have shown preservation of both chromosome 17s in DNA extracted from neurofibromas from NF1 patients. However, one study showed variable loss of the presumed normal *NF1* allele in a number of individual benign neurofibromas excised from one NF1 patient (24). These studies were hampered by contaminating tissue in the multicellular benign tumors, and by the difficulty in identifying *NF1* mutations from archived tissue. The first issue can be alleviated by examining regions of the tumor that appear clonal, and the second problem can be addressed by the development of a comprehensive mutation screen using DNA extracted from clonal regions as template for PCR. The development of a comprehensive, DNA-based screening protocol requires detailed

knowledge of the genomic structure of the *NF1* gene and identification of the intron-exon boundaries at the DNA sequence level.

In addition to tumorigenesis, neurofibromin likely plays a role in embryological development. NF1 individuals often have congenital lesions that manifest early in childhood; bone abnormalities such as sphenoid wing dysplasia and tibial pseudarthroses, plexiform neurofibromas, and learning disabilities are relatively common manifestations. Further evidence for a role in human development comes from the identification of *NF1* cDNA derived from fetal tissues which suggests that it is expressed during fetal development (25,26). This is supported by *NF1* expression studies in rodents (26,27) using antibodies against various neurofibromin domains to identify spacial and temporal expression patterns during embryogenesis. Likewise, the development of transgenic mice clearly demonstrate a role for neurofibromin in mouse embryogenesis (28,29). Nf1 transgenic mice were constructed with a neomycin gene insertion in the human equivalent mutation found in exon 31 that leads to "inactivation" of that allele. Even though the heterozygote mouse does not have features typical in human NF1, the use of Nf1 transgenic mice in experimental systems has recently provided insight for at least three cell types involved in the pathogenesis of this condition.

Schwann cells and neurons harvested from ganglia comprising the peripheral nervous system of mice with different genotypes demonstrate different phenotypes in *vitro* cell culture experiments. Paradoxically, Schwann cells from neurofibromin-deficient mice show

growth inhibition in response to growth factors typically found in human neurofibromas (30). This was interpreted to signify that the hyperplasia of Schwann cells in NF1-associated tumors cannot be explained simply as a deficiency of intracellular neurofibromin. On the other hand, cultured neurons from *Nf1*$^{-/-}$ embryos atypically survive without the addition of growth factors into the tissue culture medium (31). This finding was interpreted as a loss of dependency on growth factors needed for cell survival. Finally, hematopoietic stem cells from *Nf1*$^{-/-}$ mice demonstrate a heightened response to GM-CSF, a growth factor that stimulates colony formation through a cell-surface receptor (32,33). Cells that are null for *Nf1* have a different phenotype than those haplo-insufficient cells which emphasizes the potential significance of somatic inactivating mutations in the heterozygote organism. It further emphasizes the need to screen and detect such mutations in archived specimens in order to correlate clinical aspects of NF1 with the molecular pathology.

The regulation of gene transcription is an important theme both in embryogenesis and tumorigenesis, and studies to specifically address transcriptional regulation of *NF1* expression will require knowledge of the genomic structure involving promoters and enhancers at the 5′-end of the gene. Mouse and human DNA sequence upstream of the transcription start site are well-conserved (34), thus the comparison of rodent and human *NF1* expression is valid even in the absence of comparable NF1 phenotypes. The observation that DNA in the 5′-end of the gene is methylated (35) introduces a layer of complexity in the

identification of potential mechanisms important in regulation of *NF1* expression. Thus, detailed knowledge of the human *NF1* locus extending in the 5′ direction is essential for further studies on transcriptional regulation.

The important observations relating to NF1 which have been made over the last forty months since this project proposal was submitted continue to demonstrate the need to develop a comprehensive understanding of the structure of the *NF1* locus. This final progress report will deal with accomplishments made involving each of the following specific aims;

1. To isolate a complete set of overlapping genomic clones that span the NF1 locus, and construct a restriction enzyme map of the genomic contig. The present genomic contig would also be extended to include clones that map to the flanking regions of *NF1*.

2. To screen cosmid clones that map to flanking regions of the *NF1* locus for short nucleotide repeat sequences, and, providing loci are identified, to develop PCR-based sequence-tagged-site markers.

3. To develop a working set of oligonucleotide primers to PCR amplify genomic DNA template at all *NF1* exons, and to map exons to the genomic restriction map.

4. To screen genomic DNA for somatic *NF1* mutations in tissue derived from NF1 patients shown to carry defined germline mutations at the molecular level.

BODY

Specific Aim 1. To isolate a complete set of overlapping genomic clones that span the NF1 locus, and construct a restriction enzyme map of the genomic contig. The present genomic contig would also be extended to include clones that map to the flanking regions of *NF1*.

Originally this specific aim was to be accomplished with cosmid clones and YAC subclones. The implementation of P1-bacteriophage library screening at the University of Utah altered our approach. P1 clones generally harbor inserts that are twice as large as cosmids (approximately 60 to 100 kb), and they do not rearrange like YAC clones. We screened a premade P1-bacteriophage human genomic library (The DuPont-Merck Pharmaceutical Co., Wilmington, DE, DMPC-HFF#1 Series B) cloned into the *BamHI* site in the Ad10sacBII vector (36). An initial screening using *NF1* exon sequences identified a number of clones. Two clones, P1-9 and P1-12, were mapped back to the *NF1* locus. P1-12 lies in the middle of the gene whereas P1-9 lies toward the 5′ end of the gene. Southern analysis using RNA probes generated from the ends of the 65-kb P1-9 insert showed that P1-9 spanned one gap in the cosmid contig. P1-9 harbors *NF1* exons 2 through 11 (figure 1; also figure 1 in Li et al, 1995, appendix A (ref 4)). Clone P1-12 spans intron 27b and encompasses three embedded genes within this intron (see figure 1 in Leppig et al, 1996, appendix A (ref 49)).

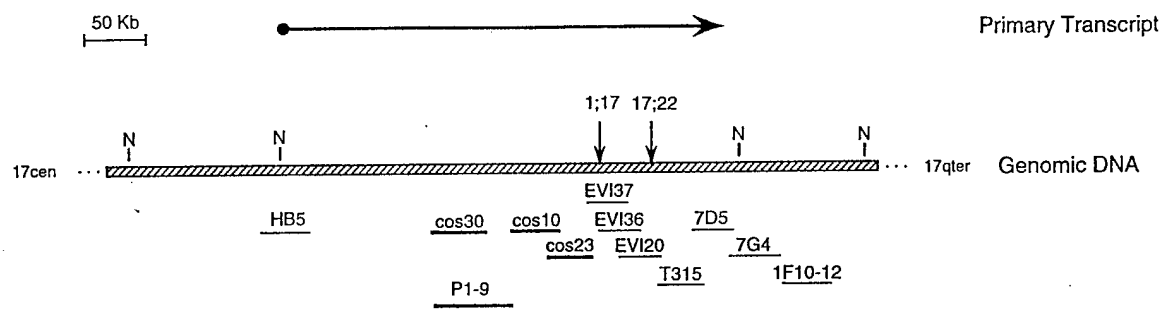

FIG. 1. The *NF1* locus. Genomic DNA is represented as a hatched bar; the length and transcriptional direction of *NF1* is depicted by the arrow above the region of genomic DNA that it spans. N denotes *NotI* restriction cleavage sites. Cosmid and P1 clones which cover all *NF1* exons are shown below the map. Breakpoints of two previously characterized chromosomal rearrangements, t(1;17) and t(17;22) are indicated by downward arrows above the genomic fragment.

In a separate screening, a random-primed probe of a restriction enzyme DNA fragment from cosmid cHB5, a clone that harbors exon 1, was used to isolate two independent P1-bacteriophage clones, P1-60 and P1-122, that map to the 5'-end of the gene (figure 2). Neither of these clones spanned the genomic contig gap harboring intron 1. The centromeric ends of each of these clones extend beyond the centromeric end of cHB5. A second screening was performed using a probe from a subcloned end-fragment of cHB5 with similar results, only P1-60 and P1-122 were identified. We collaborated with Peter O'Connell from the University of Texas at San Antonio to screen a separate P1-bacteriophage library by PCR analysis. No clones were identified in this screen. We have also used two separate probes from the centromeric ends of c30 and P1-9, to screen the P1 library in order to fill the gap which is part of intron 1. Clones that were

identified on initial screening did not map back to the *NF1* locus and likely represent false clones. These results suggest that P1 clones mapping to intron 1 and centromeric to exon 1 are under-represented in the P1 libraries. Thus, there remains a gap in intron 1 which is unfortunate because it may be relatively large, estimated between 40-115 kb based on pulsed-field estimates of restriction fragments. The potential development of microsatellite probes and identification of intron-based *cis*-regulatory elements makes it imperative to close the gap with a genomic clone even though not successful on this occasion. This is the only gap in the genomic contig for *NF1*. We also screened five YACs that mapped to *NF1* kindly provided by Robert Weiss from the Department of Human Genetics, University of Utah. The most centromeric end of each of these clones did not extend into intron 1. Even though other YAC clones spanning the *NF1* locus have been reported (37), none have been subcloned into more workable clones.

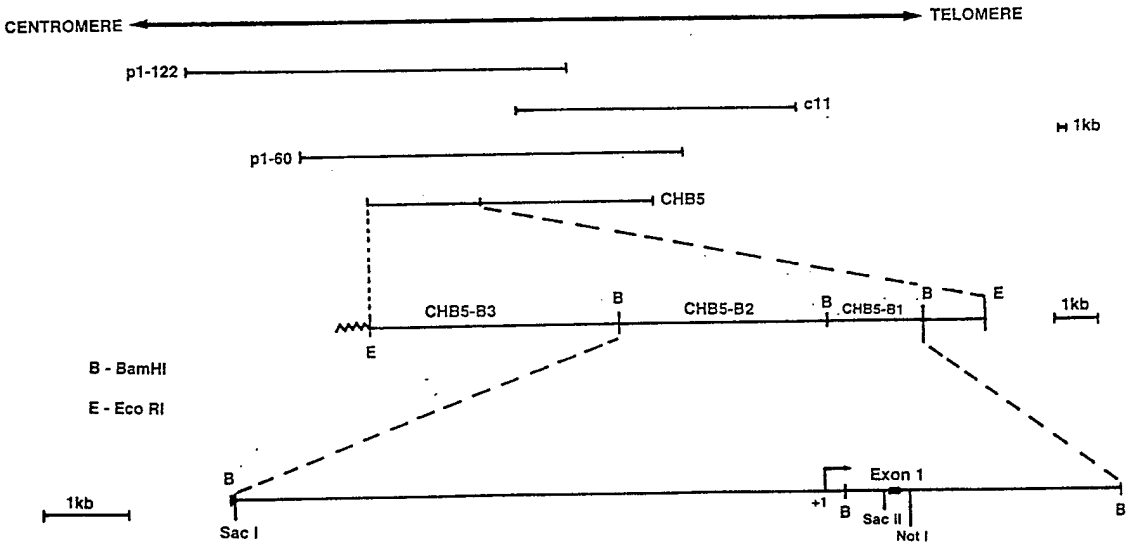

FIG. 2. Genomic clones isolated from the 5′-end of *NF1*.

The entire *NF1* coding region is represented in genomic clones, and a PCR approach was used to identify the extent of exon representation in each of the clones (4). Using exon-specific, intron-based primer pairs, various clones in the contig were used as template in routine PCR with each specific primer pair; the presence of the appropriate size band as detected with agarose gel electrophoresis confirmed the presence of each specific exon within the clone. Cosmid cHB5, P1-122 and P1-60 harbor the promotor region and exon 1, P1-9 carries exons 2 through 11, cosmid c10 contains exons 10c through 23-1, and cosmid c23 contains exons 23-2 through 27b. The remainder of the coding region of the gene, exons 28 through 49, is represented as part of a 100-kb sequence (38) that was derived from a previously obtained contig (3).

An unexpected finding in screening the P1 library with *NF1* exon sequences was the isolation of clones that did not map back to the *NF1* locus. Initially, P1 clones were partially mapped to the *NF1* locus by their ability to serve as template in PCR reactions using intron-based primer pairs that amplified individual exons. Those P1 clones that yielded a PCR product of the expected size were assumed to map to the locus. However, DNA sequence of a PCR product encompassing exon 20 from P1-7 revealed multiple base-pair substitutions in the exon sequence when compared with *NF1* cDNA. This observation suggested that P1 clones selected with *NF1* exon sequences could represent *NF1* homologous loci. This observation has been reported by other investigators (4,39,40,41,42).

In collaboration with Arthur Brothman of the core FISH laboratory at the University of Utah, we applied the technique of

FISH (fluorescence *in situ* hybridization) to map *NF1*-selected P1 probes to their respective loci on metaphase chromosome spreads (43, see appendix A). The chromosomal location of the various P1 clones is shown in table 1 (also see table 1 in Purandare et al, 1995; appendix A (ref. 43)). We sequenced those PCR products that were amplified from isolated DNA template representing homologous loci and primer sets designed from *bona fide NF1* sequence (table 2, also see table 2 in Purandare et al, 1995; appendix A (ref. 43)). By sequence analysis, the homologous loci do not represent processed *NF1* transcripts which typify pseudogenes, however there is no evidence that any other locus is transcribed. Sequence divergence is equally represented in both exons and introns. By and large, these are substitution changes which explains the equivalent size between PCR products synthesized from different templates.

TABLE 1

Chromosomal Location of Genomic Clones That Were Selected by High-Stringency Hybridization Using *NF1* cDNA Segments as Probes

Genomic clone	Chromosomal location	Method of determination	*NF1* exons
Cos HB5	17q11.2	Seq, SBA	5'UTR-1
P1-60	17q11.2	FISH	5'UTR-1
Cos 30	17q11.2	Seq, FISH	2-6
P1-9	17q11.2	Seq, FISH	2-11
Cos 10	17q11.2	Seq	10c-23-1
Cos 23	17q11.2	Seq	23-2-27b
P1-12	17q11.2	FISH	Intron 27b
Cos 7	15	Seq	
Cos A	18p11.2, 21p11.2	FISH	
P1-16	2q33–q34	FISH	
P1-15	2q33–q34, 14q11.2, 22q11.2	FISH	
P1-7	2q21, 14q11.2	FISH	
P1-4	15q11.2	FISH	
P1-10	15q11.2	FISH	

Note. Seq, sequence identity by comparison; FISH, fluorescence *in situ* hybridization; SBA, Southern blot analysis. The right-hand column shows exon representation of the *NF1*-specific genomic clones.

TABLE 2

Compilation of *NF1* Seqments That Coamplify by PCR and Show Sequence Differences between the *NF1* Locus and Homologous Loci from the Various Chromosomes

Exon	Locus	Sequence alterations
7	chr 21	9 substitutions
8	chr 18	8 substitutions
	chr 21	4 substitutions, 3-bp del
9	chr 18	3 substitutions
	chr 21	4 substitutions
11	chr 21	2 substitutions
13	chr 2	7 substitutions, 1-bp ins (A), 2-bp del
	chr 14	11 substitutions, 1-bp ins (T), 2-bp del
15	chr 14	4 substitutions
	chr 15	5 substitutions
16*	chr 12	14 substitutions, 1-bp del (G)
	chr 14	15 substitutions
17	chr 14, 22	Sequence not available
18	chr 14	9 substitutions
	chr 15	6 substitutions, 1-bp del
	chr 22	6 substitutions
19a	chr 14, 22	Sequence not available
19b	chr 15	3 substitutions, 4-bp ins
20	chr 15	11 substitutions
21	chr 15	14 substitutions, 1-bp del, 3-bp del
22	chr 15	Sequence not available
23-1	chr 15	3 substitutions
24	chr 15 (q11.2)	10 substitutions
	chr 15 (q24–qter)	8 substitutions
27a	chr 15	8 substitutions, 1-bp del
27b	chr 14	Sequence not available
	chr 15	12 substitutions, 3-bp del

A restriction enzyme map of the genomic DNA from cHB5 through c37 has not yet been constructed. The identification of homologous loci explains why it has been very difficult to interpret Southern blot analysis using *NF1* probes 5′ of exon 27b. The identification of a clone that spans inton 1 would complete the entire *NF1* contig and provide the incentive to construct such a map. The advent of rapid sequencing techniques and our ability to link new sequence to over 100-kb of continuous sequence may provide enough incentive to a human genome center lab to actually sequence the remainder of the *NF1* locus if provided the genomic clones. The work involved in sequencing might be less than that put forth in generating restriction maps by the partial digest approach. The generation of sequence would negate the need for such a map, even though the comparison between genomic clone sequence-defined restriction sites and total human DNA digestions would remain fairly complex given the homologous loci and potential polymorphisms with different alleles from each locus.

Given that knowledge regarding the regulation of *NF1* gene expression may be important in altering the haplo-insufficient state of heterozygous cells derived from NF1 patients, we have subcloned this region (see figure 2) to sequence a total of 4370 bases lying upstream of exon 1. This was performed by generating deletion mutants and sequencing the centromeric end of each of the clones. A *SacI/BamHI* subclone of cosmid cHB5 was used as the primary construct and directional deletion mutant constructs were generated. We have generated an additional 1.6 kb of sequence to that previously reported (34). There are a number of transcription

factor binding motifs upstream of the *NF1* transcriptional start site as identified by sequence analysis. To enable us to screen the *NF1* promoter for functional *cis*-regulatory elements the deletion constructs were subcloned into luciferase expression vectors that will be useful in subsequent *NF1* promoter evaluations (figure 3).

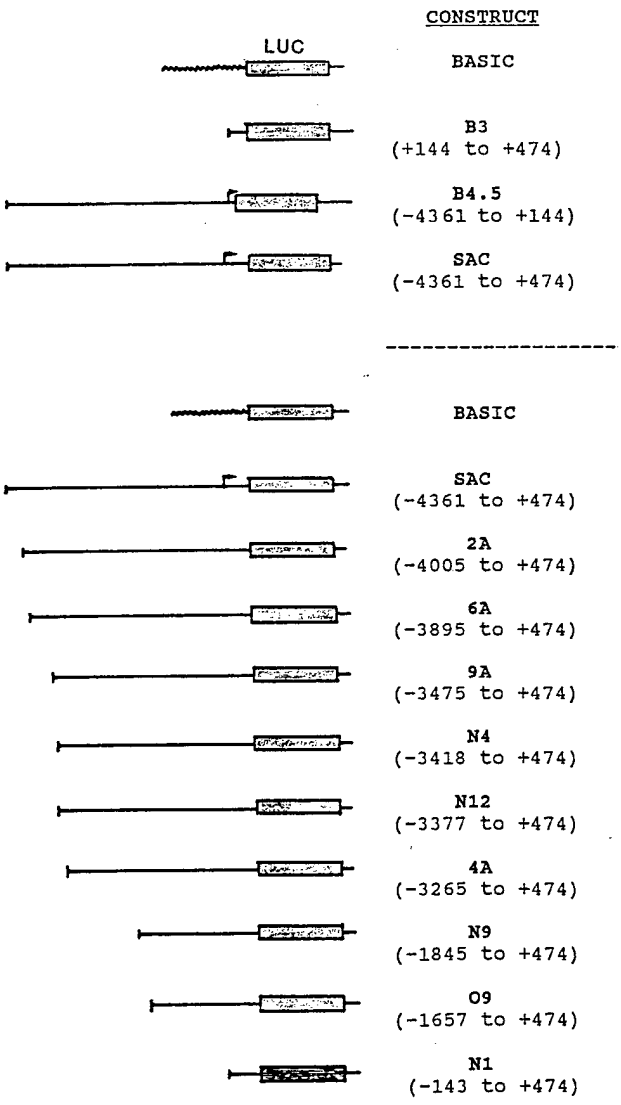

SAC I
GAGCTCTGGT CGCCAGGAGA GCCCTTCAGA GCAGCCCCAC CCTGAGCCCT GCATCTGCCA GTCAGTGCAG -4299

ACGGACCTGG TGAGAGGCAG CTTTCTTCAG CTGAAGGCAA CTCCTGGAAA GGGATTTAGC TGATAGGTGT -4229

TGACAAGTAA TGCGCCCAGC AGCTGAGGAA ATGAGCACCT TAGTCCTGAA GAGTGGTGTG CTCTTTGGTA -4159

2A
TGCTGGGATG GTTGGTTGTG CCAGTGGAGA TGGGGGTGGT GGGCAGAATG AAGGGAATAC TACTGTAAAA -4089

GCTTTTTATT TTTTATTTAT ATTTATTCAT TTATTTATTT TTTAAGACAA GGTCTAACTC TGATGCCCGG -4019

GCTGGAGTGC TGGAATGCAA TGACACCATC ACAGCTCACT GTAGCCTTGA CCTCCTGGGC TCAAGCGATC -3949

6A
CTCCCACTTC AGCTTCCCAA GTAACTGGAA CCACAGGCAC ATGCCACCAT GCCCAGCTAA TTAAAAAAAA -3879

AAATTTTGTA GAGATGAGGT TTCGCCATGT TGCCCAGGGT GGTCTGGAAC TCCTGGGCTC AAGTGATCCA -3809

CCCACCTTGG CCTCCCAAAG TGCTGGGATG ACAGGCATGA GCCACGGCTC CCAGCTTGGA ACAAAACTCT -3739

TCGAAGAAAA AATGGGCAGA GCTTGTTGCC TGACCAAAAA ACAGAGGCTG AATGAGAGAG ATGCATTTAA -3669

AACAATACGA AACACTAAGG GTTCCCTGAA TACTGTTGGA CAGTGCAAAA TGGGGGAAGT TAGGATACAA -3599

ATCTAATTCT GTTCTACTGT AAGCCTCATG CCTTTTCACT AGACTAGTGC TGGTCAAACT GGTGTTCCAT -3529

9A
GGGCTACATT CAGACAGCAG ACGTATTTTG TTTGGCTACA CAGCATTTAA AAAATGTAAA TTGGCTGCCA -3459

N4
CTATGTAAAA ATTGGAAGAG TTTACATGTA AGTTCAGATC TCTAGCTTCT CTTGAGTAAC TAGAA -3394

Figure 3. a) Deletion constructs derived from the subclones harboring the *NF1* promoter. b) Sequence from deletion constructs. The *Sac* I site is 4361 bp upstream of the transcription start site.

Specific Aim 2: To screen cosmid clones that map to flanking regions of the *NF1* locus for short nucleotide repeat sequences, and, providing loci are identified, to develop PCR-based sequence-tagged-site markers.

The purpose of this specific aim was to identify short repeats and develop microsatellite markers across the *NF1* locus to obviate the need to perform Southern blots in genotype analysis. In addition to seeking repetitive sequences to serve as genetic markers in a PCR-based allele detection system we have applied other allele detection protocols to evaluate haplotypes across the entire *NF1* locus. In collaboration with Richard Cawthon at the University of Utah we have applied MS-PCR protocols (44) developed to detect two separate alleles in exons 5 (position 702 in the cDNA) and 13 (position 2034 in the cDNA). We have also developed a detection scheme to detect two single-base, G/A, at position 10,647 in the 3'-untranslated region of exon 49 of *NF1*. Thus, we have converted a number of two-allele polymorphisms in three separate *NF1* exons by application of the MS-PCR (mutationally separated polymerase chain reaction) technique (see Purandare et al, 1996; appendix A (ref. 45)). In addition to demonstrating the feasibility of application of these primer sets and PCR conditions in genotype analysis, we applied these polymorphisms in conjunction with three other STS markers to show that linkage disequilibrium is maintained across the *NF1* locus regardless of the polymorphic systems employed or the physical distance within the locus. In addition, we demonstrated that the African population diverges from the

Caucasian and Japanese populations.

We have identified other short tandem repeats at the *NF1* locus, however we have not been able to develop a reliable PCR-based assay to exploit the STS markers. One $(CAAA)_n$ repeat was identified from sequence generated from a subclone at the end of cosmid cHB5, approximately 12 kb upstream of the promoter region. Facing oligonucleotide primers were synthesized from the DNA sequence that extends from either side of the simple tetranucleotide repeat, and, in preliminary experiments, the primers amplify the correct size band from cHB5 as template. However, we have not been able to optimize the PCR for *NF1*-specific amplification from total human DNA template. Another repetitive sequence has been identified in intron 12b. It has been difficult to DNA sequence through this CA repeat from PCR products, therefore an oligonucleotide primer has not yet been synthesized telomeric to the repeat. The identification and subcloning of a restriction enzyme fragment that harbors intron 12b will facilitate the DNA sequencing of this region and subsequent development of a PCR-based approach to identify another potentially informative site within the *NF1* gene. DNA sequence generated telomeric of *NF1* will also be scanned for repeats and STS development. In addition, any newly identified clones extending centromeric of *NF1* will be probed for potential using a set of repetitive oligonucleotides in Southern blot analysis.

Specific Aim 3. To develop a working set of oligonucleotide primers to PCR amplify genomic DNA template at all *NF1* exons, and to map exons to the genomic restriction map.

A substantial amount of effort has gone into accomplishing the goals set out in this seemingly straightforward specific aim. A significant portion of this work has been published (Li et al, 1995; see appendix A (ref. 4)). Data reported in that manuscript includes the genomic organization of *NF1* and a table of primer pairs that effectively amplify specific *NF1* exons from cloned genomic DNA (see table 1 in Li et al, 1995; appendix A (ref. 4)).

In order to develop intron-based primer pairs we defined intron/exon boundaries for exons 1 through 27b. In the majority of exons this information was available, however, during the course of this work a number of exons were shown to have introns that had not been detected previously. Thus, a significant amount of unanticipated sequencing was required before oligonucleotide primer pairs could be synthesized for each of the *NF1* exons.

We demonstrated the efficacy of each primer set using cloned genomic DNA as template, however PCR using total human DNA template resulted in a similar-sized PCR product with aberrant *NF1* sequence for a number of exons from a number of genomic clones identified by colony hybridization with *NF1* cDNA probes. This observation suggested the presence of a number of *NF1* pseudogenes which could be amplified using *NF1* intron sequence. The identification of *NF1*-related loci as presented in specific aim 1 enabled us to generate sequence derived from *non-NF1* loci. In order to perform *NF1*

mutation analysis on genomic DNA as template in PCR we were obliged to develop specific primer pairs for the *NF1* gene. Using DNA extracted from somatic cell hybrids containing single human chromosomes in a rodent background as template, we attempted PCR amplification from each human chromosome using *NF1* exon-specific primers from exons 1 through 27b. There is no evidence that any *NF1*-related loci share homology to *NF1* beyond exon 27b.

In collaboration with Dr. Richard Cawthon we committed a significant amount of effort to develop primer pairs that specifically amplify the *NF1* locus from total human DNA (table 3, also table 3 in Purandare et al, 1995; in appendix A (ref. 43)). We generated specificity by appropriate sequence selection to optimize non-*NF1* mismatching in the 3′-end. We also empirically engineered base-pair mismatches for both *NF1* and *NF1*-related sequence in order enhance priming from *bona fide NF1* sequence. Thus, using an assortment of manipulations we were able to synthesize primer pairs that could preferentially amplify the *NF1* locus (for example, see fig 3 in Purandare et al, 1996; appendix A (ref. 45)).

TABLE 3

Primer Pairs for *NF1*-Specific Amplification of Exons 1–27b

Exon	Primer sequence 5′–3′	Exon	Primer sequence 5′–3′
1	CAGACCCTCTCCTTGCCTCTT GGATGGAGGGTCGGAGGCTG	14	TCCTTTTGGGTGGAGCTTATC TATACTTGTAATATGCACGTATC
2	TTTTAAGGATAAACTGTTTACGTG TCCCCAAAACACAGTAACCC	15*	TGTGATCAGGAATAGCTTTTGAA TTAACAGATAAAAGTCAACTTTAC
3	TTTCAGTTTTCAGATGTGTGTTG TGGTCCACATCTGTACTTTG	16	TGGATAAAGCATAATTTGTCAAGT TAGAGAAAGGTGAAAAATAAGAG
4a	TTTGAAAATTTTCATAATAGAAAATGT GAGGTCAAGCTGCTGTGAG	17	CTCTGTGTGTTTAGATCAGTCA TTTATCAATTAGTACCAGTAGCAG
4b	GTCGTGGCCTCAAGTGGTC TTATAAAATCCAGATTGGTGTTC	18	AGAAGTTGTGTACGTTCTTTTCT CTCCTTTCTACCAATAAGCGC
4c	TTTCCTAGCAGACAACTATCGA CATCAAAAAAAAAATTTTAATACCAG	19a	TCATGTCAGTTAGGTTATCTGG TGTAATTAAGTAGTTATAACTCTC
5	TGACTTGAGTGATAGTTTCACAT AAAAAAAAATCAATCGTATCCTTA	19b	AACTTGAAAGATTCATGGTCTC TTTATGTTTTTTGGTGACTG
6	CATGTTTATCTTTTAAAAATGTTGCC ATAATGGAAATAATTTTGCCCTCC	20	CCACCCTGCCTGATTATCG TAATTTTTGCTTCTCTTACATGC
7	TGCTATAATATTAGCTACATCTGG CCTATGAGCTTATCAACGAAGAG	21*	AAATGAAAGTTTCATATAGAAATAC ATTTGCTATGTGCCAGGGAC
7 and 8*	TGCTATAATATTAGCTACATCTGG CTAGTCTTTCTGTTTATAAAGGAT	22	TGCTACTCTTTAGCTTCCTAC CCTTAAAAGAAGACAATCAGCC
9*	TTTGACCTCATTTGTATTACTGAG AGAACCTTTTGAAACCAAGAGTG	23-1	TTTGTATCATTCATTTTGTGTGTA AAAAACACGGTTCTATGTGAAAAG
9a (br)	TCCGCTGTGGCTCAGAACAC AGTAGAAGAGGATGCACAGCC	23-2	CTTAATGTCTGTATAAGAGTCTC ACTTTAGATTAATAATGGTAATCTC
10a	ACGTAATTTTGTACTTTTCTTCC CAATAGAAAGGAGGTGAGATTC	23a	AGCCAGAAATAGTATACATGATTGGGT CTATTTCTGCCAGAATTAGTAGA
10b	AACTATTGAGTGTTCTACTATACC TCTTGGCGATTCAGCTAAACC	24	TTGAACTCTTTGTTTTCATGTCTT GGAATTTAAGATAGCTAGATTATC
10c	CTTGGTACCCTTTAGCAGTCAC CCTTCTTTCTCCATGGAG	25	AATATAATAATTATATTTGGGAAGGT GAAAATATTTGATTCAAACAGAGC
11	GTACTCCAGTGTTATGTTTACC TAAAGTTGAAATTTAAAAATTAAAGTAC	26	GCTTTGTCTAATGTCAAGTCAC TTAAACGGAGAGTGTTCACTATC
12a	AAACCTTACAAGAAAAACTAAGCT ATTACCATTCCAAATATTCTTCCA	27a*	GTTACAAGTTAAAGAAATGTGTAG CTAACAAGTGGCCTGGTGGCAAAC
12b	TTTCTAGTGAATGTCCTTCAAGT ATGAAATTTACCAAATTTCATTCAG	27b*	TTTATTGTTTATCCAATTATAGACTT TCCTGTTAAGTCAACTGGGAAAAAC
13	CACAGTTTATTGCATTGTTAGAT GCCATGTGCTTTGAGGCAGAA		

Note. Primer pairs marked by an asterisk for exons 8, 9, 15, 21, 27a, and 27b amplify from chromosome 17 and the homologous loci. Primer pairs for exons 7 and 8 have been combined and amplify an ~700-bp PCR product, which amplifies preferentially from chromosome 17, but also amplifies from the homologous loci on chromosomes 18 and 21. Primer pairs for exon 9a (identical to exon 9br—Danglot *et al.*, 1995) were derived from sequence submitted to GenBank.

Primer pairs for each of the *NF1* exons have been synthesized, and, under routine PCR conditions, each *NF1* exon can be amplified. We designed primers at least 50 bp upstream from the 5'-end and 5 bp downstream of each exon so that both open reading frame and sequences important in splicing could be evaluated. This has enabled us to implement *NF1* screening protocols to identify sequence variants from DNA template. It was imperative to accomplish this aspect of specific aim 3 before we could begin to comprehensively screen DNA extracted from tumor tissue as proposed in specific aim 4.

In addition to laying the foundation for *NF1* mutation analysis using DNA template, we have used exon-specific primer pairs to generate PCR products representing single exons for mapping studies. The PCR products were radioactively labeled by including P^{32} dCTP as a nucleotide in the PCR, and they were used as probes in Southern analysis to identify the size of *EcoRI* fragments harboring exons 2 through 27b. This analysis is shown in table 4.

NF1 Exon	*EcoRI* Frag	Genomic Clone	Intron Size by PCR (kb)
1	15kb	cHB5	?
2	5.8kb	c30	3.1
3	5.8kb	c30	?
4a	600bp/450bp	c30	?
4b	2.1kb	c30	2
4c	>10kb	c30	0.22
5	>10kb	c30	0.8
6	>10kb	c30	?
7	550bp/1kb	P1-9	0.4
8	1kb	P1-9	?
9	9.4kb/4kb	P1-9	~4kb
10a	4.5kb	P1-9	?
10b	-	P1-9	~4kb
11	2.1kb	c10	0.54
12a	2.1kb	c10	?
12b	0.9kb	c10	1.2
13	~15kb	c10	1.3
14	~15kb	c10	0.23
15	~15kb	c10	1.3
16	~15kb	c10	0.38
17	~15kb	c10	0.28
18	~15kb	c10	0.46
19a	~15kb	c10	1.2
19b	~15kb	c10	0.55
20	~15kb	c10	0.12
21	~15kb	c10	2.2
22	~15kb	c10	0.14
23-1	~15kb	c10	?
23-2	1.7kb/1.2kb	c10	4
23a	-	c10	6
24	1.6kb	c23	0.53
25	2.2kb	c23	1.25
26	2.25kb	c23	1.27
27a	4.4kb	c23	?
27b	-	c23	?

Table 4. Southern analysis of exon-specific probe hybridization against cloned genomic DNA blots. Fragment sizes are from clones, intron sizes are from PCR products that span the intron lying downstream of the exon.

Specific Aim 4. To screen genomic DNA for somatic *NF1* mutations in tissue derived from NF1 patients shown to carry defined germline mutations at the molecular level.

We have developed techniques to comprehensively screen genomic DNA for *NF1* mutations. This applies to DNA extracted from blood, frozen tissue, and archival material that has been processed in paraffin blocks. In this approach each *NF1* exon is amplified by PCR using specific primers and standardized PCR conditions. We used a variety of protocols to evaluate the products including direct DNA sequencing, size-shift analysis, and single-strand conformer analysis.

Initially we attempted to screen *NF1* PCR products for mutations by direct DNA sequencing. We designed primer pairs to provide products between 250 and 400 basepairs in length which encompass the entire exon and include DNA sequence at least 50 basepairs upstream of the exon. Each primer is 20 to 24 bases long and contains an additional common 18-bp tag which is used in subsequent analysis. The 5′-primer contains the 21M13 (5′TGAAAAACGACGGCCAGT3′) sequence and the 3′-primer contains the M13RP1 (5′CAGCAAACAGCTATGACC3′) sequence. PCR conditions are as follows: 50 to 100 ng template, 1.2mM dNTP, 2.5 mM $MgCl_2$, 10 mM Tris (pH8.3), 50 mM KCl, 2.5 microM primers, 50 to 600 ng of genomic DNA, and 0.5 units of *Taq* polymerase in a total volume of 25 microliters. The amplification conditions are 94°C denaturation for 45 seconds, 60°C annealing for 45 seconds and 72°C extension for 1.5 minutes for 35 cycles. An aliquot of this first PCR product is

checked on an ethidium bromide stained, 4% agarose gel prior to subsequent manipulations. Direct sequencing by the magnetic bead approach uses the first exon-specific PCR product that has both 21M13 and M13RP1 tags as template for a second round of PCR. One microliter of a 1/100 dilution of PCR product ultrafiltrate is amplified using the following conditions: 1.2mM dNTP, 2.5mM $MgCl_2$, 10mM Tris(pH8.3), 50mM KCl, 5pMol of biotinylated primer (either 21M13 or M13RP1), 15pMol of non-biotinylated primer (other one of the pair), and 2 units of *Taq* polymerase in 50 microliters. The amplification is carried out by denaturation at 95°C for 30 seconds, 50°C annealing for 30 seconds, and 72°C for 1 minute for 25 cycles. Magnetic beads (Dynabeads^{Tm} M-280 Strepavidin, Lake Success, NY) with strepavidin attached are used to separate the biotinylated DNA strand in the PCR product for subsequent sequencing. PCR products are denatured with 0.1N NaOH and incubated with the beads at room temperature, and the immobilized strand is collected using a magnet (Dynal MPC^{Tm}, Lake Success, NY). This separated complex is directly sequenced by the dideoxynucleotide chain termination method using 0.5pMol of either upstream primer (21M13) or downstream primer (M13RP1) depending on the free target site in the ssDNA, T7 DNA polymerase (Sequenase version 2.0, USB, Cleveland, OH), and 0.5 microliters of [alpha-^{35}S]dATP (Amersham, Arlington Heights, IL) for each reaction. The sequencing reactions are denatured and electrophoresed on standard 6% PAGE-Urea gels. We were unable to consistently generate clean enough sequence to identify two alleles by sequence differences in control heterozygotes. Given that approximately 2/3 of reported *NF1*

mutations (NNFF Mutation Database, B. Korf and G. Schnieder, NNFF; 95 Pine Street, 16th Floor, New York, NY 10005) harbor small frame-shifting insertions or deletions, we elected to screen for small mutations entirely contained within exon-specific PCR products by mobility-shift in denaturing polyacrylamide gel electrophoresis.

The size-shift assay has been adapted for all *NF1* exons using DNA extracted from white blood cells as template in PCR. In conjunction with the preparation of template for direct sequencing reactions, aliquots of first-round PCR products were put through a centricon-100 ultrafiltration column to minimize primer and small-product carry-over to a second round of PCR. A 1/100 dilution of the ultrafiltrate was used as template in a second PCR using 21M13 and M13RP1 primers whereby one primer was end-labeled with [gamma-^{32}P]ATP by T4 polynucleotide kinase prior to PCR. PCR conditions: 1.2mM dNTP, 2.5mM $MgCl_2$, 10mM Tris(pH8.3), 50mM KCl, 5microM primers, and 0.5 units of *Taq* polymerase in 25 microliters. The isotope-labeled PCR products were denatured and electrophoresed on a standard 6% PAGE-Urea gel. The gels were dried and exposed by routine autoradiography. Examples of the application of this technique are demonstrated in the manuscript by Sawada and Viskochil which is contained in Appendix A (ref. 46).

We also used the single-strand, end-labeled PCR products for SSC (Single-strand conformer) analysis. This was accomplished by diluting the PCR product 60-fold in a buffer consisting of 20mM EDTA, 0.05% bromophenol blue, 0.05% xylene cyanol and heating to 85°C for 5 minutes to denature the DNA. Samples were electrophoresed through an 10% non-denaturing polyacrylamide gel

that contained 5% glycerol. The products were electrophoresed at 40W of power at 4°C for 6 hours. The buffers were exchanged once midway through the run. Gels were dried and exposed by routine autoradiography. We applied the size-shift and SCC protocols to 60 *NF1* exon-specific PCR products amplified from DNA extracted from white blood cells from 22 NF1 patients. The results of the complete screen is shown in table **5**. We were unable to complete screening on two individuals, NF 57-01 and 12767. Eight clearly demonstrated a size-shift with four showing sequence changes compatible with mutation. Seven demonstrated an SSC variant with 6 showing sequence differences predicting inactivation of that allele. Thus, of 20 individuals tested ten were detected to have an *NF1* mutation.

Lab #	Pt.#	Size Shift	Size Shift Variant	SSC	SSC Variant	SEQ	SEQ Variant
1	NF 56-02	X		X			
2	NF 57-01						
3	NF 64-05	X	10b	X		X	No abnormality
4	NF-65-03	X		X			
5	NF 91-01	X	31			X	CA insert, 5874
6	NF 93-03	X	33			X	No abnormality
7	NF 94-01	X		X	29	X	g(-1)→C,exon 29 dropout
8	NF 98-05	X	23.1	X		X	TGG→TGA, 3942
9	NF 107-06	X		X	20	X	g(-1)→C,exon 20 dropout
10	NF 112-01	X		X			
11	NF 117-01	X		X	27b	X	t(-7)→C, dropout 27b
12	NF 120-04	X		X	22	X	CGA→TGA, 3721
13	NF 124-02	X		X			
14	L-11578	X	23.1			X	T insert, 3912
15	12359	X		X	35	X	g(+1)C, exon 35 dropout
16	12418	X	44			X	9 bp deletion/26 plus
17	12497	X	11,34	X		X	No abnormality
18	12594	X		X	25,41	X	
19	12602	X		X			
20	12767						
21	12790			X	11,42	X	AAG→AGG, 7403
22	12930	X	19b?				
							10/22

Table 5. Summary of pilot study of *NF1* mutation detection assay.

In order to make this screening protocol more efficient we have empirically tested various multiplex protocols. By combining PCR products of different expected sizes we electrophoresed multiple exons from each template in a single lane of the gel (see figure 4). In addition, a number of primer sets are compatible for joint PCR. Up to six primer sets can be used in the same PCR reaction and processed as a group. An example of our groupings for this "stream-line analysis" is shown in table 6.

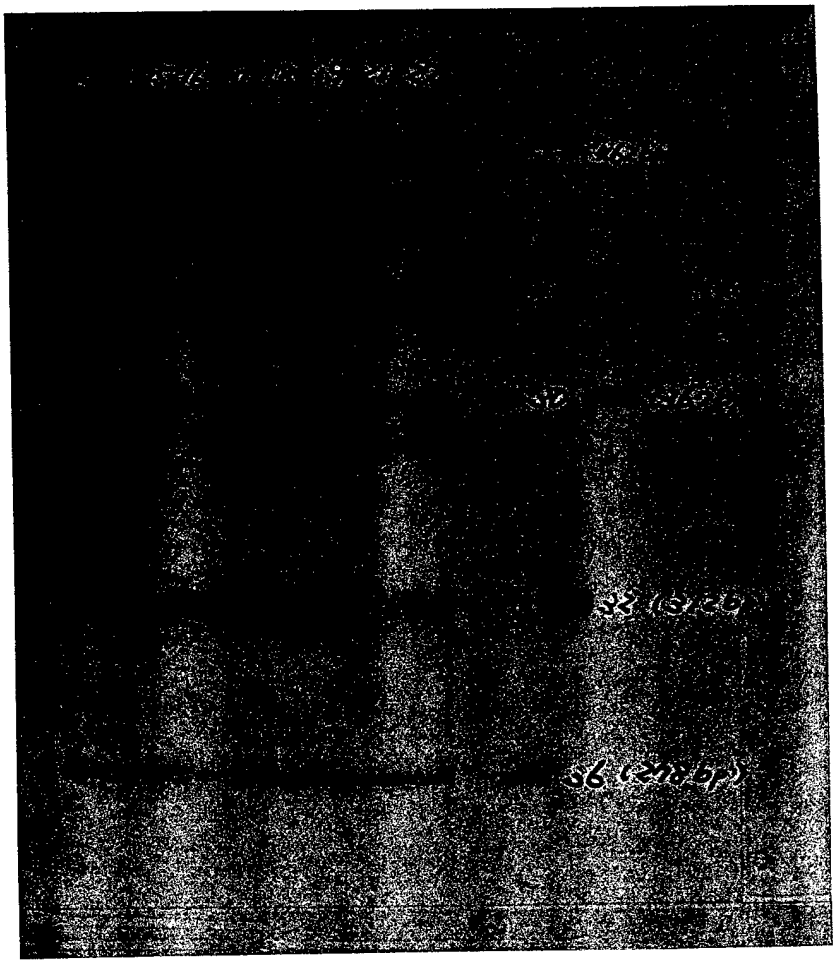

Figure 4. Size-shift assay on 6% denaturing gels. Patient DNA is labeled over each lane. The PCR products for exons 33, 34, 30, 32 and 36 are pooled for each patient run. Individual PCR products for each exon are shown on the right hand margin. The size of the PCR product is in parentheses.

GROUP	EXON	SIZE	GROUP	EXON	SIZE	GROUP	EXON	SIZE
A (75)	6	(301)	F (150)	36	(278)	L (300)	15	(275)
	43	(318)		28.1	(334)		17	(318)
	40	(328)		21	(374)		13	(382)
	42	(356)						
	49-3	(435)				SINGLE (500)	1	
	49-1	(468)	G (150)	10a	(232)		2	
				41	(339)		3	
B (75)	5	(180)		46	(347)		4b	
	48a	(245)					7	
	9a	(294)	H (150)	32	(312)		8	
	48	(360)		44	(334)		10c	
				30	(362)		11	
C (75)	37	(318)		33	(462)		19a	
	49-2	(326)					19b	
	38	(362)	I (250)	9	(248)		20	
	39	(382)		12a	(303)		24	
				18	(367)		28.2	
D (100)	4c	(190)		12b	(382)		31	
	14	(285)		4a	(415)		34	
	27a	(298)	J (500)	25	(254)		45	
	26	(342)		10b	(374)		47	
E (150)	27b	(296)		16	(549)			
	35	(311)	K (500)	23-1	(206)			
	22	(331)		23-2	(268)			
	23a	(412)		29	(530)			

Table 6. Exon groupings for joint PCR analysis in "stream-line" mutation detection. Numbers in parentheses next to the group letter indicates the amount of DNA template required for adequate imaging.

We have also performed direct mutation analysis on the first-round PCR product by including an exon-specific, end-labeled primer in the first round PCR. In this way we have eliminated the need for two PCRs and the processing of the "first-round" PCR products by Centricon ultrafiltration. An example of a size-shift

autoradiograph demonstrating the use of first-round labeled PCR product from grouped primer sets using DNA extracted from whole blood is shown in figure 5. We have begun integrating the multiplex size-shift analysis with heteroduplex analysis, however the poor separation of multiple bands on the autoradiograph precludes the use of previously designated groupings of primer sets. Thus, heteroduplex analysis is being performed on individual samples that do not show size-shift variants on the initial screen.

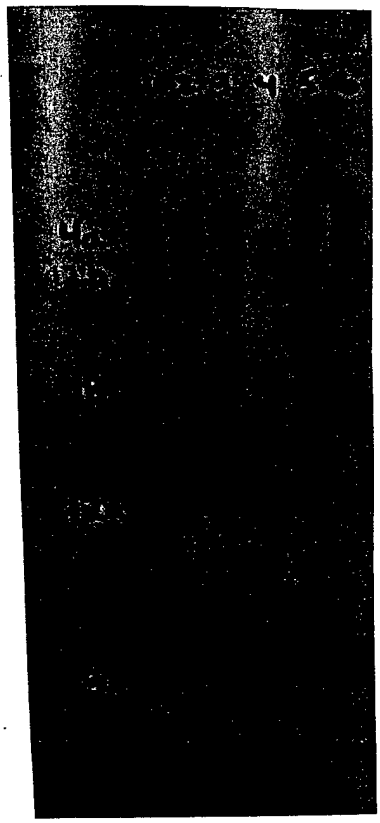

Figure 5. Size-shift assay on exons in group I. Using 250 ng of genomic DNA as template, PCR was performed by amplifying with five sets of primers whereby the upstream primer for each set was group-labeled by the T4-Kinase reaction. All five primer sets were incubated together in the PCR for each of six patient templates. Exons evaluated are 4a, 12b, 18, 12a, and 9 for patients 1 through 6 as labeled at the top of the autorad.

The primary goal of this specific aim was to examine NF1-associated tissue for the presence of somatic mutations. We were most interested in addressing the hypothesis that somatic *NF1* mutation of the normal *NF1* allele in NF1 patients must occur to

cause abnormal growth observed in neurofibromas. Furthermore, determination of the timing of the "second hit" would potentially focus future investigations for therapies either toward "up regulation" of the normal allele or toward interference of the Ras signal transduction pathway.

One difficulty with the somatic mutation analysis involves the designation of a "second hit" to the "normal" *NF1* allele in tissue. We have addressed this difficulty in two ways, one is to demonstrate linkage of the respective mutations either to each other or to known polymorphic sites that designate specific alleles. This would enable one to identify the allele harboring the somatic mutation with a specific haplotype; if the allele is distinct from the constitutional *NF1* mutant allele, then double inactivation of neurofibromin could be ascertained. The second approach is to screen abnormal tissue from individuals who are hemizygous at the *NF1* locus. In this case, any *NF1* mutation identified in DNA from archived tumor tissue would necessarily arise in the "normal" allele.

NF1 patients with large deletions encompassing the entire gene are hemizygous for *NF1*, and they appear to have a distinctive phenotype (47,48,49). We have developed *NF1* genomic clones as FISH probes in order to screen this distinctive population of NF1 individuals in order to identify those who are hemizygous. Over the last year we have identified two deletion patients, and we have collaborated with Dr. Karen Stephens at the University of Washington in Seattle to demonstrate a large deletion in one of her patients. One of our patients, identified by Virginia Johnson at

the University of South Dakota, and one from Dr. Alan Rubinstein at Mt. Sinai were shown to harbor large *NF1* deletions by FISH (Leppig et al, 1996; appendix A (ref. 49)). We have also used a single probe, P1-9, to demonstrate the loss of one *NF1* allele in metaphase chromosome spreads from white blood cells in a gentleman who has borderline mental retardation and multiple neurofibromas that presented at an early age. We continue to apply FISH analysis to screen individuals who have an atypical NF1 phenotype in order to identify those who may be hemizygous for *NF1*. We have also applied the PCR genotyping protocols (Purandare et al, 1996; appendix A (ref. 45)) to identify individuals who have two alleles at any one informative *NF1* locus. Those who are heterozygous are not candidates for whole gene deletions, therefore they are not processed for FISH analysis. Those who have only one allele at all loci may be hemizygous and are processed for FISH analysis.

In addition to whole blood samples, we have performed *NF1* mutation analysis using the DNA-based, exon-specific approach on pathological specimens. DNA was extracted from a scalp neurofibroma (shown in figure 6) which was excised from an NF1 individual previously shown to harbor a whole gene deletion (47). This individual was shown to be hemizygous for *NF1* by both somatic cell hybrid genotype analysis and FISH using P1-9 as a probe (D. Viskochil, unpublished). The neurofibroma was typical and there was a fair amount of S-100 protein staining as demonstrated in figure 6. The adjacent overlying skin (left side of figure 6) was entirely normal in appearance. DNA was extracted from the top, middle, and bottom portion of the tumor and subjected to the *NF1* mutation

screen based on PCR of individual exons.

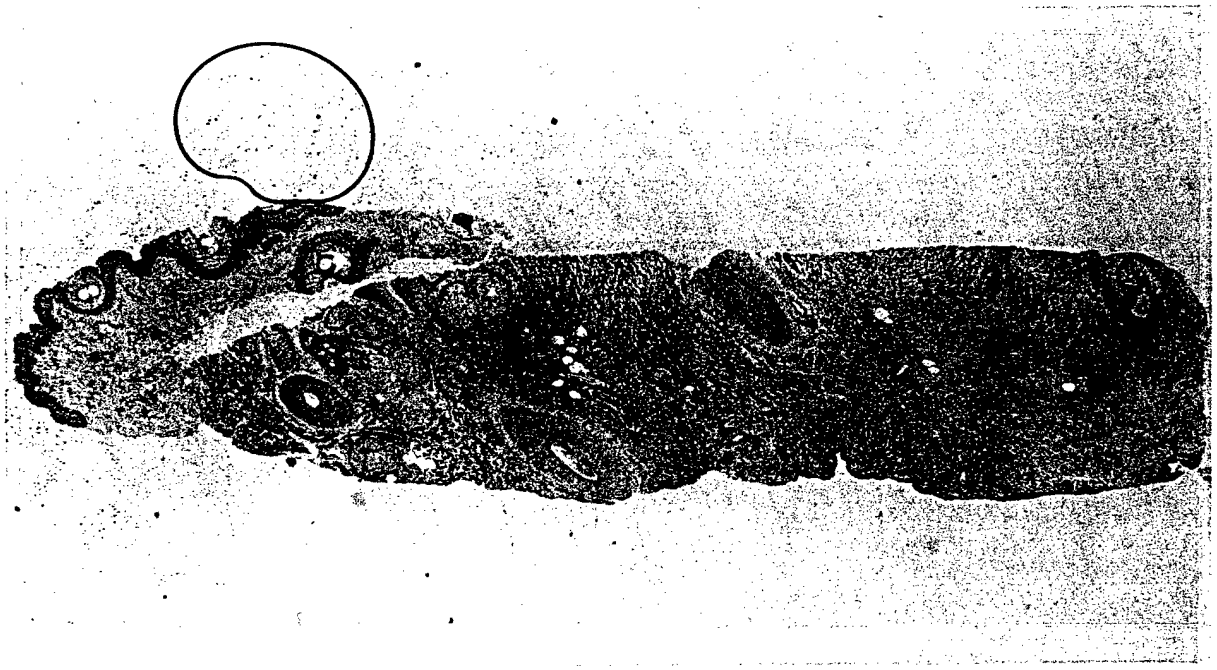

Figure 6. Scalp neurofibroma from an NF1 individual who has a large deletion of the *NF1* gene. This is an S-100 immuno-staining pattern which shows typical homogeneity of the neurofibroma in the center and to the right in the tissue sample shown. Adjacent skin to the left and upper left corner are normal.

Size-shift analysis was performed on all *NF1* exon-specific PCR products. We identified a faster migrating PCR product which amplified exon 4b as shown in the autoradiograph in figure 7a. We were unable to obtain readable sequence directly from the PCR product, therefore a separate PCR product was cloned in a pMOS vector for T-7 polymerase automated sequence analysis. Sequence from a single clone demonstrated a 4-bp deletion in *NF1* exon 4b (figure 7b). The mutation leads to inactivation of the allele by premature truncation of translation (see figure 7c, also figure 2 in Sawada et al., 1996; appendix A (ref. 50)). This work, recently

published in *Nature Genetics*, unequivocally demonstrates that cells from neurofibromas harbor "second hits" resulting in complete inactivation of both *NF1* alleles. By microdissection of adjacent skin tissue we were able to demonstrate that the somatic mutation was localized to the neurofibroma, and the proliferating cells maintained a number of cells that did not harbor the mutation (see figures 1 and 3 in Sawada et al, 1996; Appendix A (ref. 50)). Thus, the tumor was not clonal. The multicellularity of these tumors suggests that expansion of a clone of invading cells best represents the model cell proliferation of a dermal neurofibroma.

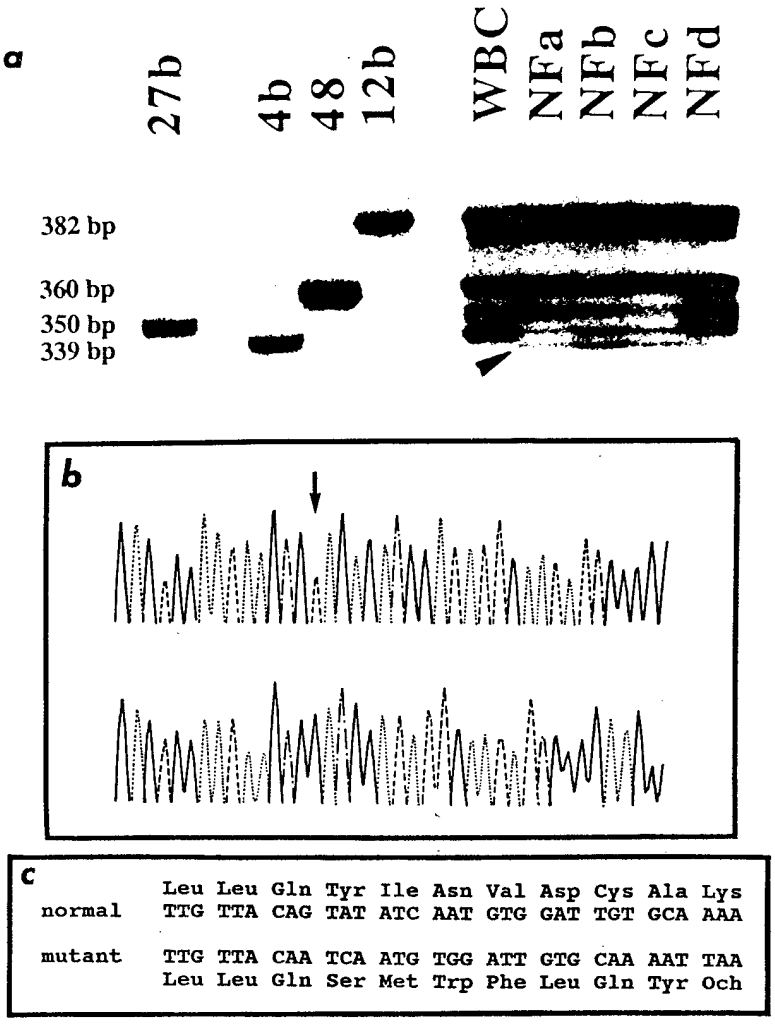

Figure 7. a) Size-shifted PCR product which was amplified from exon 4b from four separate DNA extractions from a scalp neurofibroma. The arrow shows the presence of the faster migrating band. b) DNA sequence of normal and mutant alleles. The base identified by the arrow is cDNA base 546 and it represents the site of a 4-bp deletion in the lower sequence (solid line-adenine, dotted line-thymine, dashed line-guanine, dot/dash line-cytosine). c) Deduced amino acid sequence from panel b showing frameshift ochre or stop-translation codon.

The identification of a somatic *NF1* mutation in a dermal neurofibroma suggests that cells involved in neurofibroma development can be null for intracellular neurofibromin, yet remain benign. It implies that neurofibromin deficient cells must accumulate other genetic changes to progress to malignancy. We were not able to determine the timing of somatic *NF1* mutation in this neurofibroma nor were we able to determine the cell of origin in the proliferating cell mass. Clearly there was abnormal S-100 protein staining which implies that the most likely cell type to cause this proliferation was a Schwann cell. Schwann cells are of neural crest origin and they migrate during embryogenesis. In collaboration with Karen Stephens, we are attempting to locate other excised scalp neurofibromas that have been archived in order to screen for the same somatic *NF1* mutation in exon 4b. Somatic mutation early in embryogenesis would suggest that expansion of a clone of Schwann cells should harbor the same mutation from a region, whereas a late mutation should demonstrate that a neurofibroma adjacent to this previously tested tumor does not harbor the same mutation. This study would be important to focus investigators on the possibility that $NF1^{+/-}$ cells have a predisposition to somatic mutation post-natally rather than embryologically. If somatic mutation is post-natal as suggested by the age-dependent occurrence of dermal neurofibromas in puberty, then the identification of agents that up-regulate expression from the normal *NF1* allele could be important. If *NF1* somatic mutation occurs in the embryonic time period, there would be no use in up-regulating an inactivated *NF1* allele.

This analysis demonstrates the utility of the DNA-based mutation screen using DNA extracted from archival tumor tissue. It also shows that microdissection of tissue from blocks can address the issue of timing of somatic mutation. We are also using this technique to examine the *NF1* locus as part of a genome-wide screen to identify "tumor suppressor" loci important in *NF1*-related tumor progression. We have begun a screen using an informative tetranucleotide repeat marker set that represents each chromosome arm. We have begun this study on neurofibromas and malignant peripheral nerve sheath tumors (MPNSTs) in hopes of identifying potential allelic imbalance in consistent loci which could signify genes near the genetic marker loci play a significant role in tumor development. We have focused on one individual from whom we obtained two costal neurofibromas, a primary MPNST, and a second MPNST excised later which presumably represents a metastasis from the primary MPNST. The neurofibroma DNA samples show allelic imbalance at 6 of 37 and 3 of 33 screened markers representing individual chromosome arms (none at the *NF1* locus), whereas the MPNST tumor DNAs demonstrated allelic imbalance at 8 of 21 and 6 of 18 screened genomic loci. We are in process of evaluating the arms showing allelic imbalance by testing with other markers. In addition, we are using interphase fluorescence *in situ* hybridization (FISH) with probes specific for different chromosomal arms to ascertain if allelic imbalance represents either loss of gain of chromosomal material.

We have also collected tissue on 5 individuals who have segmental NF, defined as the clinical expression of typical NF1 features

in a localized area of the body (51). A neurofibroma from one male individual is being screened for *NF1* somatic mutation by the exon-based PCR approach. If a sequence variant is identified, we intend to examine his blood and sperm DNA for the possibility of gonadal mosaicism.

Our last project is *NF1* mutation screening of MPNSTs collected as archival material from non-NF1 individuals (see Ota et al, 1996; abstract submission in Appendix B). In collaboration with David Parham from the Department of Pathology at the University of Arkansas and Cheryl Coffin from the Department of Pathology at the University of Utah, we have characterized 5 MPNST specimens by antibody studies, and we have extracted DNA from microdissected paraffin-embedded samples for *NF1* mutation screening. Genotype analysis is also being performed to identify allelic imbalance at other loci. We have demonstrated allelic imbalance in all 5 tumors using UT290, a chromosome 17 marker located just centromeric of the *NF1* locus. Three of the tumors (T3, T4, and T5) demonstrate loss of heterozygosity when compared to the constitutional DNA from the respective individuals. The other two tumors, T1 and T2, demonstrate homozygosity at locus UT290, however we have not ascertained the genotype from normal tissue to confirm this finding as allelic imbalance. After screening 90% of the *NF1* exons by size-shift analysis, we have identified one sequence variant from exon 3 in T2. This sequence change predicts inactivation of the *NF1* allele. This study is not completed, nevertheless it appears that there is loss of heterozygosity near the *NF1* locus in MPNSTs derived from non-NF1 individuals. We are attempting to complete the

screening in pursuit of the hypothesis that complete inactivation of the *NF1* locus is required for MPNST development. In addition to the analysis at the *NF1* locus we have expanded the genotype analysis to include additional loci, both on chromosome 17 and other chromosomal arms.

CONCLUSIONS

We have more fully characterized the *NF1* locus by isolating genomic clones that provide a complete contig of sequence spanning the coding region of the gene. These clones were essential for the complete elucidation of the *NF1* intron-exon boundaries. The identification of these boundaries enabled us to design a direct gene mutation screen that uses genomic DNA template derived from various sources, including archival material. We have synthesized *NF1*-specific oligonucleotides as primer sets for use in the PCR to obtain products for mutation analysis and radioactive probes. This work provided us with an opportunity to screen for somatic mutations in NF1-associated tumors. Even though others have raised the possibility that both *NF1* alleles are inactivated in neurofibromas, we were the first to prove this hypothesis by identifying *NF1* mutations in both alleles of a dermal neurofibroma, the constitutional mutation was a large deletion and the somatic mutation was a 4-basepair deletion in exon 4b. The significance of this finding lies in the rational design of therapeutic modalities in the targeting of either *NF1* expression or downstream signaling, ie through Ras signaling. The presence of two "inactivating" *NF1*

mutations in a benign neurofibroma suggests that therapy might be best directed toward the attenuation of Ras signaling. However, we now have the tools to address the issue of timing of somatic mutations, embryological versus post-natal. Clarifying the timing of the inactivating event may provide insight as to the pathogenesis of the myriad medical complications associated with this condition.

This finding brings out another important concept which should be fully evaluated. If both *NF1* alleles are "inactivated" within a neurofibroma, yet it remains benign, then there must be other genetic changes that lead to the overgrowth of NF1-affected tissue in the progression to malignancy. The identification of these loci may be extremely important in the characterization of modifying loci in this clinically variable condition.

In addition to providing the reagents for intensive *NF1* mutation analysis, we have explored a number of issues related to the molecular biology of NF1. We were able to demonstrate that *NF1*-homologous loci are distributed throughout the human genome, yet their significance or impact on NF1 is not understood. We developed a PCR-based assay system to easily genotype the *NF1* locus, both at the DNA and the RNA levels. We applied these assays to examine disequilibrium in three different populations; Caucasian, Japanese, and African. Application of the PCR genotype analysis will also apply to allelic gene-expression studies and rapid screening of those NF1 individuals who may harbor whole gene deletions. We developed probes to demonstrate the feasibility of fluorescence *in situ* hybridization at the *NF1* locus and we have identified

individuals who have large *NF1* deletions. This will be important both in the identification and mapping of deletion breakpoints, and screening for contiguous genes.

Finally, we have subcloned and sequenced a substantial segment of the promoter region of the *NF1* gene. The deletion constructs that have been synthesized should prove useful in the functional analysis of potential *cis*-regulatory elements of *NF1* transcription.

REFERENCES

1. Cawthon, R.M., Weiss, R., Xu, G., Viskochil, D., Culver, M. et al. (1990). A major segment of the neurofibromatosis type 1 gene: cDNA sequence, genomic structure, and point mutations. *Cell* 62: 193-201.

2. Viskochil, D. H., Buchberg, A. M., Xu, G., Cawthon, R. M., Stevens, J. et al. (1990). Deletions and a translocation interrupt a cloned gene at the neurofibromatosis type 1 locus. *Cell* 62:187-92.

3. Wallace, M. R., Marchuk, D. A., Anderson, L. B., Letcher, R., Odeh, H. M. et al. (1990). Type 1 neurofibromatosis gene: Identification of a large transcript disrupted in three patients. *Science* 249:182-86.

4. Li, Y., O'Connell P., Huntsman Breidenbach H., Cawthon R., Stevens J., Xu G., Neil S., Robertson M., White R., and Viskochil, D. (1995). Genomic organization of the neurofibromatosis 1 gene (*NF1*). *Genomics* 25: 9-18.

5. Marchuk, D. A., Saulino, A. M., Tavakkol, R., Swaroop, M., Wallace, M. R. et al. (1991). cDNA Cloning of the type 1 neurofibromatosis gene: complete sequence of the *NF1* gene product. *Genomics* 11:931-40.

6. Ballester, R., Marchuk, D., Boguski, M., Saulino, A, Letcher, R.et al. (1990). The *NF1* locus encodes a protein functionally related to mammalian GAP and yeast *IRA* proteins. *Cell* 63:851-59.

7. Martin, G., Viskochil, D., Bollag, G., McCabe, P. C., Crosier, W. J. et al. (1990). The GAP-related domain of the NF1 gene product interacts with ras p21. *Cell* 63:843-49.

8. Xu, G., Lin, B., Tanaka, K., Dunn, D., Wood, D. et al. (1990). The catalytic domain of the NF1 gene product stimulates ras GTPase and complements IRA mutants of *S. Cerevisiae*. *Cell* 63:835-41.

9. Golubic, M., Tanaka, K., Dobrowolski, S., Wood, D., Tsai, M. et al. (1991). The GTPase stimulatory activities of the neurofibromatosis type 1 and the yeast IRA2 proteins are inhibited by arachidonic acid. *EMBO J* 10:2897-2903.

10. Buchberg, A., Cleveland L., Jenkins N., and Copeland N. (1990). Sequence homology shared by neurofibromatosis type-1 gene and RA-1 and IRA-2 negative regulators of the RAS cyclic AMP pathway. *Nature* 347: 291-294.

11. Xu, G., O'Connell, P., Viskochil, D., Cawthon, R., Robertson, M. et al. (1990). The neurofibromatosis type 1 gene encodes a protein related to GAP. *Cell* 62:599-608.

12. Shannon, K.M., O'Connell P., Martin G., Paderanga D., Olson K., Dinndorf P., and McCormick F. (1994). Loss of the normal *NF1* allele from the bone marrow of children with type 1 neurofibromatosis and malignant myeloid disorders. *NEJM* 330: 597-601.

13. Skuse, G.R., Kosciolek B., and Rowley P. (1990) Loss of heterozygosity in malignancies in von Recklinghausen neurofibromatosis: The allele remaining in the tumor is derived from the affected parent. *Am J Hum Genet* 49:600-607.

14. Basu, T., Gutmann, D., Fletcher J., et al. (1992). Aberrant regulation of ras proteins in malignant tumour cells from type 1 neurofibromatosis patients. *Nature* 356:713-715.

15. DeClue, J.E., Papageorge, A., Fletcher, J., et al. (1992). Abnormal regulation of mammalian p21 contributes to malignant tumor growth in von Recklinghausen (type 1) neurofibro-matosis. *Cell* 69:265-273.

16. Legius, E., Marchuk, D., Collins, F., and Glover, T. (1993). Somatic Deletion of the neurofibromatosis type 1 gene in a neurofibrosarcoma supports a tumour suppressor gene hypothesis. *Nature Genetics* 3:122-126.

17. Ponder, B.A.J., Xu, W., Ponder, M.A., et al. (1990) Allele loss in tumors from patients with neurofibromatosis type 1 (NF-1). *Am J Hum Genet* 47:A14.

18. Skuse, G.R, Kosciolek, B.A, Rowley, P.T. (1989). Molecular genetic analysis of tumors in von Recklinghausen neurofibromatosis: Loss of heterozygosity for chromosome 17. *Genes Chrom Cancer* 1: 36-41.

19. Menon, A.G., Anderson, K.M., Riccard, V.M., et al. (1990). Chromosome 17p deletions and p53 gene mutations associated with the formatin of malignant neurofibromsarcomas in von Recklinghausen neurofibromatosis. *Pro Natl Acad Sci USA* 87: 5435-5439.

20. Shimizu, E., et al. (1993). Loss of Heterozygosity on Chromosome Arm 17p in Small Cell Lung Carcinomas but not in Neurofibromas, in a Patient with von Recklinghausen Neurofibromatosis. *Cancer* 71: 725-728.

21. Lothe, R., et al (1995). Alterations at chromosome 17 loci in peripheral nerve sheath tumors. J of *Neuropaht and Neurol* 54: 65-73.

22. Stark, M., Assum, G., and Krone, W. (1995). Single-Cell PCR Performed with Neurofibroma Schwann Cells Reveals the Presence of Both Alleles of the Neurofibromatosis Type 1 (NF1) Gene. *Human Genetics* 96: 619-623.

23. Glover, T.W., et al. (1995). Molecular and cytogenetic analysis of tumors in von Recklinghausen neurofibromatosis. *Genes Chromosomes and Cancer* 3: 62-70.

24. Colman, S.D., Williams C.A., and Wallace, M.R. (1995). Benign Neurofibromas in Type 1 Neurofibromatosis (NF1) Show Somatic Deletions of the *NF1* Gene. *Nature Genetics* 11: 90-92.

25. Gutmann, D. H., Geist, R.T., Wright, D.E., Snider, W.D. (1995). Expression of the neurofibromatosis1 (NF1) isoforms in developing and adult rat tissues. *Cell Growth Differ* 6 (3): 315-323.

26. Huynh, D.P., Nechiporuk T., and Pulst S. (1994). Differential expression and tissue distribution of type I and type II neurofibromins during mouse fetal development. *Developmental Biology* 161: 538-551.

27. Daston, M.M. and Ratner, N. (1992). Neurofibromin, a predominantly neuronal GTPase activating protein in the adult, is ubiquitously expressed during development. *Developmental Dynamics* 195: 216-226.

28. Brannan, C.I., Perkins A., Vogel, K., Ratner N., Nordlund, M., Reid S., Buchberg A., Jenkins N., Parada L., and Copeland N. (1994). Targeted disruption of the neurofibromatosis type-1 gene leads to developmental abnormalities in heart and various neural crest-derived tissues. *Genes & Development* 8: 1019-1029.

29. Jacks, T., Shih T., Schmitt E., Bronson R., Bernards A., and Weinberg R. (1994). Tumor predisposition in mice heterozygous for a targeted mutation in Nf1. *Nature Genetics* 7: 353-361.

30. Kim, H.A., Rosenbaum, T., Marchioni, M.A., Ratner, N., DeClue, Jeff E.(1995). Schwann cells from defficient mice exhibit activation of p21 ras, inhibition of cell proliferation and morphological changes. *Oncogene* 11: 325-335.

31. Vogel, K.S., Brannan, C.I., Jenkins, N.A., Copeland, N.G., and Parada, L.F. (1995). Loss of Neurofibromin Results in Neurotrophin-Independent Survival of Embryonic Sensory and Sympathetic Neurons. *Cell* 82: 733-742.

32. Bollag, G., *et al* (1995). Loss of NF1 results in activation of the ras signalling pathway and leads to aberrant growth in haematopoietic cells. *Nature Genet.* 12, 144-148.

33. Largespada, D., Brannan, C., Jenkins, N., and Copeland, N. (1996). *NF1* deficiency causes Ras-mediated granulocyte/macrophage colony stimulating factor hypersensitivity and chronic myeloid leukemia. *Nature Genet.* 12, 137-143.

34. Hajra, A., Martin-Gallardo A., Tarle S., Freedman M., Wilson-Gunn S., Bernards A., and Collins F. (1994). DNA sequences in the promoter region of the *NF1* gene are highly conserved between human and mouse. *Genomics* 21: 649-652.

35. Rodenhiser, D.I., Coulter-Mackie M., and Singh S. (1993). Evidence of DNA methylation in the neurofibromatosis type 1 (NF1) gene region of 17q11.2. *Human Molecular Genetics* 2: 439-444.

36. Pierce, J. and Sternberg, N. (1992). Using bacteriophage P1 system to clone high molecular weight genomic DNA. *Methods Enzymol* 216: 549-574.

37. Marchuk, D.A., Tavakkol, R., Wallace, M., Brownstein, B., Taillon-Miller, P., Fong, C-T, Leguis, E., Anderson, L., Glover, T., and Collins, F. (1995). A yeast artificial chromosome contig encompassing the type 1 neurofibromatosis. *Genomics* 13: 672-680.

38. Weiss, R., Dunn, D., DiSera, L. Wheatley, W., Kimball, A., Rote, C., Cherry, J., Duval, B., Lee, R., Ferguson, M., and Gesteland, R. (1992). The human neurofibromatosis type 1 locus: Genomic sequence of the 3" region, 1-100849. GenBank Accession No. L05367.

39. Legius, E., Marchuk D., Hall B., Anderson L., Wallace M., Collins F., and Glover, T. (1992). NF-1 related locus on chromosome 15. *Genomics* 13: 1316-1318.

40. Gasparini, P., Grifa A., Origone P., Coviello D., Antonacci R., and Rocchi M. (1993). Detection of a neurofibromatosis type 1 (NF-1) sequence by PCR: Implications for the diagnosis and screening of genetic diseases. *Mol Cell Probes* 7: 415-418.

41. Cummings, L., Glatfelter A., and Marchuk D. (1993). *NF1*-related loci on chromosomes 2,12, 14, 15, 20, 21, and 22: A potential role for gene conversion in the high spontaneous mutation rate in NF1? *Am J Hum Genet* 53: 672A.

42. Hulsebos, T.J.M. Localization of *NF1*-related sequences on chromosome 22 (1995). *Am J Hum Gen* 57: Abstract 353 .

43. Purandare, S., Breidenbach, H.H., Li, Y., Zhu, X.L., Sawada, S., Neil, S.M., Brothman, A., White, R., Cawthon, R., and Viskochil, D.H. (1995). Identification of Neurofibromatosis 1 (NF1) Homologous Loci by Direct Sequencing, Flourescence in *Situ* Hybridization, and PCR Amplification of Somatic Cell Hybrids. *Genomics* 30: 476-485.

44. Rust, S., Funke H., and Assman G. (1993). Mutagenically separated PCR(MS-PCR): A highly specific one-step procedure for easy mutation detection. *Nucleic Acids Research* 21: 3623-3629.

45. Purandare, S.M., Cawthon, R., Nelson, L.M., Sawada, S., Watkins, W.S., Ward, K., Jorde,L.B., and Viskochil, D.H. (1996). Genotyping of PCR-Based Polymorphisms and Linkage-Disequilibrium Analysis at the NF1 Locus. *Am J Hum Genet* 59:159-166.

46. Sawada, S. and Viskochil, D. (1995). Detection of a Germline Mutation at the Neurofibromatosis 1 Locus. *Jpn J Dermatol* 105: 1187-1196.

47. Kayes, L., Riccardi, V., Burke, W., Bennet, R., and Stephens, K. (1992). Large de novo DNA deletion in a patient with sporadic neurofibromatosis 1, mental retardation and dysmorphism. *J Med Genet* 29: 686-690.

48. Wu, B.L., Austin, M.A., Schneider, G.H., Boles, R.G., Korf, B.R. (1996). Deletion of the entire NF1 gene detected by FISH: four deletion patients associatedwithsevere manifestations. *Am J Med Genet* 59:528-535.

49. Leppig, K., Viskochil D., Neil S., Rubenstein A., Johnson V., Zhu XL., Brothman A., and Stephens K. (1995). The detection of contiguous gene deletions at the neurofibromatosis locus with fluorescence in situ hybridization. *Cytogenet Cell Genet* 72:95-98.

50. Sawada, S., Florell, S., Purandare, S., Ota, M., Stephens, K., and Viskochil, D. (1996). Identification of NF1 mutations in both alleles of a dermal neurofibroma. *Nat Genet* (14) 110-112.

51. Viskochil D and Carey J. (1992). Nosological Considerations of the neurofibromatoses. *J Dermatol* 19(11):873-880.

APPENDIX A

1. Sawada S., Florell S., Purandare S., Ota M., Stephens K., and Viskochil D. (1996). Identification of *NF1* Mutations in both Alleles of a Dermal Neurofibroma. *Nature Genetics* **14**:110-112.

2. Purandare S., Cawthon R., Nelson L., Sawada S., Watkins W., Ward K., Jorde L., and Viskochil D. (1996). Genotyping of PCR-Based Polymorphisms and Linkage-Disequilibrium Analysis at the *NF1* Locus. *American Journal of Human Genetics* **59**:159-166.

3. Leppig K., Viskochil D., Neil S., Rubenstein A., Johnson V., Zhu X., Brothman A., and Stephens K. (1996). The Detection of Contiguous Gene Deletions at the Neurofibromatosis 1 Locus with Fluorescence in situ Hybridization. *Cytogenetics and Cell Genetics* **72**:95-98.

4. Purandare S., Breidenbach H., Li Y., Zhu X., Sawada S., Neil S., Brothman A., White R., Cawthon R., and Viskochil D. (1995). Identification of Neurofibromatosis 1 (*NF1*) Homologous Loci by Direct Sequencing, Fluorescence *in situ* Hybridization, and PCR Amplification of Somatic Cell Hybrids. *Genomics* **30**:476-485.

5. Sawada S. and Viskochil D. (1995). Detection of a Germline Mutation at the Neurofibromatosis 1 Locus. *Japan Journal of Dermatology* **105**:1187-1196.

6. Li Y., O'Connell P., Breidenbach H., Cawthon R., Stevens J., Xu G., Neil S., Robertson M., White R., and Viskochil D. (1995). Genomic Organization of the Neurofibromatosis 1 Gene (*NF1*). *Genomics* **25**:9-18.

Identification of *NF1* mutations in both alleles of a dermal neurofibroma

Shun'ichi Sawada[1,4], Scott Florell[2], Smita M. Purandare[4,5], Mayumi Ota[1,4], Karen Stephens[3] & David Viskochil[4]

A hallmark clinical feature of neurofibromatosis 1 (NF1) is multiple dermal neurofibromas, benign tumours that typically appear in early adolescence and increase in numbers throughout life. The pathogenesis of these tumours is not known. One domain of the *NF1* gene product, neurofibromin, stimulates the intrinsic GTPase of Ras[1–3], and inactivation of both *NF1* alleles has been demonstrated in specific malignancies[4–15]. These observations support the contention that the *NF1* gene product is a tumour suppressor that is involved in the Ras signal transduction pathway. Even though accumulating evidence demonstrates that *NF1* acts as a tumour suppressor in some cells, mutations have not been identified in both *NF1* alleles in dermal neurofibromas. Using standard techniques to analyse DNA extracted from benign neurofibromas, numerous investigators failed to identify loss of heterozygosity (LOH) in multiple tumours[6–8,14–16]. In contrast to these reports, Colman *et al.*[17] demonstrated *NF1* LOH of dermal neurofibromas derived from 2 of 5 NF1 patients, yet the constitutional *NF1* mutations in these patients were not identified, and the extent of the somatic deletions beyond the *NF1* locus were not established. In this study, we show that a dermal neurofibroma from an NF1 individual who has a constitutional deletion of the entire *NF1* locus harbours a 4-bp deletion of *NF1* exon 4b in the other allele. This is the first definitive identification of a somatic mutation which is limited to the *NF1* locus in a benign neurofibroma from an NF1 individual in whom the constitutional *NF1* mutation is known.

Patient UWA128-3, was previously shown to have a large submicroscopic deletion of the *NF1* locus by both somatic cell hybrid analysis[18] and fluorescence *in situ* hybridization of lymphoblastoid cells[19]. The deletion extends at least 145 kb centromeric and 135 kb telomeric to *NF1*[18,20]. As part of her medical care, she electively had a scalp neurofibroma surgically removed, and a portion of this spheroid, 2.5 cm tumour was subdivided and frozen for subsequent *NF1* mutation analysis (Fig. 1). We have developed a direct-gene mutation screen using flanking intron-based primers to PCR-amplify *NF1* exons[21] followed by detection of abnormally migrating products in polyacrylamide gel electrophoresis. DNA extracted from two adjacent halves of the top tumour section and patient DNA extracted from lymphoblastoid cells was evaluated using this protocol. The PCR product representing *NF1* exon 4b[22] from the frozen tumour DNA demonstrated a size-shift by denaturing gel electrophoresis as compared with the constitutional DNA (Fig. 2*a*). This pattern suggested the presence of a small deletion in exon 4b. No other mutations were detected from other exon-specific PCR products.

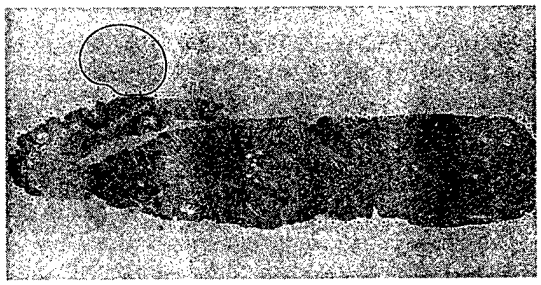

Fig. 1 Scalp neurofibroma from an NF1 individual who is constitutionally hemizygous for the *NF1* locus. An S-100 protein immunohistochemistry stain of a section from the top third of the tumour showing typical features of a neurofibroma; spindle cells with wavy, dark-stained nuclei, low mitotic index, and lack of necrosis. The infiltrative nature of this tumour is evidenced by its invasion of skin appendages, including a hair follicle and eccrine sweat ducts. The fracture plane on the left portion of the section was used for microdissection. As marked, normal tissue was harvested from left of the fracture plane and tumour tissue was scraped from the right. Magnification ×20.

The initial exon 4b PCR product from tumour DNA was sequenced using a fluorescence dye-primer sequencing protocol (Applied Biosystems), and it suggested divergence between two alleles. We were not able to obtain

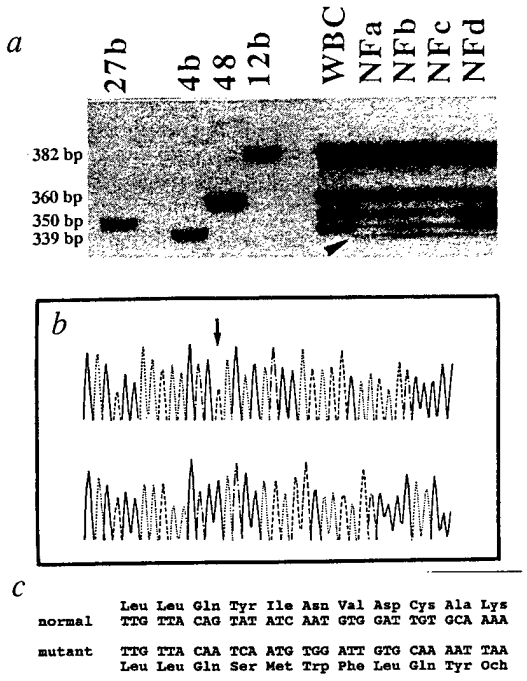

Fig. 2 *NF1* mutation analysis. *a*, Four ^{33}P end-labelled PCR products representing exons 27b, 4b, 48, and 12b from DNA template from the NF1 patient's lymphoblasts (WBC) and duplicate samples (NFa, NFb, NFc, and NFd) of two adjacent neurofibroma sections were electrophoresed on a 6% polyacrylamide denaturing gel. The arrow depicts an aberrantly migrating band which presumably is derived from exon 4b. The left hand side of the autoradiograph shows individual PCR products synthesized from cloned genomic DNA template. *b*, Segments of DNA sequences from two independent clones harbouring *NF1* exon 4b PCR products amplified from DNA template extracted from the neurofibroma shown in Fig. 1. The upper sequence represents normal *NF1* cDNA from bases 532–570. The base identified by the arrow is cDNA base 546, and it represents the site of a 4-bp deletion shown in the lower sequence. solid line-adenine, dotted line-thymine, dashed line-guanine, dot/dash line-cytosine. *c*, DNA and deduced amino acid sequences from two independent clones containing PCR products represented in panel *b*. Normal is the wild-type *NF1* allele, and mutant is the *NF1* allele that harbours a 4-bp deletion of cDNA bases 546–549 in *NF1* exon 4b. This frame-shift results in an ochre triplet, 9 codons downstream.

[1]*Department of Dermatology, Jikei University School of Medicine, 19-18, Nishishinbashi 3-chrome, Minato-ku, Tokyo 105, Japan*
[2]*Department of Pathology, University of Utah, Salt Lake City, Utah 84112, USA*
[3]*Division of Medical Genetics, PO Box 357720, Department of Medicine, University of Washington, Seattle, Washington 98195, USA*
[4]*413 MREB, Division of Medical Genetics, Department of Pediatrics, University of Utah, Salt Lake City, Utah 84112, USA*
[5]*Present address: Department of Neurology, Baylor College of Medicine, Houston, Texas 77030, USA*

Correspondence should be addressed to D.V.

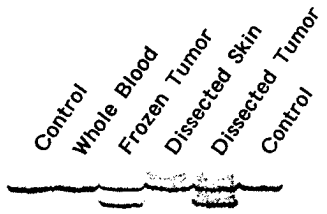

Fig. 3 End-labelled PCR products representing *NF1* exon 4b amplified from various DNA templates which were then electrophoresed on a 6% polyacrylamide gel under denaturing conditions and exposed for autoradiography. The control is DNA extracted from blood from an unrelated individual. Whole blood represents DNA extracted from patient UWA128-3 who has a large constitutional *NF1* deletion. Frozen tumour represents DNA extracted from a section of the whole neurofibroma. Dissected skin represents DNA extracted from normal tissue in the neurofibroma, as marked to the left of the fracture plane in Fig.1. Dissected tumour represents DNA extracted from the tissue that represents homogeneous-appearing tumour as marked to the right of the fraction plane in Fig. 1.

unambiguous sequence from direct sequencing, therefore the PCR product for exon 4b from the tumour DNA was cloned into the pMOS *Blue* T-vector (Amersham Life Sciences) using the TA-cloning strategy for subsequent sequencing. We sequenced six clones; two were wild-type sequence and four showed a 4-bp deletion of bases 543–546 in the *NF1* cDNA sequence[23] (Fig. 2*b*). This frame-shift mutation leads to the insertion of an ochre codon 9 amino acids downstream of the deletion site (Fig. 2*c*). Thus, DNA extracted from this dermal neurofibroma has a large *NF1* deletion in one allele and a 4-bp deletion in exon 4b in the second allele.

This is the first definitive identification of a somatic mutation which is limited to the *NF1* locus in a benign neurofibroma from an NF1 individual in whom the constitutional *NF1* mutation is known. The 4-bp deletion in exon 4b would lead to a premature truncation product which predicts a neurofibromin peptide that would not contain the GAP-related domain. Given the unknown function of the N terminus of neurofibromin, and the lack of evidence demonstrating a dominant-negative model for mutant neurofibromin in the NF1 phenotype, we contend that this somatic mutation is inactivating in nature and results in complete loss of intra-cellular neurofibromin activity. This observation is significant because, unlike haematopoietic stem cells[4,24,25], the absence of intracellular neurofibromin in target cells of the peripheral nervous system, in and of itself, does not result in malignancy. This study does not, however, rule out the possibility that somatic mutations at other loci contribute to neurofibroma development. Thus, while these results are consistent with a model whereby a second hit in *NF1* initiates neoplasia, the somatic *NF1* mutation may simply be one of many mutation events.

The identification of two inactivating mutations in a benign dermal neurofibroma indicates that additional genetic changes are important in the development of malignant peripheral nerve sheath tumours (MPNSTs). These soft-tissue malignancies have intra-tumour heterogeneity as demonstrated by anaplastic foci embedded within a background of more benign-appearing neurofibroma tissue. This study suggests that the background neurofibroma tissue could harbour two inactivating *NF1* mutations, and additional genetic alterations involving multiple foci within a MPNST could cause the malignant transformation observed in a number of larger, deep neurofibromas. The identification of other genetic loci that may be important in the development of NF1-associated malignancies could define biochemical pathways important in tumour progression within susceptible tumours. For example, as a logical extension of the reports of granulocyte/macrophage colony stimulating factor (GM-CSF) hypersensitivity in neurofibromin-deficient murine hematopoietic stem cells[24,25], depletion of neurofibromin in certain cells within peripheral nerves may render them more growth-responsive to humoral factors, especially those factors that are expressed during puberty and pregnancy. If so, treatment strategies directed toward other linked biochemical pathways may be warranted.

The clonal nature of neurofibromas has been a source of controversy for many years[26,27]. Even though quite homogeneous by histological appearance, these tumours are not unicellular by immunohistochemical evaluations[28]. We screened DNA from separate sections of the tumour to evaluate the distribution of target cells harbouring the somatic *NF1* mutation. We dissected a tumour (Fig. 1) along the markings which are separated by the cleavage plane in the left side of the section; normal-appearing tissue left of the cleavage plane was separated from the tumour depicted on the right side of the section. This separation was performed directly on the slide of a 4-micron section. DNA was extracted and amplified by the PCR using an end-labelled, intron-based primer upstream of exon 4b with a non-radioactive reverse primer lying downstream of exon 4b. The abnormally migrating allele was not present in adjacent epidermis, whereas it was present in the microdissected tumour tissue (Fig. 3). Our PCR assays were not quantitative, therefore the ratios of abnormal to normal alleles in the PCR (Fig. 3) may not represent actual ratios of cells harbouring the second hit in this neurofibroma. Nevertheless, the presence of both a normal and a 4-bp deletion allele in a homogeneous-appearing section of tumour suggests that an uncharacterized cell population that harbours a somatic *NF1* mutation has expanded and infiltrated the normal-appearing tissue.

More precise knowledge of the timing of somatic *NF1* mutations in neurofibroma progenitor cells would be important in the development of treatment strategies. If somatic mutations of the wild-type *NF1* allele were to occur pre-natally, then systemic treatment to increase expression of that allele would not be expected to be effective in preventing neurofibromas, whereas, other treatment strategies focusing on the downstream pathways of neurofibromin (such as targeting of Ras signalling) would be more rational. The demonstration of a mosaic pattern of mutation distribution in this neurofibroma suggests that further evaluation of cells with the 4-bp deletion in this tumour and other scalp tissue from this individual, including dermal neurofibromas, could provide insight both to the timing in development of this somatic mutation event and the identification of neurofibroma progenitor cells.

In summary, this is the first demonstration of mutations in both *NF1* alleles in a neurofibroma, and it supports the hypothesis that a second hit in the normal allele is necessary although perhaps not sufficient for the development of neurofibromas in NF1. Based on this singular case, one cannot generalize that all neurofibromas result from inactivating somatic *NF1* mutations, however it suggests that any somatic events leading to diminished neurofibromin activity could contribute to tumour formation.

Methods

Preparation of tissue. Freshly excised neurofibroma (approximately a 2.5-cm spheroid tumour) was dissected into three sections and frozen in liquid nitrogen within 1 h of excision. Frozen tissue was thawed on ice and carefully examined using a stereozoom dissecting microscope to enable sectioning perpendicular to the skin surface. One quarter was fixed in 10% buffered formalin and submitted for standard paraffin embedding for subsequent microdissection and immunohistochemical staining on sequential sections.

DNA isolation. Genomic DNA was extracted from the remaining half of the tumour using the animal tissue protocol from a Puregene™ DNA Isolation Kit (Gentra Systems). This involved homogenization of the tumour tissue with a mortar and pestle, SDS cell lysis, Proteinase K digestion and isopropanol precipitation. The DNA was diluted to 100 ng/μl in distilled water for use as template in the polymerase chain reaction assays.

Microdissection of formalin-fixed, paraffin-embedded tissue. Five consecutive 4-micron sections were cut from the formalin-fixed, paraffin-embedded tissue block and applied to glass microscope slides, one section per slide. The first section was stained with standard haematoxylin and eosin (H&E); the next two sections were deparaffinized and stained with aniline blue but were not coverslipped, and the last two sections were stained for S-100 and vimentin proteins by standard immunohistochemical techniques. Tissue microdissection was performed as described[29].

Immunohistochemical staining for S-100 and vimentin. Mounted sections were deparaffinized in xylene and absolute ethanol. The tissues were then rehydrated by successive dips in 95% ethanol, 70% ethanol, and distilled water. Immunoperoxidase staining was performed on the Ventana ES instrument (Ventana Medical Systems, Tucson, AZ) using the avidin-biotin-peroxidase complex in accord with manufacturers instructions. Primary antibody to S-100 (polyclonal rabbit anti-cow; Dako Corp., Carpinteria, CA) and vimentin (monoclonal mouse anti-pig) proteins were used at dilutions of 1:700 and 1:200, respectively. The immunostaining was developed using diaminobenzidine (DAB) as the chromogen, then counterstained with Mayer's haematoxylin.

PCR protocol and primer preparation. PCR was carried out using either 100 ng of DNA isolated from the fresh tumour or 1 μl of Proteinase K digest from either normal or tumour from formalin-fixed, paraffin-embedded microdissected tissue as DNA template. Initial PCR amplification for *NF1* mutation screening was carried out using primers[22] and techniques[21] described. First-round PCR synthesis was performed routinely using *NF1* exon-specific primers tagged with universal 18-bp sequences at the 5'-end. The PCR products are subjected to centricon filtration (Amicon), and an aliquot of retentate is used as template for a second round of PCR using end-labelled UP primer with non-radioactive RP primers to generate radioactive PCR products which were electrophoresed in both denaturing polyacrylamide and MDE (AT Biochem) gels. Abnormally migrating products were further evaluated for *NF1* mutations. Subsequent analysis of exon 4b was performed using the following protocol; primers I4B (5'–GTGAGAT-ACCACACCTGTCCC–3') and rI4B (5'–TTCATGATACTAGTT-TTTGACCC–3') were used in a final PCR volume of 25 μl which contained 2.5 pmol I4b, 1.4 pmol ^{33}P end-labelled rI4B, 1.1 pmol rI4B, 20 mM Tris-HCl pH 8.4, 50 mM KCl, 140 mM deoxynucleotides, 2.5 mM $MgCl^2$, 0.5 U *Taq* polymerase (Life Technologies) and 0.2 mM spermidine. The reaction was heated to 94 °C for 5 min prior to cycling at 94 °C for 30 s, annealing at 56 °C for 30 s, and extension at 72 °C for 30 s for 30 cycles. DNA template from microdissected formalin-fixed tissue required an additional 10 cycles. Primers were end-labelled using γ^{33}P-ATP (2000 Ci/mmol, DuPont) and *T4 polynucleotide kinase* (Promega) and standard labelling conditions[30]. PCR products from DNA extracted from formalin-fixed, paraffin-embedded tissue were diluted 1:2 with formamide containing dye solution, and PCR products from DNA extracted from fresh tissue were diluted 1:5 with distilled water prior to 1:2 dilution with formamide-dye solution. Aliquots were electrophoresed in 6% polyacrylamide, 8.3 M Urea, TBE (90 mM Tris-Borate pH7.5, 2 mM EDTA) gels at 80 W for 5 h at room temperature. The gel was dried on filter paper under vacuum and exposed to X-OMAT film at room temperature for 24–72 h.

Acknowledgements

We thank the individual with NF1 who participated in these studies; S. Neil for technical assistance; E. Meehan (HHMI, U. of Utah) for the synthesis of oligonucleotides; M. Robertson for DNA sequencing support (Huntsman Cancer Center Core Sequencing Facility); S. Perkins for immunohistochemistry studies (Department of Pathology, U. of Utah); and R. Cawthon, W. Samowitz and S. Bidichandani for helpful discussions. This work was supported by grants from the American Cancer Society EDT17A (K.S.) and the Department of the Army, DAMD 17-93-J-3070 (D.V.).

Received 29 February; accepted 1 July 1996.

1. Ballester, R. *et al.* The NF1 locus encodes a protein functionally related to mammalian GAP and yeast IRA proteins. *Cell* **63**, 851–859 (1990).
2. Martin, G.A. *et al.* The GAP-related domain of the NF1 gene product interacts with ras p21. *Cell* **63**, 843–849 (1990).
3. Xu, G. *et al.* The catalytic domain of the NF1 gene product stimulates ras GTPase and complements IRA mutants of *S. Cerevisiae*. *Cell* **63**, 835–841 (1990).
4. Shannon, K. *et al.* Loss of the normal *NF1* allele from the bone marrow of children with type 1 neurofibromatosis and malignant myeloid disorders. *New Engl. J. Med.* **330**, 597–601 (1994).
5. Xu, W. *et al.* Loss of *NF1* alleles in pheochromocytomas from patients with type 1 neurofibromatosis. *Genes Chromosom. & Cancer* **4**, 337–342 (1992).
6. Menon, A.G. *et al.* Chromosome 17p deletions and p53 gene mutations associated with the formation of malignant neurofibrosarcomas in von Recklinghausen neurofibromatosis. *Proc. Natl. Acad. Sci U.S.A.* **87**, 5435–5439 (1990).
7. Skuse, G.R., Kosciolek, B.A. & Rowley, P.T. Loss of heterozygosity in malignancies in von Recklinghausen neurofibromatosis: The allele remaining in the tumor is derived from the affected parent. *Am. J. Hum. Genet.* **49**, 600–607 (1990).
8. Glover, T.W. *et al.* Molecular and cytogenetic analysis of tumors in von Recklinghausen neurofibromatosis. *Genes Chrom. Cancer* **3**, 62–70 (1991).
9. Basu, T. *et al.* Aberrant regulation of RAS proteins in malignant tumour cells from type 1 neurofibromatosis patients. *Nature* **356**, 713–715 (1992).
10. DeClue, J.E. *et al.* Abnormal regulation of mammalian p21 contributes to malignant tumor growth in von Recklinghausen (type 1) neurofibromatosis. *Cell* **69**, 265–273 (1992).
11. Legius, E., Marchuk, D., Collins, F. & Glover, T. Somatic deletion of the neurofibromatosis type 1 gene in a neurofibrosarcoma supports a tumour suppressor gene hypothesis. *Nature Genet.* **3**, 122–126 (1993).
12. Reynolds, J. *et al.* Molecular characterization of a 17q11.2 translocation in a malignant schwannoma cell line. *Hum. Genet.* **90**, 450–456 (1992).
13. Anderson, L. *et al.* Mutations in the neurofibromatosis 1 gene in sporadic malignant melanoma cell lines. *Nature Genet.* **3**, 118–121 (1993).
14. Skuse, G.R., Kosciolek, B.A. & Rowley, P.T. Molecular genetic analysis of tumors in von Recklinghausen neurofibromatosis: Loss of heterozygosity for chromosome 17. *Genes Chrom. Cancer* **1**, 36–41 (1989).
15. Shimizu, E. *et al.* Loss of heterozygosity on chromosome arm 17p in small cell lung carcinomas but not in neurofibromas, in a patient with von Recklinghausen neurofibromatosis. *Cancer* **71**, 725–728 (1993).
16. Lothe, R. *et al.* Alterations at chromosome 17 loci in peripheral nerve sheath tumors. *J. Neuropath. Exp. Neurol.* **54**, 65–73 (1995).
17. Colman, S.D., Williams, C.A. & Wallace, M.R. Benign neurofibromas in type 1 neurofibromatosis (NF1) show somatic deletions of the *NF1* gene. *Nature Genet.* **11**, 90–92 (1995).
18. Kayes, L. *et al.* Deletions spanning the neurofibromatosis 1 gene: Identification and phenotype of five patients. *Am. J. Hum. Genet.* **54**, 424–436 (1994).
19. Leppig, K. *et al.* The detection of contiguous gene deletions at the neurofibromatosis 1 locus with fluorescence in situ hybridization. *Cytogenet. Cell Genet.* **72**, 95–98 (1996).
20. Marchuk, D. *et al.* A yeast artificial chromosome contig encompassing the type 1 neurofibromatosis gene. *Genomics* **13**, 672–680 (1992).
21. Sawada, S. & Viskochil, D. Detection of a germline mutation at the neurofibromatosis 1 locus. *Jap. J. Dermatol.* **105**, 1187–1196 (1995).
22. Li, Y. *et al.* Genomic Organization of the neurofibromatosis 1 (NF1) locus. *Genomics* **25**, 9–18 (1995).
23. Marchuk, D.A. *et al.* cDNA cloning of the type 1 neurofibromatosis gene: complete sequence of the *NF1* gene product. *Genomics* **11**, 931–40 (1991).
24. Bollag, G. *et al.* Loss of *NF1* results in activation of the ras signalling pathway and leads to aberrant growth in haematopoietic cells. *Nature Genet.* **12**, 144–148, (1996)
25. Largaespada, D., Brannan, C., Jenkins, N. & Copeland, N. *Nf1* deficiency causes Ras-mediated granulocyte/macrophage colony stimulating factor hypersensitivity and chronic myeloid leukemia. *Nature Genet.* **12**, 137–143 (1996).
26. Fialkow, P.J., Sagebiel, R.W., Gartler, S.M. & Rimoin, D.I. Multiple cell origin of hereditary neurofibromas. *New Engl. J. Med.* **284**, 298–300 (1971).
27. Skuse, G., Kosciolek, B. & Rowley, P. The neurofibroma in von Recklinghausen neurofibromatosis has a unicellular origin. *Am. J. Hum. Genet.* **49**, 600–607 (1991).
28. Enzinger, F. & Weiss, S. Benign tumors of peripheral nerves. in *Soft Tissue Tumors*. (eds Gay, S. & Gery, L.) 821–885 (Mosby-Yearbook, St. Louis, 1988).
29. Samowitz, W., Slattery, M.L. & Kerber, R.A. Microsatellite instability in human colonic cancer is not a useful clinical indicator of familial colorectal cancer. *Gastroent.* **109**, 1765–1771 (1995).
30. Sambrook, J., Fritsch, E. & Maniatis, T. *Molecular Cloning: A Laboratory Manual*. 2nd edn. (Cold Spring Harbor Laboratory, Cold Spring Harbor, New York, 1989).

Am. J. Hum. Genet. 59:159–166, 1996

Genotyping of PCR-Based Polymorphisms and Linkage-Disequilibrium Analysis at the *NF1* Locus

S. M. Purandare,[1,*] R. Cawthon,[2] L. M. Nelson,[3] S. Sawada,[4] W. S. Watkins,[2] K. Ward,[2,3] L. B. Jorde,[2] and D. H. Viskochil[1]

Departments of [1]Pediatrics, [2]Human Genetics, and [3]Obstetrics and Gynecology, University of Utah, Salt Lake City; and [4]Jikei University, Tokyo

Summary

Six polymorphisms across the *NF1* gene have been adapted for genotyping through application of PCR-based assays. Three exon-based polymorphisms—at positions 702, 2034, and 10647 in the *NF1* cDNA—were genotyped by mutagenically separated PCR (MS-PCR). A fourth polymorphism, DV1.9, is an L1 insertion element in intron 30, and the other two polymorphisms, GXAlu and EVI-20, are short tandem repeats in intron 27b. All the polymorphisms were evaluated in a cohort of 110 CEPH individuals who previously had been analyzed by use of eight RFLPs at the *NF1* locus. Pairwise linkage-disequilibrium analyses with the six PCR-based polymorphisms and their flanking markers demonstrated disequilibrium between all tested loci. Genotypes of the four diallelic polymorphisms (702, 2034, 10647, and DV1.9) were also evaluated in cohorts from the CEPH, African, and Japanese populations. The CEPH and Japanese cohorts showed similar heterozygosities and linkage-disequilibrium coefficients. The African cohort showed a higher degree of heterozygosity and lower linkage-disequilibrium values, compared with the CEPH and Japanese cohorts.

Introduction

Neurofibromatosis type 1 (NF1) is an autosomal dominant condition affecting 1/3,500 individuals worldwide. It is a clinical diagnosis that requires the presence of two of seven diagnostic criteria (NIH Consensus Development Conference 1988). The age-dependent onset, high number of sporadic cases, and wide variability in clinical expression can make diagnosis difficult in specific cases. Direct *NF1* gene mutation analysis is available on a limited basis as an aid for clinical diagnosis. However, the various screening techniques are not yet comprehensive in detecting all *NF1* mutations. The size and complexity of the *NF1* gene partially account for the relatively low mutation-detection rate. The *NF1* primary transcript is ~335 kb in length, and the processed mRNA, comprising 57 core exons, is ~12 kb (Li et al. 1995). The presence of *NF1*-related loci (Purandare et al. 1995) further complicates DNA-based, direct-gene screening protocols. An alternative to direct-gene mutation analysis in NF1 families with multiple affected members is linkage analysis using several flanking and intragenic polymorphisms (Ward et al. 1990; Hofman and Boehm 1992; Lazaro et al. 1993*a*; Rodenheiser et al. 1993). The most widely used intragenic STS markers include GXAlu, a tetranucleotide repeat in intron 27b (Xu et al. 1992), and EVI-20, a CA repeat in intron 27b (Accession no. L05367). Other polymorphisms include a $(GATN)_n$ repeat in intron 26 (Andersen et al. 1993), an additional CA/GT-repeat polymorphism in intron 27b (Lazaro et al. 1993*b*), and a CA/GT-repeat polymorphism in intron 38 (Lazaro et al. 1994).

Development of PCR-based assays for analysis of polymorphisms would be beneficial for both direct-gene mutation analysis and linkage analysis. For example, the demonstration of absence of heterozygosity at multiple polymorphic loci in the *NF1* gene could identify individuals who harbor large *NF1* deletions. Likewise, this analysis could prove useful in somatic *NF1* mutation analysis for allelic loss in tumor tissue. Genotyping with exon-based polymorphisms across the *NF1* gene would also allow assessment of mRNA expression from both alleles in heterozygous individuals. This would be useful in the detection of cases with unequal mRNA levels of an *NF1* allele because of mutation, which would be especially important in avoiding false-negative results in screening methods that use *NF1* mRNA as the template (e.g., reverse-transcriptase PCR–based methods such as the protein-truncation test; Heim et al. 1995). In addition to its use in the testing of individuals, genotype analysis by PCR could be broadly applied in population studies.

Received December 19, 1995; accepted for publication April 1, 1996.

Address for correspondence and reprints: Dr. David H. Viskochil, Department of Pediatrics, 413, MREB, University of Utah, Salt Lake City, UT 84112.

*Present address: Department of Neurology, Baylor College of Medicine, Houston.

0002-9297/96/5901-0023$02.00

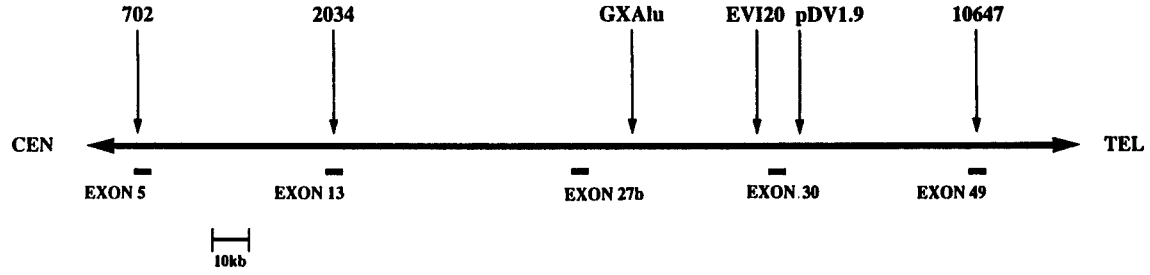

Figure 1 Sequence of polymorphisms across the *NF1* gene. The distance between 702 and 2034 is estimated at 50 kb, and that between 2034 and GXAlu is estimated at 75 kb, by Southern analysis. The distances between GXAlu/EVI20 (31 kb), EVI20/pDV1.9 (11 kb), and DV1.9/10647 have been approximated from the genomic sequence, GenBank Accession no. L05367.

We have developed a PCR-based assay for the analysis of six *NF1* polymorphisms, which span ~200 kb of genomic DNA (fig. 1). The three exon-based polymorphisms—at *NF1* cDNA positions 702, 2034, and 10647—have been evaluated by a mutagenically separated PCR (MS-PCR)–based approach. Additionally, two STS polymorphisms in intron 27b of the *NF1* gene, GXAlu (Xu et al. 1990) and EVI-20, were analyzed. An L1 insertion-element polymorphism, DV1.9, in intron 30 (Bleyl et al. 1994), was also evaluated by PCR methodology.

The six polymorphic loci were analyzed for linkage disequilibrium in a CEPH cohort that previously had been shown to be in high linkage disequilibrium for *NF1* RFLP markers (Jorde et al. 1993). The diallelic polymorphisms at *NF1* cDNA positions 702, 2034, 10647, and DV1.9 were also analyzed in two additional cohorts, an African population and an Japanese population. Allele frequencies, heterozygosity, and linkage-disequilibrium analyses were evaluated for each of these populations.

In discussing the results of this analysis, we address the following: the effect of linkage disequilibrium on the reliability of genetic diagnosis of NF1; the relationship between linkage disequilibrium and physical distance in the *NF1* region; the consistency of disequilibrium-distance relationships based on microsatellite polymorphisms, versus those based on RFLPs; and variation of disequilibrium patterns among human populations including the implications of this variation for human evolutionary origins.

Subjects and Methods

Subjects and DNA Methods

The six polymorphisms at positions 702, 2034, EVI-20, GXAlu, DV1.9, and 10647 were evaluated in 95–110 unrelated CEPH individuals. The polymorphisms at positions 702, 2034, and 10647 were evaluated in 60 African and 50 Japanese unrelated individuals, and from this cohort 52 African and 32 Japanese individuals were genotyped at DV1.9. DNA was prepared from blood or lymphoblastoid cell lines by standard methods (Bell et al. 1981).

Development of MS-PCR

The three exon-based polymorphisms—at positions 702, 2034, and 10647—were adapted for MS-PCR analysis (Rust et al. 1993). MS-PCR is a technique whereby both normal and mutant alleles are amplified in the same reaction tube by using different-length allele-specific primers. For each polymorphism, MS-PCR primers were designed such that one of the two allele-specific primers was 23–29 bp in length, whereas the other primer was 43–49 bp in length (see fig. 2, *top*). The short primer was designed to contain a mismatch

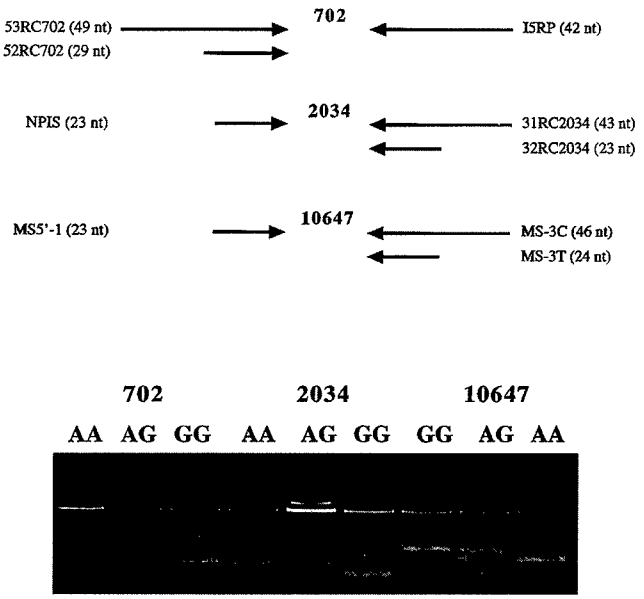

Figure 2 MS-PCR primers for the three exon-based polymorphisms, at 702, 2034, and 10647 (*top*)—and agarose gel electrophoresis (4% [3:1 Nusieve:Seakem LE]) (*bottom*) of these polymorphisms, with heterozygotes (A/G and G/A) and homozygotes (AA and GG) for both alleles for each of the three polymorphisms.

in one of the three bases adjacent to the 3′-terminal base. In the corresponding region, the longer primer was designed to have a mismatch at a position different from that of the short primer, all within three bases adjacent to the 3′-terminal base. In addition, the long primer has two consecutive mismatches at positions corresponding to the 5′ end of the short primer, which should inhibit hybridization with short heteroduplex molecules. For each MS-PCR set, a shared complementary-strand primer was located at a distance from the polymorphic site to yield two distinct PCR products 80–120 bp in length. Each MS-PCR required empirical optimization of the optimum annealing temperature, template concentration, and relative concentration of the allele-specific primers, to yield equally intense signals from both the alleles. (The longer allele-specific primer was used at a molar concentration lower than that used for the shorter one). In order to ensure accurate genotyping, DNA isolated from known homozygotes for either allele and a known heterozygous individual were used as controls in every analysis. The conditions for all three polymorphisms at positions 702, 2034, and 10647 are as follows: The template is total genomic DNA, 50 ng in a final PCR volume of 25 μl. Final concentrations of other components are 1 × PCR buffer (Gibco BRL), 20 μM each dNTP, 0.25 mM spermidine, 0.1% Triton X-100, and 0.025 units of *Taq* polymerase/μl. The thermal cycling conditions for all three MS-PCRs are 94°C for 5 min; 94°C for 10 s, 60°C for 10 s, and 72°C for 10 s, repeated for five cycles; followed by 94°C for 10 s, 56°C for 10 s, and 72°C for 10 s, repeated for 30 cycles. The PCR products were electrophoresed on a 4% (3:1 Nusieve:Seakem LE) agarose gel and were analyzed; an example of is which shown in the bottom section of figure 2.

The primers (all used in a single tube) and their concentrations used for 702 are as follows: The upstream primers are 52RC702 (5′-AAAATTATCCAGATG-AATTTACAAAAGTG-3′ at 0.5 μM [final concentration]) and 53RC702 (5′-GGCATTTTGGAACTGGGT-AGCCAATTATCCAGATGAATTTACAAACCTA-3′ at 0.125 μM [final concentration]). The downstream primer, I5RP (5′-CAGGAAACAGCTATGACCAAA-AAAAAATCAATCGTATCCTTA-3′ at 0.5 μM [the 18 bases at the 5′ end are not in the template]), is intron based. The longer product, the "A allele," is 120 bp; the shorter product, the "G allele," is 100 bp. For MS-PCR of 702 from cDNA, we replace the downstream (intron-based) primer with a primer in exon 6: 4T5D (5′AATACGACACCAAGTCAAATAGCTTTTCTG3′ [the last five bases at the 5′ end are not in the template]). Otherwise, all PCR conditions are the same as those used for 702 MS-PCR from genomic DNA.

The primers and their concentrations used for 2034 are as follows: the upstream primer is NPIS (5′-ACT-TCCACCCTTGACTCTCAGGA-3′ at 0.5 μM), and the downstream primers are 31RC2034 (5′-GTACAG-GGCCACTTCTAGTTACGTCTGGGCTTGTCGGCA-ACTT-3′ at 0.17 μM [final concentration]) and 32RC2034 (5′-TGGTCTGGGCTTGTCGGCACATC-3′ at 0.5 μM [final concentration]). The longer product, the "A allele," is 97 bp; and the shorter product, the "G allele," is 77 bp. For MS-PCR of 2034 from cDNA, we replace the upstream (intron-based) primer with a primer in exon 12, 13T15U (5′TCGACATCGCCT-CTCTCCGGAAGGGAA3′ [the last five bases at the 5′ end are not in the template]). Otherwise, all PCR conditions are the same as those for 2034 MS-PCR from genomic DNA.

The primers and their concentrations used for 10647 are as follows: the upstream primer is MS5′-1 (5′-GGT-GTTATGCTATTTTGCTCTTC-3′ at 0.4 μM), and the downstream primers are MS3-T (5′-GAAATACTA-CACCCTTGGTAAGCT-3′ at 0.4 μM) and MS3-C (5′-TGCTGATCATTTCAGGCGGTATTCAATACTACA-CCCTTGGTAGACC-3′ at a final concentration of 0.05 μM). The longer product, the "G allele," is 130 bp; and the shorter product, the "A allele," is 108 bp.

Intron-Based Polymorphism Analysis

PCR to amplify the EVI-20 CA repeat region from total genomic DNA was performed in a reaction volume of 25 μl containing 100–150 ng of DNA, 0.5 μM of each of the primers M15-169A (5′-CCCATACCTAGT-TCTTAAAGTCTG-3′) and M15-169B (5′-TAACAA-TTGTGGAACTGCAGCAATTATT-3′), 2.0 mM $MgCl_2$, 10 mM Tris-HCl pH 8.4, 40 mM NaCl, 200 μM of each dNTP, 1.25 units of *Taq* polymerase (Gibco BRL), and 0.01 μM radiolabeled M15-169B. The end-labeled primer was prepared as follows: 0.1 μM M15-169B, 50 mM Tris-Hcl pH 7.5, 10 mM $MgCl_2$, 5.0 mM DTT, 8.4 units T4 polynucleotide kinase (MBR, Milwaukee), and 6.0 μl ^{32}P-ATP (3,000 Ci/mmol; NEN) in a total volume of 10 μl, incubated at 37°C for 30 min. After an initial 5-min denaturation at 94°C, PCR amplification was performed for 30 cycles, with denaturation at 94°C for 30 s, annealing at 62°C for 30 s, and extension at 72°C for 1 min. The samples were diluted in formamide dye (10 μl was added to the 25-μl reaction), and 3 μl were loaded on a 7% polyacrylamide gel that contained 5.6 M urea, 32% formamide, 90 mM Tris-borate pH 7.5, and 2 mM EDTA pH 8.0. Electrophoresis was performed at 90 W for 3 h in 90 mM Tris-borate and 2 mM EDTA, and the gel was preelectrophoresed before the samples were loaded. The gels were placed on Whatmann 3mm filter paper and were exposed to X-ray film overnight. PCR genotype analysis for DV1.9 (Bleyl et al. 1994) and GXAlu (Xu et al. 1992) was performed as described elsewhere.

Disequilibrium Analysis

Weir's (Weir and Cockerham 1989; Weir 1990) composite measure of disequilibrium (Δ), which is appropriate for genotypic data, was applied to the CEPH, Japanese, and African data. The alleles of the multiallelic loci were grouped into diallelic systems in which the most frequent allele constituted one system and in which the remaining alleles were summed to constitute the other. The 95% confidence limits for Δ were estimated by using Fisher's Z-transformation (Weir 1979). A test of the null hypothesis that $r = .0$ was performed by using a χ^2 test, whereby $\chi^2 = Nr^2$ (N = number of chromosomes in the sample).

Results and Discussion

Identification and Analysis of the Polymorphisms

The six *NF1* polymorphisms evaluated by PCR are represented on a genomic map in figure 1. The polymorphism at 702 was identified by comparison of the *NF1* cDNA sequence with that of Marchuk et al. (1991), which revealed different purine bases at that position. SSCP analysis of RT-PCR products spanning position 702 revealed a common electrophoretic variant, and sequencing of the bands confirmed that the A/G variation at 702 was a common polymorphism (R. Cawthon, unpublished data). This polymorphism was also reported, by Hoffmeyer and Assum (1994), as an *Rsa*I RFLP. The polymorphism at position 2034 of the *NF1* cDNA was identified during initial sequencing of the *NF1* gene. Independent cDNA clones showed different purine bases at this position (Xu et al. 1990). SSCP and sequence analysis of RT-PCR products spanning this site in 37 NF1 patients and several controls revealed a polymorphism that was located at base 2034 of the *NF1* cDNA (R. Cawthon, unpublished data). The polymorphism at 2034 has also been reported as a *Tsp*509 I RFLP, by Regnier et al. (1995). A polymorphism at position 10647 was identified on the basis of a sequence discrepancy between *NF1* cDNA clone 21D and a sequence discrepancy between *NF1* cDNA clone 21D and genomic clone 7D5 (Li et al. 1995). Sequencing PCR products from several controls confirmed the presence of this polymorphism. All three exon-based polymorphisms were adapted for MS-PCR analysis. The bottom section of figure 2 shows an example of the MS-PCR for the three exon-based polymorphisms, at positions 702, 2034, and 10647. The allele frequencies for all three exon-based polymorphisms are presented in table 1.

The three intron-based polymorphisms—GXAlu, EVI-20, and DV1.9—cluster within 42 kb of genomic DNA (see fig. 1). The GXAlu polymorphism was identified from sequence from a genomic clone cosmid EVI36 (Xu et al. 1992). It lies in an Alu repeat of *NF1* intron 27b (approximate position 2000 in GenBank Accession no. L05367) and maps 3.5 kb centromeric to the end of the *OMGP* gene. The allele frequencies for the major alleles in the GXAlu polymorphism in 91 CEPH individuals whom we evaluated are as follows: allele 1 (407 bp), .09; allele 2 (403 bp), .65; and allele 3 (399 bp), .26. The calculated heterozygosity for this polymorphism is .51. These values are similar to those reported by Xu et al. (1992) and Lazaro et al. (1993*a*). The CA-repeat polymorphism, EVI-20 (approximate position 33200 in GenBank Accession no. L05367), was identified from a genomic clone, cosmid EVI20, which spans *NF1* exons 28–31. The CA repeat lies 440 bp telomeric to exon 1 of the embedded *EVI2A* gene and 3.7 kb centromeric to *NF1* exon 28. The heterozygosity of this polymorphism is .76, and genotyping of 89 unrelated individuals revealed six alleles. The frequencies of the six major alleles, on the basis of 178 chromosomes, are as follows: allele 1 (203 bp), .15; allele 2 (201 bp), .07; allele 3 (199 bp), .10; allele 4 (195 bp), .38; allele 5 (193 bp), .28; and allele 6 (191 bp), .02. Similar allele frequencies have been reported by Lazaro et al. (1993*a*). Mendelian codominant inheritance was demonstrated in 5 CEPH families and in 175 families who requested diagnostic DNA testing for NF1. The DV1.9 polymorphism, which has been reported elsewhere, represents the 3′ end of the Ta subclass L1 insertion element (Bleyl et al. 1994). It lies in the middle of intron 30, 2 kb downstream of *NF1* exon 30 and 2 kb upstream of *NF1* exon 31. Allele frequencies for the CEPH cohort are shown in table 1

Table 1

Allele Frequencies and Heterozygosities for the CEPH, Japanese, and African Populations

	CEPH	Japanese	African
702:			
Allele frequency: A/G	.73/.27	.58/.42	.38/.62
Heterozygosity: observed/expected	.32/.40[a]	.52/.50	.67/.48[b]
2034:			
Allele frequency: G/A	.73/.27	.51/.49	.65/.35
Heterozygosity: observed/expected	.34/.40	.56/.50	.46/.46
DV1.9:			
Allele frequency: 1/2	.35/.65	.52/.48	.62/.38
Heterozygosity: observed/expected	.41/.48	.47/.49	.69/.47[c]
10647:			
Allele frequency: G/A	.74/.26	.49/.51	.20/.80
Heterozygosity: observed/expected	.30/.38[d]	.54/.50	.36/.32

[a] $\chi^2 = 4.4$; $P < .05$.
[b] $\chi^2 = 10.15$; $P < .01$.
[c] $\chi^2 = 9.73$; $P < .01$.
[d] $\chi^2 = 3.98$; $P < .05$.

Table 2

Δ Values and 95% Confidence Intervals, Based on Genotype Analysis of the CEPH Population

Polymorphism	Type[a]	Distance (kb)	Δ	95% Confidence Interval
fHB5-E.3/702	D/D	60–140	.94	.90–.96
fHB5-E.3/2034	D/D	135–215	.94	.92–.96
702/pHu39.3	D/D	130	.85	.79–.90
2034/pHu39.3	D/D	80	.81	.73–.87
702/GXAlu	D/R	125	.73	.61–.81
2034/GXAlu	D/R	75	.75	.64–.83
2034/EVI-20 CA	D/R	106	.72	.60–.80
EVI-20 CA/10647	R/D	55	.71	.59–.80
DV1.9/10647	D/D	44	.70	.60–.79
10647/f7G4-GL2	D/D	4–8	.75	.65–.83
EVI-20/DV1.9	R/D	11	.78	.68–.85
GXAlu/EVI-20	R/R	31	.47	.27–.62

[a] D = diallelic; and R = repeat polymorphism.

and agree with results of previous studies of this diallelic polymorphic site (Xu et al. 1991; Bleyl et al. 1994).

Correlation of Linkage Disequilibrium versus Physical Distance and Polymorphism Type

Linkage disequilibrium at the *NF1* locus has been demonstrated previously by haplotype analysis using eight diallelic restriction-site polymorphisms in a CEPH cohort (Jorde et al. 1993). As an extension of this study, the same cohort was genotyped by PCR methodology, at six polymorphic loci (for approximate map positions, see fig. 1), and linkage-disequilibrium analysis was performed by using multiple loci. Table 2 shows 12 pairwise evaluations of nine polymorphic loci spanning the *NF1* locus. The physical distances between the loci are included. Locus 702 (exon 5) and locus 2034 (exon 13) lie between fHB5-E.3 (intron 1) and pHu39.3 (intron 27b), and DV1.9 (intron 30) and locus 10647 (exon 49) lie between pHu39.3 and f7G4-GL.2. By genotype analysis, loci 702 and 2034 show high linkage disequilibrium both with each other and with their respective flanking markers. Likewise, locus 10647 is in high linkage disequilibrium with its flanking markers. These results, based on use of diallelic polymorphisms in PCR genotyping, are consistent with previous results, which used diallelic RFLP markers in Southern analysis (Jorde et al. 1993).

Linkage-disequilibrium analyses based on genotypes were performed in the CEPH population, by using the two STS polymorphisms, and these were shown to be in disequilibrium with their flanking markers (table 2). The determination of genotypes by using different types of polymorphic markers within a single gene locus provides the opportunity to evaluate not only the relationship of distance to disequilibrium but also disequilibrium determination between repeat and single-base systems. Even though they are only 31 kb apart, the disequilibrium coefficient between the two short repeat polymorphisms, GXAlu and EVI-20, is .47, which is the only coefficient <.70, for all pairwise comparisons at the *NF1* locus (table 2). Lower disequilibrium values have sometimes been observed for repeat polymorphisms (Elbein 1992), and the apparent anomaly for GXAlu and EVI-20 may be explained by virtue of both being relatively highly mutable repeat polymorphisms.

Previous analysis had not demonstrated linkage disequilibrium between disease alleles and any of the diallelic RFLPs examined (Jorde et al. 1993). We extended this analysis to an exon-based polymorphism, by comparing MS-PCR–based genotypes at position 2034 in a Utah NF1 cohort and in unaffected individuals from a Utah CEPH cohort. The allele frequencies at position 2034, for a cohort of 30 NF1 individuals from Utah, are .77 (G allele) and .23 (A allele), with .36 heterozygosity (H. H. Breidenbach, personal communication). This is not significantly different than allele frequencies at 2034 from 30 individuals from Utah CEPH kindreds: .75 (G allele), .25 (A allele), and .38 heterozygosity. Likewise, a comparison between 20 Japanese NF1 patients and 50 unaffected Japanese individuals showed a similar congruence (data not shown). As would be expected for an autosomal dominant condition that has a high incidence of sporadic occurrence, there is no association of haplotype with disease.

Genotype and Disequilibrium Analysis in the CEPH, Japanese, and African Cohorts

Genotyping was carried out in CEPH individuals from Utah and from non-Utah kindreds and in two other cohorts, representing the Japanese (50 individuals) and African (60 individuals) populations. The allele frequencies and heterozygosity of the three exon-based polymorphisms for the CEPH, Japanese, and African populations are presented in table 1. The observed genotype frequencies at position 702 significantly differed from Hardy-Weinberg expectations for the CEPH and African populations. The CEPH cohort demonstrated fewer heterozygotes than expected, whereas the African cohort revealed more heterozygotes than expected. In addition, at 10647 the CEPH cohort showed fewer heterozygotes than expected, and at DV1.9 the African population showed greater heterozygosity than expected (table 1).

Genotype analysis for the 702 and 2034 polymorphisms in the CEPH and Japanese cohorts showed that a G/G genotype at 2034 is usually seen with an A/A genotype at 702 and that the A/A genotype at 2034 is usually seen with a G/G genotype at 702. However, the most common genotypes seen in the African population are G/G at 2034, with A/G at 702, and A/A at 2034,

Table 3

Δ Values and 95% Confidence Intervals, Based on Genotype Analysis of CEPH, Japanese, and African Individuals, for 702, 2034, DV1.9, and 10647

	CEPH	Japanese	African
702/2034:			
Δ	.90	.82	.61
95% Confidence interval	.87–.93	.71–.90	.42–.75
702/DV1.9:			
Δ	.55	.60	.89
95% Confidence interval	.40–.67	.33–.79	.81–.94
702/10647:			
Δ	.84	.75	.41
95% Confidence interval	.77–.88	.60–.85	.17–.60
2034/DV1.9:			
Δ	.60	.76	.54
95% Confidence interval	.46–.71	.56–.88	.31–.70
2034/10647:			
Δ	.90	.91	.34
95% Confidence interval	.86–.93	.85–.95	.09–.55
DV1.9/10647:			
Δ	.71	.73	.45
95% Confidence interval	.59–.74	.51–.86	.21–.60

also with A/G at 702. Thus, in contrast to the CEPH and Japanese populations, the African population is usually heterozygous at 702, regardless of the homozygous genotype at 2034. With respect to allele representation at the 702 and 2034 loci, the differences between the CEPH and Japanese populations and the African population suggested that linkage-disequilibrium patterns might also differ between the three populations.

Disequilibrium analysis using genotypes was performed for pairwise comparisons of 702, 2034, DV1.9, and 10647 in the CEPH, African, and Japanese cohorts (table 3). The CEPH and Japanese cohorts were not significantly different from each other, for any comparison. The African cohort showed significantly lower disequilibrium for three pairwise evaluations: 702 versus 2034 and 702 versus 10647, both with respect to the CEPH cohort; and 2034 versus 10647, with respect to both the CEPH and the Japanese cohorts. The African cohort, which is not in Hardy-Weinberg equilibrium for 702 and DV1.9 (see table 1), exhibits significantly higher disequilibrium for this pair of loci than do the Japanese and CEPH cohorts. This anomalously high value may result from the fact that most of the Africans are double heterozygotes for these two polymorphisms. In general, the African cohort demonstrated lower disequilibrium than did the CEPH and Japanese cohorts, and at four of six pairwise comparisons it significantly differed from the other two populations. Thus, the African disequilibrium patterns tend to diverge from those of Caucasians and Japanese, in accordance with a number of genetic distance analyses (Bowcock et al. 1994; Deka et al. 1995; Jorde et al. 1995).

Our analysis of linkage disequilibrium across the *NF1* locus shows that the African cohort has higher heterozygosity and lower disequilibrium than do the CEPH and Japanese cohorts. This result is similar to the recent finding that African populations have more haplotypic variation (and thus less linkage disequilibrium) for polymorphisms near the CD4 locus than do non-African populations (Tishkoff et al. 1996). Because linkage disequilibrium diminishes through time, these disequilibrium patterns are consistent with an African origin of modern humans. Detailed analyses at additional loci are needed in order for this hypothesis to be evaluated more conclusively.

Clinical Applications

The application of six PCR-based assays to the genotyping of polymorphisms across the *NF1* locus should prove useful in the clinical setting. Eighty-four percent of 96 CEPH individuals were heterozygous at one or more of the six loci. Furthermore, the intron-based markers—GXAlu, EVI-20, and DV1.9—have been implemented successfully in diagnostic family-linkage evaluations (L. Nelson, unpublished). The addition of the three exon-based polymorphisms extends the coverage of the gene from 42 kb (GXAlu to DV1.9) to >200 kb (702 to 10647). This could be important in the identification of large *NF1* deletions. For example, NF1 patients who are not heterozygous at any of the multiple *NF1* polymorphic sites could be appropriately screened for large deletions, by FISH studies (Leppig et al. 1996).

Implementation of the MS-PCR assays for the polymorphisms at 702, 2034, and 10647 would also provide a straightforward assay for the qualitative assessment of *NF1* mRNA levels. For example, the use of exon-based polymorphisms has enabled investigators to analyze the processing of mutant *NF1* RNA transcripts (Hoffmeyer et al. 1995). This would also be important in mRNA-based mutation-detection protocols, such as the protein-truncation test, whereby significantly reduced mRNA levels of a mutant allele could lead to false-negative results. Ideally, as part of the initial mutation-screening evaluation, genotyping at the exon-based polymorphisms should be performed for every NF1 patient, at the genomic level. For the heterozygous individuals, both *NF1* alleles should be determined to be present in the cDNA transcribed from mRNA, prior to initiation of mutation-detection analysis.

Finally, the application of PCR-based protocols to the evaluation of the *NF1* locus would enhance detection of the loss of *NF1* alleles in various tumor tissues, including archival material. The conversion of diallelic polymorphism detection to MS-PCR–based methods would enable investigators to examine the *NF1* locus by using

limited amounts of DNA template. It also has a potential advantage over STS markers. Recent evidence suggests that microsatellite instability exists at a number of loci in genomic DNA from neoplasms (Pykett et al. 1994; Dams et al. 1995; Honchel et al. 1995), as well as in benign neurofibromas (Ottini et al. 1995). The potential misinterpretation of convergence to homozygosity due to microsatellite instability as reduction to hemizygosity—or loss of heterozygosity at a "tumor suppressor" locus—could be circumvented by the careful application of MS-PCR. The MS-PCR protocols described here have been successfully applied to the identification of genotypes from DNA extracted from sections of paraffin-embedded tissue (S. M. Purandare, unpublished data).

In summary, we have converted polymorphism analysis at the *NF1* locus to a PCR-based assay system. Application of both diallelic and multiallelic PCR systems to genomic DNA samples provides ready access to the *NF1* locus, for both linkage analysis and population studies. Linkage disequilibrium is maintained across the *NF1* locus regardless of the polymorphic systems used or the physical distance between loci. Using these techniques, we have shown that the African population diverges from the Caucasian and Japanese populations. The lack of recombination at the *NF1* locus strengthens family-linkage studies for *NF1* testing. Finally, the adaptation of intron- and exon-based systems provides a framework to more fully evaluate the *NF1* locus at the molecular level.

Acknowledgments

The Japanese DNA samples were provided by Ituro Inoue and Jean-Marc Lalouel. Some of the African DNA samples were provided by Trefor Jenkins. R.C. was supported by National Neurofibromatosis Foundation grant MGN 1 R55 and National Cancer Institute grant CA 57511-01. L.B.J. and W.S.W. were supported by NSF grant DBS-9310105 and NIH grant HG00347. D.H.V. was supported by U.S. Department of the Army grant DAMD 17-93-J-3070.

References

Andersen LB, Tarle SA, Marchuk DA, Legius E, Collins FS (1993) A compound nucleotide repeat in the neurofibromatosis (NF1) gene. Hum Mol Genet 2:1083

Bell GI, Karem JH, Rutter JR (1981) Polymorphic DNA region adjacent to the 5′ end of the human insulin gene. Proc Natl Acad Sci USA 78:5759–5763

Bleyl S, Ainsworth P, Nelson L, Viskochil D, Ward K (1994) An ancient Ta subclass L1 insertion results in an intragenic polymorphism in an intron of the NF1 gene. Hum Mol Genet 3:517–518

Bowcock AM, Ruiz-Linares A, Tomfohrde J, Minch E, Kidd JR, Cavalli-Sforza LL (1994) High resolution of human evolutionary trees with polymorphic microsatellites. Nature 368:455–457

Dams E, Van de Kelft EJZ, Martin JJ, Verlooy J, Willems PJ (1995) Instability of microsatellites in human gliomas. Cancer Res 55:1547–1549

Deka R, Jin L, Shriver MD, Yu LM, DeCroo S, Hundrieser J, Bunker CH, et al (1995) Population genetics of dinucleotide $(dC\text{-}dA)_n \cdot (dG\text{-}dT)_n$ polymorphisms in the world populations. Am J Hum Genet 56:461–474

Elbein SC (1992) Linkage disequilibrium among RFLPs at the insulin-receptor locus despite intervening Alu repeat sequences. Am J Hum Genet 51:1103–1110

Heim RA, Kam-Morgan LN, Binnie CG, Corns DD, Cayouette MC, Farber RA, Aylsworth AS, et al (1995) Distribution of 13 truncating mutations in the neurofibromatosis 1 gene. Hum Mol Genet 4:975–981

Hoffmeyer S, Assum G (1994) An Rsa I polymorphism in the transcribed region of the neurofibromatosis (NF1) gene. Hum Genet 93:481–482

Hoffmeyer S, Assum G, Greisser J, Kaufmann D, Nurnberg P, Krone W (1995) On unequal allelic expression of neurofibromin in neurofibromatosis type 1. Hum Mol Genet 4: 1267–1272

Hofman K, Boehm CD (1992) Familial neurofibromatosis type 1: clinical experience with DNA testing. J Pediatr 120:394–398

Honchel R, Halling KC, Thibodeau SN (1995) Genomic instability in neoplasia. Semin Cell Biol 6:45–52

Jorde LB, Bamshad MJ, Watkins WS, Zenger R, Fraley AE, Krakowiak PA, Carpenter KD, et al (1995) Origins and affinities of modern humans: a comparison of mitochondrial and nuclear genetic data. Am J Hum Genet 57:523–538

Jorde LB, Watkins WS, Viskochil D, O'Connell P, Ward K (1993) Linkage disequilibrium analysis in the neurofibromatosis I (NFI) region: implications for gene mapping. Am J Hum Genet 53:1038–1050

Lazaro C, Gaona A, Estivill X (1994) Two CA/GT repeat polymorphisms in intron 27 of the human neurofibromatosis (NF1) gene. Hum Genet 93:351–352

Lazaro C, Gaona A, Ravella A, Volpini V, Casals T, Fuentes J, Estivill X (1993*a*) Novel alleles, hemizygosity, and deletions at an Alu repeat within the neurofibromatosis type 1 gene. Hum Mol Genet 2:725–730

Lazaro C, Gaona A, Xu G, Weiss R, Estivill X (1993*b*) A highly informative CA/GT repeat polymorphism in intron 38 of the human neurofibromatosis type 1 (NF1) gene. Hum Genet 92:429–430

Leppig KA, Viskochil D, Neil SM, Rubenstein A, Johnson VP, Zhu XL, Brothman AR, et al (1996) The detection of contiguous gene deletions at the neurofibromatosis 1 locus with fluorescence *in situ* hybridization. Cytogenet Cell Genet 72:95–98

Li Y, O'Connell P, Breidenbach HH, Cawthon R, Stevens J, Xu G, Neil SM, et al (1995) Genomic organization of the neurofibromatosis 1 gene (*NF1*). Genomics 25:9–18

Marchuk D, Saulino A, Tavakkol R, Swaroop M, Wallace M, Andersen L, Mitchell A, et al (1991) cDNA cloning of the type 1 neurofibromatosis gene: complete sequence of the NF1 gene product. Genomics 11:931–940

Marchuk D, Tavakkol R, Wallace M, Brownstein B, Taillon-Miller P, Fong C, Legius E, et al (1992) A yeast artificial

chromosome contig encompassing the type 1 neurofibromatosis 1 gene. Genomics 13:672–680

NIH Consensus Development Conference (1988) Neurofibromatosis conference statement. Arch Neurol 45:575–578

Ottini L, Esposito DL, Richetta A, Carlesimo M, Palmirotta R, Veri MC, Battista P, et al (1995) Alterations of microsatellites in neurofibromas of von Recklinghausen's disease. Cancer Res 55:5677–5680

Purandare SM, Breidenbach HH, Li Y, Zhu XL, Sawada S, Neil SM, Brothman A, et al (1995) Identification of NF-1 homologous loci by direct sequencing, fluorescent in situ hybridization and PCR amplification of somatic cell hybrids. Genomics 30:476–485

Pykett MI, Murphy M, Harnish PR, George DL (1994) Identification of microsatellite instability phenotype in meningiomas. Cancer Res 54:6340–6344

Regnier V, Danglot G, Nguyen VC, Bernheim A (1995) A Tsp509I variant in exon 13 of the neurofibromatosis type 1 (NF1) gene allows the identification of both alleles at the mRNA level. Hum Genet 96:131–132

Rodenheiser D, Ainsworth P, Coulter-Mackie M, Singh S, Jung J (1993) A genetic study of neurofibromatosis type 1 (*NF1*) in southwestern Ontario. II. A PCR based approach to molecular and prenatal diagnosis using linkage. J Med Genet 30:363–368

Rust S, Funke H, Assmann G (1993) Mutagenically separated PCR (MS-PCR): a highly specific one step procedure for easy mutation detection. Nucleic Acids Res 21:3623–3629

Tishkoff S, Dietzsch E, Speed W, Pakstis A, Cheung K, Kidd J, Bonne-Tamir B, et al (1996) Global patterns of linkage disequilibrium at the CD4 locus support a recent African origin of non-African humans. Science 271:1380–1387

Ward K, O'Connell P, Carey JC, Leppert M, Jolley S, Plaetke R, Ogden B, et al (1990) Diagnosis of Neurofibromatosis 1 by using tightly linked, flanking DNA markers. Am J Hum Genet 46:943–949

Weir BS (1979) Inferences about linkage disequilibrium. Biometrics 35:235–254

——— (1990) Genetic data analysis. Sinauer, Sunderland, MA, pp 102–103

Weir BS, Cockerham CC (1989) Complete characterization of disequilibrium at two loci. In: Feldman MW (ed) Mathematical evolutionary theory. Princeton University Press, Princeton, pp 86–109

Xu W, Liu L, Ponder M, Ponder BA (1991) A Taq I polymorphism in the human NF1 gene. Nucleic Acids Res 19:4570

Xu G, Nelson L, O'Connell P, White R (1992) An Alu polymorphism intragenic to the neurofibromatosis type 1 gene. Nucleic Acids Res 19:3764

Xu G, O'Connell P, Viskochil D, Cawthon R, Robertson M, Culver M, Dunn D, et al (1990) The neurofibromatosis type 1 gene encodes a protein related to GAP. Cell 62:599–608

Cytogenet Cell Genet 72:95–98 (1996)

Cytogenetics and Cell Genetics

The detection of contiguous gene deletions at the neurofibromatosis 1 locus with fluorescence in situ hybridization

K.A. Leppig,[1] D. Viskochil,[4] S. Neil,[4] A. Rubenstein,[5] V.P. Johnson,[6] X.L. Zhu,[4] A.R. Brothman,[4] and K. Stephens[2,3]

Departments of [1] Pediatrics, Division of Medical Genetics, [2] Medicine, Division of Medical Genetics, and [3] Pathology, University of Washington, Seattle, WA;
[4] Department of Pediatrics, University of Utah, Salt Lake City, UT;
[5] Department of Neurology, Mount Sinai School of Medicine, New York, NY; and
[6] Departments of Obstetrics and Gynecology, Pediatrics, and Laboratory Medicine, University of South Dakota, Vermillion, SD (USA)

Abstract. Neurofibromatosis type 1 (NF1) is a common genetic disorder characterized primarily by the development of multiple neurofibromas and pigmentary changes. The recent identification of contiguous gene deletions in NF1, a previously unrecognized molecular basis for this disorder, raises important questions regarding deletion frequency in the patient population and the role that contiguous genes may play in the physical manifestations of NF1 patients. To facilitate the identification of patients with large NF1 deletions, we have isolated clones carrying large genomic segments from the NF1 locus and tested their efficacy as probes for fluorescence in situ hybridization (FISH). Clone P1-9 spans approximately 65 kb of the NF1 gene, including exons 2–11, and clone P1-12 carries ~ 55 kb of NF1 intron 27B. FISH studies performed with P1-9, P1-12, and a set of overlapping 1F10 cosmid clones mapping telomeric to the NF1 locus identified large deletions in two new neurofibromatosis type 1 patients who, like previously characterized deletion patients, had mildly dysmorphic facial features and large numbers of cutaneous neurofibromas.

Neurofibromatosis 1 (NF1) is a common autosomal dominant genetic disorder characterized primarily by the development of multiple neurofibromas and pigmentary abnormalities, which include café au lait spots, axillary and inguinal freckling, and Lisch nodules. A hallmark of the disorder is phenotypic variability, which is observed both in the severity of the primary clinical features and in the manifestation of additional unusual, rather atypical, physical features (reviewed by Viskochil and Carey, 1992). The characterization of the NF1 gene has provided the necessary resources to address the hypothesis that specific NF1 mutant alleles predispose to distinctive clinical features. However, NF1 mutational analyses have been hampered by the large size and complexity of the gene, which is approximately 335 kb in length and comprised of 59 known exons that encode a 2,818 amino acid peptide (Marchuk et al., 1991; Li et al., 1995). In general, the relatively few NF1 mutations that have been characterized are unique and scattered throughout the NF1 gene, thus precluding genotype/phenotype correlations (reviewed by Upadhyaya et al., 1994).

Recently, each of five patients identified with NF1 contiguous gene deletions were noted to be remarkable for their mildly dysmorphic features and large numbers of cutaneous neurofibromas relative to age (Kayes et al., 1992, 1994). These patients had deletions greater than 700 kb and were hemizygous for NF1 and three other genes, EVI2A, EVI2B, and OMG, encoded by the complementary strand of NF1 intron 27B (Kayes et al., 1994; Li et al., 1995). Other genes flanking NF1 that may be encompassed in the interstitial deletions of these patients have yet to be identified. These data raise critical questions

Supported by grants from the American Cancer Society (EDT17A to K.S.), the Texas Neurofibromatosis Foundation (K.A.L.), the National Institute of Neurological Disorders and Stroke (K08 NS01492 to D.V.), and the U.S. Department of Defense (DAMD 17-93-J-3070 to D.V.).

Received 8 February 1995; revision accepted 26 June 1995.

Request reprints from Dr. Karen Stephens, Division of Medical Genetics RG-25, University of Washington, Seattle, WA 98195 (USA); telephone: 206-543-8285; fax: 206-685-4829; e-mail: millie @u.washington.edu.

KARGER
E-mail karger@karger.ch
Fax + 41 61 306 12 34

0301–0171/96/0721–0095$8.00

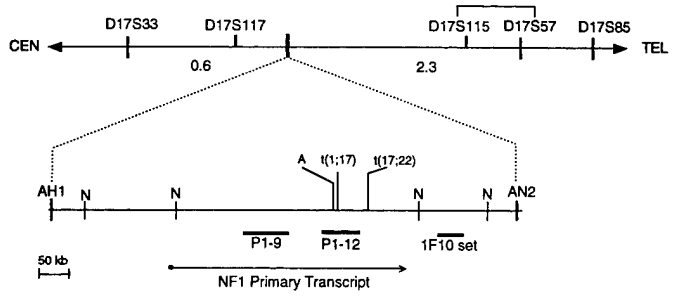

Fig. 1. Genetic map of chromosome 17 and an expanded physical map of the NF1 locus. Sex-averaged genetic distances (cM) are shown between NF1 and the flanking genetic markers D17S33 and D17S57 (Goldgar et al., 1989). The positions of D17S117, D17S115, and D17S85 are indicated (Fain et al., 1989; O'Connell et al., 1989b); brackets indicate that the relative order of D17S115 and D17S57 is unknown. The physical map represents a 700-kb region bordered by the yeast artificial chromosome contig end clones AH1 and AN2 (Marchuck et al., 1992). *Not*I (N) restriction sites and the NF1 primary transcript that spans ~ 335 kb of a 350-kb *Not*I fragment (Li et al., 1995) are indicated. NF1 intragenic landmarks include the two translocation breakpoints (Ledbetter et al., 1989; Menon et al., 1989) and the *Alu*I/*Alu*II (**A**) polymorphic tetranucleotide sequence-tagged site (Xu et al., 1991). P1 bacteriophage clones P1-9 and P1-12 and the set of 1F10 selected cosmid clones used for FISH analyses are shown.

regarding the frequency of large deletions in the patient population and the role that contiguous genes may play in the physical manifestations of some NF1 patients. To facilitate the identification of additional patients with large NF1 deletions, we isolated clones carrying large genomic segments of the NF1 gene, tested their efficacy as probes for fluorescence in situ hybridization (FISH), and identified two new NF1 patients with large deletions.

Materials and methods

Isolation of NF1 genomic clones

Overlapping cosmid clones, carrying human genomic DNA in the pWE15 vector (Stratagene, San Diego, CA), were identified by a probe, p1F10 (O'Connell et al., 1989a), which maps within 100 kb telomeric of the NF1 locus (Viskochil et al., 1990; Jorde et al., 1993). P1 bacteriophage clones containing human genomic DNA were identified with NF1 probes by a high-density screening protocol (Li et al., 1995). Clones were mapped to the NF1 locus by Southern analysis using membranes with EcoRI-digested genomic clones representing the NF1 contig and RNA probes from the ends of the inserts (Li et al., 1995). The P1-bacteriophage clones were further mapped by their ability to serve as template for PCR under standard conditions using facing primers encompassing specific NF1 exons. PCR products were sequenced, and the observed exon sequence was identical to known NF1 cDNA (Li et al., 1995).

FISH analysis

FISH studies were performed as previously described (Chance et al., 1993) on metaphase chromosome preparations of immortalized lymphoblastoid cell lines of each patient. After hybridization at 37 °C for 36–50 h, the slides were washed in 50% formamide, 2 × SSC at 48 °C for the P1 probes and 43 °C for the cosmid probe set. Biotin signals were detected using fluorescein-conjugated avidin, amplified with biotinylated goat anti-avidin followed by a second layer of fluoresceinated avidin. Chromosomes were counterstained with propidium iodide.

Two different methods were used to identify the chromosome 17 homologs. Chromosomes were stained with Hoechst 33258 and aminoactinomycin D, which results in the chromosomes having a Q-band-like pattern (Chance et al., 1993). Scorable metaphase cells were limited to those in which both copies of chromosome 17 could be identified by their banding pattern; a minimum of 20 metaphase cells were analyzed and scored for each hybridization. Symmetrical signals on both chromatids of a chromosome were required for a positive hybridization result, while lack of symmetrical signals on both chromatids defined a negative hybridization result. In the second method, an additional chromosome 17-specific P1 probe, P1-U, which maps to chromosome region 17q24→q25, was hybridized simultaneously with the NF1-specific probe. P1-U was selected with a PCR probe synthesized with rat sequence primers and a human cDNA template for the *N*-methyl-D-aspartate receptor subunit, NR2C (M. Singh et al., 1995, manuscript submitted for publication). Scorable metaphase cells were limited to those with positive signals for the control probe P1-U on both homologs of chromosome 17. In multiple FISH studies, the P1-U signal was present typically on all four chromatids, and P1-9 was present either on four, in controls, or on two paired chromatids in the NF1 deletion cases. Thus, in scorable metaphases, the hybridization efficiency of P1-9 approached 100%. Comparable studies using the 1F10 cosmid clone set as probe demonstrate a hybridization efficiency just under 90% (eg., 32 of a possible 36 chromatids detected in the hybridization represented in Fig. 2A).

NF1 patients

Patient UWA160-1, referred by A.R., is a white female with sporadic NF1. The patient was diagnosed at 11 yr of age based on the presence of multiple café au lait spots, bilateral axillary freckling, and several cutaneous neurofibromas. In addition, she had short stature, a broad neck, and learning disabilities, prompting a cytogenetic evaluation for Turner syndrome, which demonstrated a normal 46,XX karyotype. UWA160-1 required surgeries for the correction of spinal stenosis and bilateral Madelung deformity. She attended special education through high school and currently works as a teacher's aide. At 35 yr of age, the patient has coarse facial features distinctive from other family members, short stature, and 100–500 cutaneous neurofibromas.

Patient J.L., referred by V.P.J., is a 19-yr-old white female, with no family history of NF1. Physical finding included axillary freckling, 10–50 clinically apparent cutaneous neurofibromas (a number of which appeared by age 6), and unusual facial features consisting of hypertelorism, ptosis, and a broad fleshy nose. She also had intermittent left exotropia, mild pectus excavatum, and lax joints, and one grand mal seizure at age 12. The patient attended special education classes throughout grade school and high school. Her full-scale IQ was 56 at 16 yr of age, and she currently lives in a group home and has a job in a sheltered workshop.

Results

Identification of NF1 genomic clones

To facilitate the detection of deletions by FISH, we developed NF1 genomic clones for use as highly efficient hybridization probes. Two P1 bacteriophage clones were identified and mapped relative to the NF1 gene (Fig. 1). Clone P1-9, identified by a probe synthesized as a cDNA PCR product containing exons 8–10c, contained ~ 65 kb of DNA and harbored NF1 exons 2 through 11. Clone P1-12, identified by a PCR probe from the OMG gene (Viskochil et al., 1991), carried approximately 55 kb of DNA and spanned NF1 intron 27b, which contains the polymorphic marker *Alu*I/*Alu*II, as well as the genes for OMG, EVI2A, and EVI2B (Fig. 1). The 1F10 probe set shown in Fig. 1 actually consisted of a mixture of three overlapping cosmid clones (1F10-1, 1F10-12, and 1F10-30) that map to an adjacent 90-kb *Not*I fragment lying telomeric to the *Not*I fragment that harbors the NF1 gene (Fig. 1). The 3′ end of the NF1 gene lies ~ 15 kb centromeric of the shared *Not*I site (Li et al., 1995); therefore, the cosmid clones lie beyond the NF1 gene.

NF1 FISH

Clones P1-9, P1-12, and the 1F10 cosmid set were tested for their ability to detect the NF1 deletion in metaphase chromosomes prepared from lymphoblasts from patients with bona fide NF1 contiguous gene deletions characterized previously by somatic cell hybrid analyses (Kayes et al., 1994). As expected, hybridization signals were evident on only one chromosome 17 homolog for each probe/patient combination tested. Thus, these probes are highly sensitive and specific for the detection of NF1 deletions (data not shown).

Based on our previous data, which suggested that NF1 patients with mildly dysmorphic facies may be more likely to carry heterozygous NF1 contiguous gene deletions (Kayes et al., 1994; Leppig et al., 1994), two such patients were selected initially for FISH analyses. As shown in Fig. 2A for patient J.L., both chromosome 17 homologs had positive hybridization signals from the distal 17q control probe, P1-U, while only one homolog had positive signal from the 1F10 cosmid set. Additional FISH studies with probes P1-9 and P1-12 demonstrated that patient J.L. was also deleted for these sequences (data not shown). As illustrated for patient UWA160-1 in Fig. 2B and 2C, probe P1-9 gave positive signal on only one homologue of chromosome 17. The deletion was delineated by FISH with P1-12 and the 1F10 cosmid set, both of which were found to be deleted in this patient (data not shown). These FISH data define the minimal deleted region for both patients as extending from NF1 exon 2 through the 3′ untranslated region of the gene and into adjacent telomeric sequences.

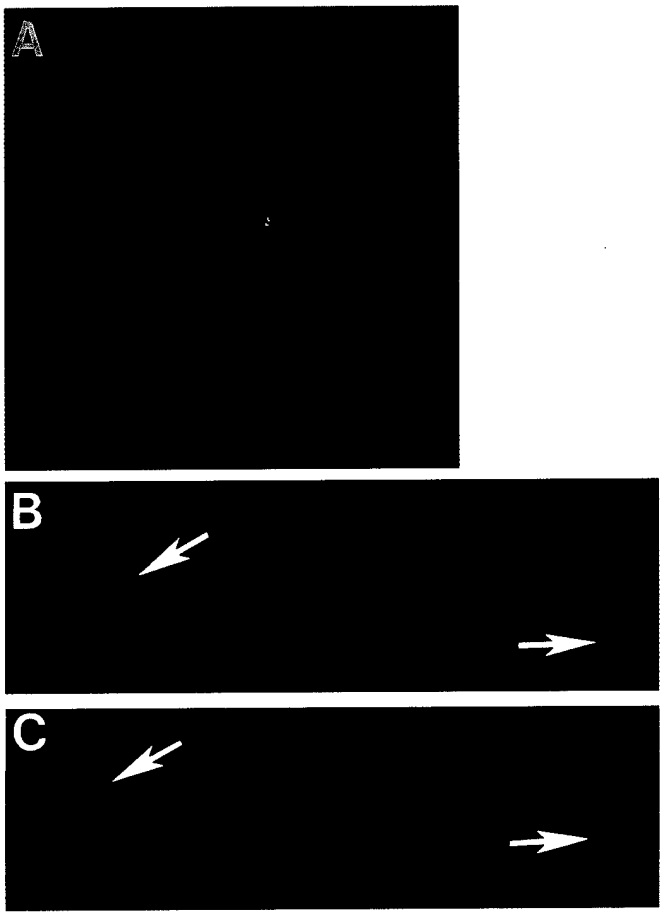

Fig. 2. FISH of NF1 patients. (**A**) The set of 1F10 cosmid probes and the chromosome 17-specific control probe P1-U hybridized to metaphase chromosomes from patient J.L. Grayscale images were captured individually using a CCD camera (Photometrics) and merged in pseudocolor using a software program designed specifically for FISH (Oncor). (**B, C**) Arrows indicate the chromosome 17 homologs. (**B**) Propidium iodide-stained metaphase chromosomes of patient UWA160-1 with the biotin-labeled hybridization signal from probe P1-9. (**C**) The same metaphase and microscopic field as in panel **B** observed through a filter to permit the identification of the chromosome 17 homologs from their quinacrine-like banding pattern obtained by actinomycin D and Hoechst staining.

Discussion

We have developed genomic clones from the NF1 locus for FISH analysis that will facilitate rapid and unambigous detection of large deletions in NF1 patients. These FISH probes demonstrated deletions in five previously defined deletion patients and two new patients, UWA160-1 and J.L. The deletions were at least 275 kb and minimally included four genes: NF1, OMG, EVI2A, and EVI2B. Although P1-9, which carries NF1 exons 2–11, was deleted, it is not known whether either deletion extends through the 5′ end of the NF1 gene. A maximum telomeric limit to the deletion of UWA160-1 has been established by heterozygosity at D17S800, which maps just telomeric to D17S57 (Fig. 1; K. Stephens, unpublished data). The five previously described deletions were at least 700 kb and exceeded the region bounded by the YAC end clones AH1 and AN2 (Fig. 1; Kayes et al., 1994).

Although genotype/phenotype comparisons will be most informative when the full extent of each patient's deletion has been delineated, patients UWA160-1 and J.L. display the key phenotypic findings noted previously in other NF1 contiguous gene deletion patients (Kayes et al., 1994). These include a sufficient number of skin and pigmentary changes to fulfill the NIH consensus criteria for a diagnosis of NF1 (Stumpf et al., 1988), mildly dysmorphic facies, and large numbers of cutaneous neurofibromas relative to age (approximately > 85 percentile). The 10–50 cutaneous neurofibromas of patient J.L. places her in the upper ~ 13% of her age group (Huson et al., 1988). It is difficult to assess patient UWA160-1, since the timing of her tumor development is not known; however, typical of the majority of NF1 patients over age 30 (Huson et al., 1988), she has between 100 and 500 cutaneous neurofibromas. Although cutaneous neurofibromas rarely appear prior to 10 yr of age (Huson et al., 1988), it is intriguing that of the five NF1 contiguous gene deletion patients for whom medical records of sufficient detail were available (including J.L.), each had developed multiple cutaneous neurofibromas well before the age of 10. Together, these data suggest that NF1 contiguous gene deletion may predispose to early onset of cutaneous neurofibromas due to NF1 hemizygosity or haplo-insufficiency for a contiguous gene with a role in tumorigenesis.

The observation of Madelung deformity in patient UWA160-1 may be either a coincidence or evidence for a

Madelung deformity gene contiguous to the NF1 locus. Individual UWA160-1 is one of two NF1 patients reported previously (patient No. 2 in Taff et al., 1987) to have Madelung deformity (MIM 12730 in McKusick, 1992), an autosomal dominant condition marked by dorsal dislocation of the ulnar head. The NF1 region may become a candidate location for a Madelung deformity gene if the deletion of UWA160-1 is found to be larger than that of the other six deletion patients without the deformity.

With the probes described in this article, FISH can be employed to rapidly and unambiguously identify those NF1 patients with an NF1 contiguous gene deletion. The application of FISH analysis now enables investigators to easily address unresolved issues regarding the frequency of NF1 contiguous gene deletion and the resulting associated physical manifestations.

Acknowledgements

We thank Molly Weaver for technical support. Lymphoblast immortalization for patient J.L was performed by the General Clinical Research Center at the University of Utah (under grant M01-RR0064).

References

Chance PF, Alderson MK, Leppig KA, Lensch MW, Matsunami N, Smithe B, Swanson PD, Odelberg SJ, Disteche CM, Bird TD: DNA deletion associated with hereditary neuropathy with liability to pressure palsies. Cell 72:143–151 (1993).

Fain PR, Goldgar DE, Wallace MR, Collins FS, Wright E, Nguyen K, Barker DF: Refined physical and genetic mapping of the NF1 region of chromosome 17. Am J hum Genet 45:721–728 (1989).

Goldgar DE, Green P, Parry DM, Mulvihill JJ: Multipoint linkage analysis in neurofibromatosis type 1: an international collaboration. Am J hum Genet 44:6–12 (1989).

Huson SM, Harper PS, Compston DAS: Von Recklinghausen neurofibromatosis: a clinical and population study in south-east Wales. Brain 111:1355–1381 (1988).

Jorde LB, Watkins WS, Viskochil D, O'Connell P, Ward K: Linkage disequilibrium in the neurofibromatosis 1 (NF1) region: implications for gene mapping. Am J hum Genet 53:1038–50 (1993).

Kayes LM, Burke W, Riccardi VM, Bennett RL, Ehrlick P, Rubenstein A, Stephens K: Deletions spanning the neurofibromatosis 1 gene: identification and phenotype of five patients. Am J hum Genet 54:424–436 (1994).

Kayes LM, Riccardi VM, Burke W, Bennett RL, Stephens K: Large de novo DNA deletion in a patient with sporadic neurofibromatosis, mental retardation and dysmorphism. J med Genet 29:686–690 (1992).

Ledbetter DH, Rich DC, O'Connell P, Leppert M, Carey JC: Precise localization of NF1 to 17q11.2 by balanced translocation. Am J hum Genet 44:20–4 (1989).

Leppig KA, Viskochil D, Kaplan P, Stephens KG: Is NF-1 gene deletion the molecular mechanism of neurofibromatosis type 1 with distinctive facies? Am J hum Genet 55:A229 (1994).

Li Y, O'Connell P, Breidenbach HH, Cawthon R, Stevens J, Xu G, Neil S, Robertson M, White R, Viskochil D: Genomic organization of the neurofibromatosis 1 gene. Genomics 25:9–18 (1995).

Marchuk DA, Saulino AM, Tavakkol R, Swaroop M, Wallace MR, Andersen LB, Mitchell AL, Gutman DH, Boguski M, Collins FS: cDNA cloning of the type 1 neurofibromatosis gene: complete sequence of the NF1 gene product. Genomics 11:931–940 (1991).

Marchuk DA, Tavakkol R, Wallace MR, Brownstein BH, Taillon-Miller P, Fong C-T, Legius E, Andersen LB, Glover TW, Collins FS: A yeast artificial chromosome contig encompassing the type 1 neurofibromatosis gene. Genomics 13:672–680 (1992).

McKusick VA: Catalogs of autosomal dominant autosomal recessive and X-linked phenotypes, in McKusick VA: Mendelian Inheritance in Man, 10th Ed, p 326 (Johns Hopkins University Press, Baltimore 1992).

Menon AG, Ledbetter DH, Rich DC, Seizinger BR, Rouleau GA, Michels VF, Schmidt MA, Dewald G, DallaTorre CM, Haines JL, Gusella JF: Characterization of a translocation within the von Recklinghausen neurofibromatosis region of chromosome 17. Genomics 5:245–249 (1989).

Stumpf S, Alksne JF, Annegers JF, Brown SS, Conneally PM, Housman D, Leppert MF, Miller JP, Moss ML, Pileggi AJ, Rapin I, Strohman RC, Swanson LW, Zimmerman A: Neurofibromatosis Conference statement. Archs Neurol 45:575–578 (1988).

Taff I, Trepel R, Rubinstein A, Wallace S, Handelsman J: Dyschondrosteosis (Madelung's deformity) associated with von Recklinghausen neurofibromatosis (VRNF): extension of the spectrum of dysplastic phenomena associated with NF. Neurology 37(Suppl 1):204 (1987).

Upadhyaya M, Shaw DJ, Harper PS: Molecular basis of neurofibromatosis type 1 (NF1): mutation analysis and polymorphisms in the NF1 gene. Hum Mutat 4:83–101 (1994).

Viskochil D, Buchberg AM, Xu G, Cawthon RM, Stevens J, Wolff RK, Culver M, Carey JC, Copeland NG, Jenkins NA, White R, O'Connell P: Deletions and a translocation interrupt a cloned gene at the neurofibromatosis type 1 locus. Cell 62:187–192 (1990).

Viskochil D, Carey JC: Nosological considerations of the neurofibromatoses. J Dermatol 19:873–880 (1992).

Viskochil D, Cawthon R, O'Connell P, Xu G, Stevens J, Culver M, Carey J, White R: The gene encoding the oligodendrocyte-myelin glycoprotein is embedded within the neurofibromatosis type 1 gene. Mol Cell Biol 11:906–912 (1991).

Xu G-F, Nelson L, O'Connell P, White R: An *Alu* polymorphism intragenic to the neurofibromatosis type 1 gene (NF1). Nucl Acids Res 19:3764 (1991).

GENOMICS 30, 476–485 (1995)

Identification of Neurofibromatosis 1 (*NF1*) Homologous Loci by Direct Sequencing, Fluorescence *in Situ* Hybridization, and PCR Amplification of Somatic Cell Hybrids

SMITA M. PURANDARE,* HEIDI HUNTSMAN BREIDENBACH,† YING LI,† XIAO LIN ZHU,† SHUN'ICHI SAWADA,‡ SHANNON M. NEIL,* ARTHUR BROTHMAN,* RAY WHITE,§ RICHARD CAWTHON,† AND DAVID VISKOCHIL*,[1]

*Departments of *Pediatrics and †Human Genetics and §Oncological Sciences and Huntsman Cancer Institute, University of Utah, Salt Lake City, Utah 84112; and ‡Department of Dermatology, The Jikei University School of Medicine, Tokyo 105, Japan*

Received April 3, 1995; accepted July 27, 1995

Using fluorescence *in situ* hybridization (FISH), we have identified seven *NF1*-related loci, two separate loci on chromosome 2, at bands 2q21 and 2q33–q34, and one locus each on five other chromosomes at bands 14q11.2, 15q11.2, 18p11.2, 21q11.2–q21, and 22q11.2. Application of PCR using *NF1* primer pairs and genomic DNA from somatic cell hybrids confirmed the above loci, identified additional loci on chromosomes 12 and 15, and showed that the various loci do not share homology beyond *NF1* exon 27b. Sequenced PCR products representing segments corresponding to *NF1* exons from these loci demonstrated greater than 95% sequence identity with the *NF1* locus. We used sequence differences between *bona fide NF1* and *NF1*-homologous loci to strategically design primer sets to specifically amplify 30 of 36 exons within the 5′ end of the *NF1* gene. These developments have facilitated mutation analysis at the *NF1* locus using genomic DNA as template.

INTRODUCTION

Neurofibromatosis 1 is an autosomal dominant disorder that afflicts approximately 1 in 3500 individuals worldwide (Crowe *et al.,* 1956; Riccardi, 1992). It manifests in an age-related fashion and is characterized mainly by cafe au lait spots, neurofibromas, and Lisch nodules of the iris. The *NF1* gene maps to chromosome 17q11.2 (Barker *et al.,* 1987), and, even though it was cloned in 1990 (Cawthon *et al.,* 1990; Viskochil *et al.,* 1990; Wallace *et al.,* 1990), its complete genomic organization was reported only recently (Li *et al.,* 1995). It is a large and complex gene that spans approximately 335 kb of genomic DNA and encodes a protein (neurofibromin) of 2818 amino acids (Marchuk *et al.,* 1991). The intron/exon boundaries of the coding region were recently characterized, and it was established that *NF1* is composed of 60 exons, inclusive of three alternatively spliced insertion exons (Li *et al.,* 1995; Danglot *et al.,* 1995). The *NF1* promoter region (Hajra *et al.,* 1994) and the 3′ untranslated region, which spans 3.5 kb of genomic DNA (Li *et al.,* 1995), have also only recently been characterized. *NF1* functions in part as a tumor suppressor gene, whereby inactivating mutations lead to loss of neurofibromin function associated with typical NF1-related tumors as well as other malignancies (Andersen *et al.,* 1993; Basu *et al.,* 1992; DeClue *et al.,* 1992; Johnson *et al.,* 1993; Legius *et al.,* 1993; Li *et al.,* 1992; The *et al.,* 1993; Shannon *et al.,* 1994; Xu *et al.,* 1992). This function is mediated, at least in part, by the GAP (GTPase activating protein)-related domain that, *in vitro,* stimulates hydrolysis of p21ras-GTP (Ballester *et al.,* 1990; Martin *et al.,* 1990; Xu *et al.,* 1990a). Thus, inactivating *NF1* mutations could play a significant role in tumorigenesis via altered signal transduction through p21ras.

Reliable identification of *NF1* mutations by PCR-based screening of *NF1* exons in genomic DNA would be useful for studies of NF1 disease and for analysis of the role of somatic *NF1* mutations both in sporadic tumorigenesis and in the variability of its clinical expression. The large size of the gene, high mutation rate, and the predominance of small deletions/insertions and point mutations have complicated the detection of *NF1* mutations. In addition, other loci have been observed to coamplify with the *NF1* gene in some PCR reactions when performed with primer pairs that lie upstream of exon 28, including segments that encode the catalytic domain of neurofibromin. An *NF1* related locus on chro-

Sequence data from this article have been deposited with the EMBL/GenBank Data Libraries under Accession Nos. U35684–U35699.

[1] To whom correspondence should be addressed at the Division of Medical Genetics, 413 MREB, University of Utah, Salt Lake City, UT 84112. Telephone: (801) 581-8943. Fax: (801) 585-5241.

0888-7543/95 $12.00

mosome 15 (GenBank Accession No. M84131) was reported by Legius *et al.* (1992), and a different locus on chromosome 15 that mapped to band 15q24–qter (NF1HHS; EMBL Accession No. X72619) was detected by Gasparini *et al.* (1993). *NF1*-homologous loci on chromosomes 14 and 22 were reported by Marchuk *et al.* (1991), and an *NF1*-related locus on chromosome 21 at 21q11.2 was reported by Suzuki *et al.* (1994). Other *NF1*-related loci, reported in abstract form, have been identified on chromosomes 2, 12, and 20 (Cummings *et al.,* 1993). The extent of homologies between *NF1* and the various *NF1*-related loci has not been elucidated.

In the process of sequencing genomic DNA clones both to determine *NF1* exon boundaries and to develop intron-based PCR primers for individual *NF1* exons, we identified exonic sequences from some of our genomic clones that did not match *NF1* cDNA sequence. In addition, sequence of several PCR products generated from total human genomic DNA from non-NF1 controls revealed genomic sequence that was clearly derived from more than one locus. This strongly suggested the presence of additional loci in the genome. We used the genomic clones as probes in FISH (fluorescence *in situ* hybridization) analysis to identify seven *NF1*-related loci, and we used PCR of monochromosomal somatic cell hybrids to identify two additional loci. To improve *NF1* mutation analysis using total genomic DNA as a template, we have designed a number of oligonucleotide primer pairs to amplify specifically from the *NF1* locus on chromosome 17 by PCR. Implementation of these primer pairs would simplify germline and somatic mutation detection using PCR-based methods and genomic DNA as a template.

MATERIALS AND METHODS

Isolation of NF1 genomic clones. P-1 bacteriophage clones containing human genomic DNA were identified with *NF1* exon probes by a high-density screening protocol (Li *et al.,* 1995). Pooled probes containing sequence from exons 8 through 10c, 18 through 21, and 26 through 27b were labeled by using *NF1* cDNA as template and exon-based oligonucleotides as primers. Hybridization was carried out under standard high-stringency conditions as previously described (Li *et al.,* 1995). Multiple P-1 bacteriophage clones were identified, and they were partially mapped to the *NF1* locus by their ability to serve as template for PCR under standard conditions using facing primers encompassing specific *NF1* exons. Cosmid clones carrying human genomic DNA prepared from peripheral blood leukocytes in the pWE15 vector (Stratagene, San Diego, CA) were isolated by standard techniques as previously described (Li *et al.,* 1995).

DNA sequencing. *NF1*-specific primers tagged with 21m13 (upstream primer) and m13RPI (downstream primer) sequences were used for PCR amplification of the purified genomic DNAs from cosmid and P1 clones. The PCR products were purified and sequenced using a test site protocol provided by Applied Biosystems Inc. (Foster City, CA) as previously described (Li *et al.,* 1995). Subcloned genomic DNA in Bluescript was sequenced by the dideoxy method as described previously (Li *et al.,* 1995).

FISH analysis. Metaphase chromosome preparations of lymphoblastoid cell lines were prepared by standard techniques. FISH was performed as previously described for cosmid probes (Xu *et al.,* 1994) and P1-bacteriophage probes (Albertsen *et al.,* 1994). In brief, chromosomes were first G-banded using trypsin/Wright stain, and representative cells were photographed. Slides were destained in fixative and then used for hybridizations. Genomic clones were labeled with biotin using the BioNick kit labeling system (BRL, Gaithersburg, MD). Approximately 250 ng of probe and 15 μg of human Cot-1 DNA were mixed, denatured at 75°C, and preannealed at 37°C for 1–4 h before placement on the slide. After hybridization at 37°C for 16 h, the slides were washed in 50% formamide at 37°C and 2× SSC at 47°C for both P1 and cosmid clones. Biotin signals were detected using fluorescein-conjugated avidin and amplified with biotinylated goat anti-avidin, followed by a second layer of fluorescein–avidin. Fluorescence was visualized using a Olympus BX50 epifluorescence microscope equipped with filter sets specific for FITC. Chromosomes were counterstained with propidium iodide and the metaphases that were photographed by banding were identified and photographed showing hybridization for chromosome signals. FISH signals for each metaphase were mapped to the respective chromosomal band by visual comparison of photographs.

PCR amplification of monochromosomal somatic cell hybrids. The DNA from human/rodent somatic cell hybrid cultures with a reduced number of human chromosomes (Repository No. NA 10868) was obtained from Coriell Cell Repositories (Human Genetic Mutant Cell Repositories, Camden, NJ). PCR amplification of exons 1–27b from DNA from monochromosomal somatic cell hybrids and from mouse and hamster, depending on the rodent background, was performed using primer pairs previously described (Li *et al.,* 1995). PCRs were performed on a Perkin–Elmer Cetus thermocycler. In general, all of the PCRs were performed for 30 cycles, in a final volume of 50 μl. The monochromosomal somatic cell hybrid DNA template used was 50 ng in a final volume of 50 μl except for exons 8, 9, 10a, 10c, and 23-2, where the concentration of the DNA template used was 50 ng in 25 μl. A master mix was made for 25 tubes that had the following components at final concentrations: 1× PCR buffer (Gibco–BRL, Grand Island, NY), 0.2 m*M* each dNTP, 1.5 m*M* $MgCl_2$, 0.5 μM upstream and downstream primers, and water up to 25 or 50 μl. The PCR mixes were assembled on ice using a dedicated set of pipettes, and the mixture was UV irradiated at 254 nm for 10 min (Stratalinker). The mixture was aliquoted into microfuge tubes, and 1 unit of *Taq* polymerase and the appropriate DNA template were added. The cycling conditions consisted of initial denaturation at 94°C for 5 min followed by 30 cycles of denaturation at 94°C for 1 min, 56°C for 1 min, and 72°C for 1 min followed by a final extension of 72°C for 5 min.

RESULTS

Identification and Characterization of Genomic Clones

We used *NF1* cDNA segments to isolate genomic clones from cosmid and P1-bacteriophage libraries to achieve full coverage of the *NF1* locus as a contig. Approximately 400 kb of genomic DNA is encompassed by either cosmid or P1 clones, yet, even though all 60 *NF1* exons are represented in genomic clones from this contig (Li *et al.,* 1995), a gap remains in intron 1. To fill this gap and further refine the contig map in the 5′ end of *NF1,* a PCR-based approach was used to identify the extent of exon representation in each of the genomic clones. Using intron-based primer pairs flanking each exon, we PCR-amplified genomic DNA from all of the clones in the contig. The presence of the appropriate size band as detected by agarose gel electrophoresis confirmed the presence of that specific exon and enabled us to compile the *NF1* exon content of each clone.

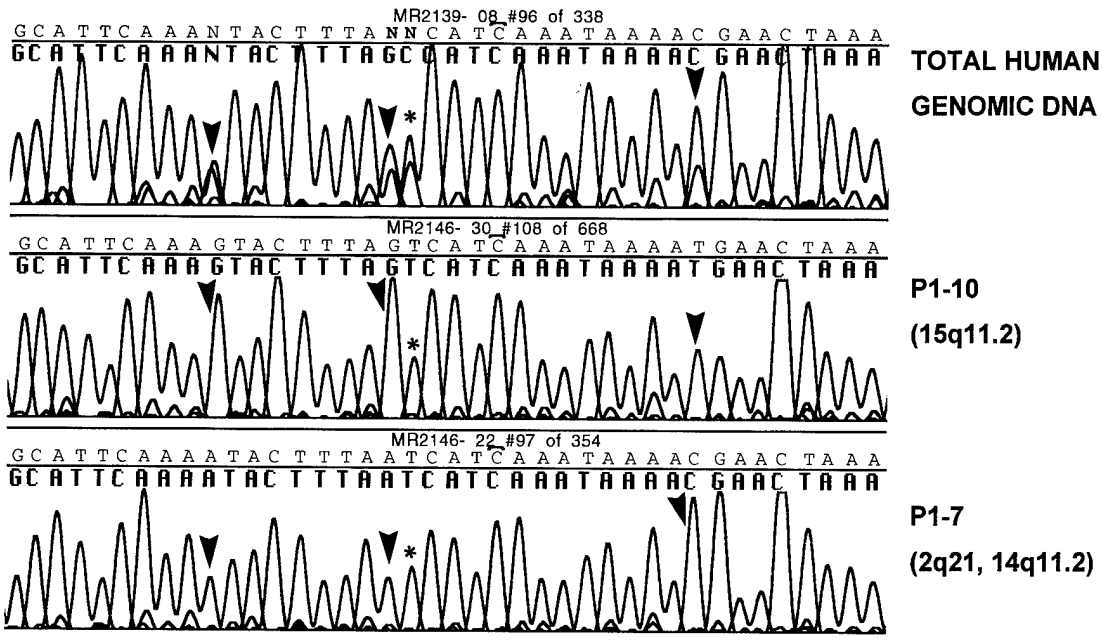

FIG. 1. An example of sequence analysis of a PCR product flanking exon 18 using total human genomic DNA and DNA from P1 clones P1-10 and P1-7 as template. Total human genomic DNA shows coamplification of more than one base at the positions marked by arrowheads. The first arrowhead shows coamplification of a G and an A and P1-10 shows a G, while P1-7 shows an A. Similarly, the second arrowhead shows coamplification of a G and an A and P1-10 shows a G, while P1-7 shows an A. The third arrowhead shows coamplification of a T and a C, and P1-10 shows a T, while P1-7 shows a C. The base marked by an asterisk shows coamplification of a T and a C, and P1-10 and P1-7 both show a C; the T comes from chromosome 22 not represented by either of these clones, but identified by PCR amplification of somatic cell hybrids.

We used the same primer pairs in *NF1*-mutation analysis to amplify uncloned total genomic DNA template, and sequences from some PCR products were ambiguous even though 4% agarose gels showed only single bands. In our efforts to optimize the sequencing protocols from uncloned genomic DNA template, we sequenced PCR products from the various genomic clones, each of which represent single alleles. Exon DNA sequence from PCR products synthesized with intron-based primers using cos 30 and P1-9 DNA template was identical to *NF1* cDNA sequence for multiple exons. However, using identical analysis, other cosmid and P1 clones, namely P1-4, P1-7, P1-15 and cos A, which were originally identified with *NF1* cDNA probes, revealed discrepancies with the *NF1* cDNA sequence. Figure 1 shows an example of sequence analysis of a PCR product flanking exon 18 using total human genomic DNA and DNA from P1 clones P1-10 and P1-7 as template. Total human genomic DNA shows coamplification of more than one base at the positions marked by arrowheads, and both bases are represented by the two P1 clones, which differ from the *NF1* locus at those sites. To characterize these separate loci better, we applied the technique of fluorescence *in situ* hybridization to map various *NF1* cDNA-selected genomic clones to their respective loci on metaphase chromosome spreads.

Fluorescence in Situ Hybridization

FISH analysis was performed for two cosmids, cos A and cos 30, and eight P1-bacteriophage clones, P1-4, P1-7, P1-9, P1-10, P1-12, P1-15, P1-16, and P1-60. Examples of FISH mapping studies are shown in Fig. 2 for three P1 clones, P1-10, P1-16, and P1-7. The left-hand photo in Fig. 2A shows strong hybridization of P1-10 to a D group chromosome, and the right-hand photo shows a G-banding pattern of the same metaphase spread, which enabled us to map the locus to chromosome 15 at band 15q11.2. Twenty cells that showed signal on both homologues were evaluated for the number of chromatids with signal (expect four per cell) to estimate the efficiency of hybridization, which was 63% for P1-10. The left-hand photo of Fig. 2B shows hybridization of P1-16 to an A group chromosome, and the right-hand photo locates the map position to bands q33–q34 on chromosome 2. The efficiency of hybridization is 53% for P1-16. The FISH photo in Fig. 2C shows weaker hybridization signal of P1-7 to a group A chromosome and a group D chromosome, and

FIG. 2. FISH analysis on the left and G-banded chromosome analysis on the right for identical metaphase spreads. (**A**) FISH mapping of P1-10 to chromosome 15q11.2. (**B**) FISH mapping of P1-16 to chromosome 2q33–q34. (**C**) FISH mapping of P1-7 to chromosomes 2q21 and 14q11.2.

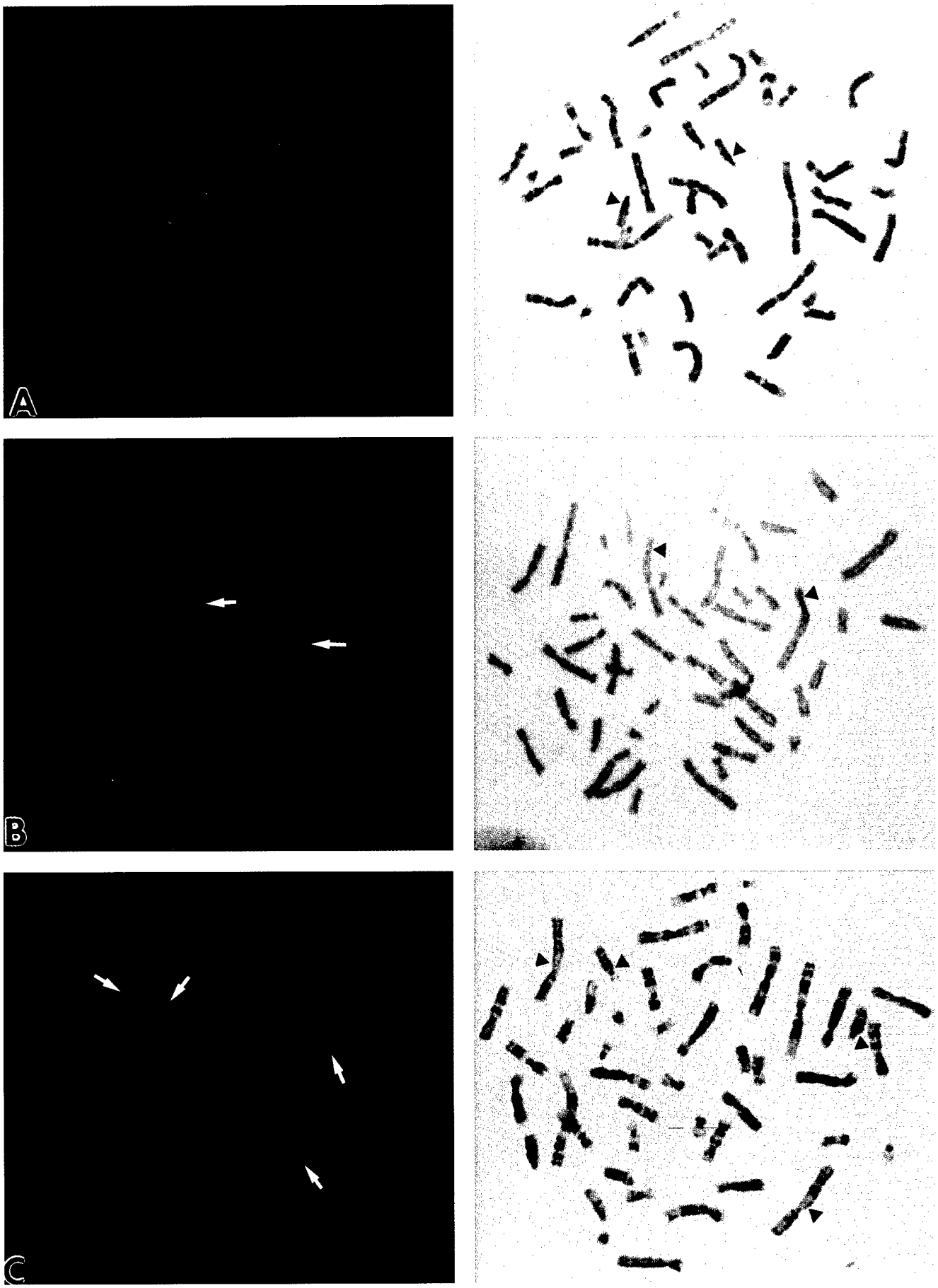
A
B
C

TABLE 1

Chromosomal Location of Genomic Clones That Were Selected by High-Stringency Hybridization Using *NF1* cDNA Segments as Probes

Genomic clone	Chromosomal location	Method of determination	*NF1* exons
Cos HB5	17q11.2	Seq, SBA	5′UTR-1
P1-60	17q11.2	FISH	5′UTR-1
Cos 30	17q11.2	Seq, FISH	2-6
P1-9	17q11.2	Seq, FISH	2-11
Cos 10	17q11.2	Seq	10c-23-1
Cos 23	17q11.2	Seq	23-2-27b
P1-12	17q11.2	FISH	Intron 27b
Cos 7	15	Seq	
Cos A	18p11.2, 21p11.2	FISH	
P1-16	2q33–q34	FISH	
P1-15	2q33–q34, 14q11.2, 22q11.2	FISH	
P1-7	2q21, 14q11.2	FISH	
P1-4	15q11.2	FISH	
P1-10	15q11.2	FISH	

Note. Seq, sequence identity by comparison; FISH, fluorescence *in situ* hybridization; SBA, Southern blot analysis. The right-hand column shows exon representation of the *NF1*-specific genomic clones.

the adjacent photo maps the FISH signals to chromosome 2 at band 2q21 and chromosome 14 at band 14q11.2. The efficiency of hybridization was estimated to be 99% for the chromosome 2 locus and 93% for the chromosome 14 locus for 20 metaphases evaluated. The chromosomal location of other clones mapped by FISH analysis is shown in Table 1. These loci have been designated as *NF1* loci (NF1-L) and they map to chromosome 2, *NF1L2* at 2q21 and *NF1L3* at 2q33–q34, chromosome 14, *NF1L4* at 14q11.2, chromosome 15, at 15q11.2, chromosome 18, *NF1L5* at 18p11.2, chromosome 21, at 21q11.2–q21, and chromosome 22, *NF1L6* at 22q11.2. The loci on chromosome 15 and 21 have been previously designated, as they have also been reported by other authors.

Monochromosomal Somatic Cell Hybrid PCR Analysis

NF1-homologous loci were also characterized by PCR amplification and direct sequencing of PCR products from monochromosomal somatic cell hybrids. Using DNA extracted from somatic cell hybrids containing single human chromosomes in a rodent background, we attempted amplification from each monochromosomal somatic cell hybrid with a combination of both intron-based and exon-based primers corresponding to *NF1* exons 1 through 27b. Exon-based primers over different segments of the *NF1* gene did not identify intronless (processed) pseudogenes. Each intron-based, exon-specific primer set was used to PCR amplify monochromosomal somatic cell hybrid DNA. The exonic segments of the *NF1* gene that coamplify from both the *NF1* locus and other chromosomes are listed in Table 2, and the respective sequence differences are also presented. In summary, PCR amplification of somatic cell hybrids confirmed the FISH mapping studies for chromosomes 2, 14, 15, 18, 21, and 22 and identified other homologous loci on chromosomes 12 and 15.

NF1-Related Loci on Chromosome 15

We used PCR amplification of somatic cell hybrids and FISH analysis to demonstrate two loci on chromosome 15. We previously identified one locus by evaluation of an SSCP variant PCR product. The primers FLR5, 5′-GTTAGCCAGCGTTTCCCTCAG-3′, and FLR3, 5′-GATTCTAGGTGGTGGCTTTTTATC-3′, PCR amplify a 129-bp product spanning a segment of exon 24 in the *NF1*-GRD that encodes the highest density of amino acid residues completely conserved in neurofibromin, p120GAP, and the yeast IRA proteins. When this primer pair was used against total human genomic DNA, a clean product of the expected size was seen on agarose gel electrophoresis. However, when the products were analyzed by single-stranded conformer analysis (PCR-SSCP, Orita *et al.,* 1989), a single com-

TABLE 2

Compilation of *NF1* Seqments That Coamplify by PCR and Show Sequence Differences between the *NF1* Locus and Homologous Loci from the Various Chromosomes

Exon	Locus	Sequence alterations
7	chr 21	9 substitutions
8	chr 18	8 substitutions
	chr 21	4 substitutions, 3-bp del
9	chr 18	3 substitutions
	chr 21	4 substitutions
11	chr 21	2 substitutions
13	chr 2	7 substitutions, 1-bp ins (A), 2-bp del
	chr 14	11 substitutions, 1-bp ins (T), 2-bp del
15	chr 14	4 substitutions
	chr 15	5 substitutions
16*	chr 12	14 substitutions, 1-bp del (G)
	chr 14	15 substitutions
17	chr 14, 22	Sequence not available
18	chr 14	9 substitutions
	chr 15	6 substitutions, 1-bp del
	chr 22	6 substitutions
19a	chr 14, 22	Sequence not available
19b	chr 15	3 substitutions, 4-bp ins
20	chr 15	11 substitutions
21	chr 15	14 substitutions, 1-bp del, 3-bp del
22	chr 15	Sequence not available
23-1	chr 15	3 substitutions
24	chr 15 (q11.2)	10 substitutions
	chr 15 (q24–qter)	8 substitutions
27a	chr 15	8 substitutions, 1-bp del
27b	chr 14	Sequence not available
	chr 15	12 substitutions, 3-bp del

Note. For exon 16 marked by an asterisk, alterations are reported in comparison with *NF1* cDNA position 2455 to 2745. Sequence from each locus has been submitted to GenBank.

plex pattern was obtained from all individuals tested. When an *NF1* genomic clone from this region, cos 10, was used as a template, a subset of the complex pattern was seen. This suggested that a locus elsewhere in the genome was coamplifying along with *NF1*. Direct sequencing of PCR products prepared from each SSC band revealed two sequences, one matching the known *NF1* sequence, the other differing by basepair substitutions at seven sites in exon 24 (bases 4111 through 4269): at bases 4122 (G to A), 4140 (C to T), 4144 (G to A), 4151 (T to C), 4179 (C to G), 4187 (C to A), and 4199 (C to T). This locus was mapped to chromosome 15 by performing the same PCR-SSCP analysis on a panel of human/rodent somatic cell hybrids from BIOS (New Haven, CT). Sublocalization within chromosome 15 was not possible using this hybrid system; however, this sequence is identical to that of NF1-HHS (Gasparini *et al.,* 1993), which was localized to q24 to qter from chromosome 15. The demonstration of an *NF1*-related locus on chromosome 15 at band q11.2 by FISH, using P1-4 and P1-10 clones as probes, predicted the presence of a second separate locus on this chromosome. The sequence of a PCR product for exon 24 from P1-4 differs by three bases from the NF1-HHS sequence at bases 4117 (C/A), 4188 (C/T), and 4244 (A/G), which supports the hypothesis that there are two loci on chromosome 15. We compared sequences from exons 20, 21, and 27a between clone P1-4 and the *NF1*-related locus, and the sequences were identical for 541 bp, which suggests that the *NF1*-related locus (Legius *et al.,* 1992) maps to 15q11.2. However, there are significant sequence differences between the *NF1*-related locus and P1-4 in exon 24, where only 6 bases are identical. This observation raises the possibility that these two loci are also distinct.

Development of Primer Pairs for NF1 Mutation Analysis

To evaluate the usefulness of our intron-based, exon-specific primer pairs in *NF1* mutation analysis, we have examined PCR amplification of uncloned genomic DNA for exons 1 through 27b, using previously published *NF1* primer sets (Li *et al.,* 1995). Some primer pairs coamplify from *NF1* and homologous loci; therefore, based on sequence differences, we redesigned most primer sets to be *NF1*-specific (Table 3).

Primer pairs for exons 8, 9, 15, 21, 27a, and 27b do not specifically amplify *NF1* from uncloned genomic DNA; therefore, to remain useful in mutation detection analysis, we attempted to separate PCR products amplified from different loci both by denaturing polyacrylamide gel electrophoresis and SSCP. Sequence analysis of aberrant bands revealed the presence of basepair substitutions, deletions, and insertions among exon and intron sequence in the homologous loci; thus, these loci likely represent nonprocessed pseudogenes. Radiolabeled PCR products amplified from total human genomic DNA, DNA specific to chromosome 17, and DNA from the homologous loci from the respective monochromosomal somatic cell hybrids were subjected to denaturing gel electrophoresis to detect size shifts. As part of this analysis the absence of amplification from the rodent background was documented for all exons except exon 23a, where we were able to separate human from amplified rodent DNA by SSCP analysis. Products for exons 21, 27a, and 27b from the individual chromosomes demonstrated fragment size variants of 1–3 bp that were easily separated on denaturing gels. For example, as shown in Fig. 3 for 27a, the PCR product from total human DNA amplified from both chromosome 17 and the homologous locus on chromosome 15. The difference in migration of the PCR product represents a basepair deletion in the chromosome 15 locus for exon 27a, which was confirmed by sequence analysis showing a basepair deletion of guanine at position 4451 in the *NF1* cDNA sequence. In addition, we performed single-stranded conformer analysis (Orita *et al.,* 1989) for the products that did not show a size shift on denaturing gel electrophoresis (exons 9 and 15). SSCP analysis of these products demonstrated the presence of aberrant bands indicative of multiple basepair substitutions, which, by DNA sequencing, showed 4 basepair substitutions in exon 9 and 5 basepair substitutions in exon 15. Using these techniques, *NF1* mutations represented by aberrant bands distinct from defined homologous loci could be identified, even when primers coamplify *NF1*-homologous loci.

DISCUSSION

Even though *NF1*-related loci had previously been reported for sequences in the 5′ region of the *NF1* gene, we were surprised by the number of non-*NF1* genomic clones that were isolated under normal stringency screening conditions. More surprising was the observation that clones from different loci amplified equivalently sized products (by 4% agarose gels) when intron-based, *NF1* exon-specific primer pairs were used in PCR. Only when PCR products were sequenced did it become clear that many clones represented *NF1*-homologous loci.

The clones with the divergent sequences mapped to different loci based on fluorescence *in situ* hybridization analysis. Given the degree of homology at multiple exons, including flanking intron sequences between numerous genomic clones representing different loci, it was surprising that the majority of clones hybridized to specific chromosomal regions by FISH without cross-hybridizing to other loci. Three clones specifically hybridized to a single locus, while three other non-*NF1* clones hybridized to multiple loci: cos A represents the homologous locus on 21q11.2 by sequence identity and cross-hybridizes to 18p11.2; P1-7, which likely represents NF1L2 at 2q21, cross-hybridizes to 14q11.2; and P1-15 hybridizes to 2q33–q34, 14q11.2, and 22q11.2.

TABLE 3

Primer Pairs for *NF1*-Specific Amplification of Exons 1–27b

Exon	Primer sequence 5′–3′	Exon	Primer sequence 5′–3′
1	CAGACCCTCTCCTTGCCTCTT	14	TCCTTTTGGGTGGAGCTTATC
	GGATGGAGGGTCGGAGGCTG		TATACTTGTAATATGCACGTATC
2	TTTTAAGGATAAACTGTTTACGTG	15*	TGTGATCAGGAATAGCTTTTGAA
	TCCCCAAAACACAGTAACCC		TTAACAGATAAAAGTCAACTTTAC
3	TTTCACTTTTCAGATGTGTGTTG	16	TGGATAAAGCATAATTTGTCAAGT
	TGGTCCACATCTGTACTTTG		TAGAGAAAGGTGAAAAATAAGAG
4a	TTTGAAAATTTTCATAATAGAAAATGT	17	CTCTGTGTGTTTAGATCAGTCA
	GAGGTCAAAGCTGCTGTGAG		TTTATCAATTACTACCAGTAGCAG
4b	CTCCTGGCCTCAAGTGGTC	18	AGAAGTTGTGTACGTTCTTTTCT
	TTATAAAATCCAGATTGGTGTTC		CTCCTTTCTACCAATAAGCGC
4c	TTTCCTAGCAGACAACTATCGA	19a	TCATGTCACTTAGGTTATCTGG
	CATCAAAAAAAAAAATTTTAATACCAG		TGTAATTAAGTAGTTATAACTCTC
5	TGACTTGAGTGATAGTTTCACAT	19b	AACTTGAAAGATTCATGGTCTC
	AAAAAAAAATCAATCGTATCCTTA		TTTATGTTTTTTGGTGACTG
6	CATGTTTATCTTTTAAAAATGTTGCC	20	CCACCCTGGCTGATTATCG
	ATAATGGAAATAATTTTGCCCTCC		TAATTTTTGCTTCTCTTACATGC
7	TGCTATAATATTAGCTACATCTGG	21*	AAATGAAAGTTTCATATAGAAATAC
	CCTATGAACTTATCAACGAAGAG		ATTTGCTATGTGCCAGGGAC
7 and 8*	TGCTATAATATTAGCTACATCTGG	22	TGCTACTCTTTAGCTTCCTAC
	CTAGTCTTTCTGTTTATAAAGGAT		CCTTAAAAGAAGACAATCAGCC
9*	TTTGACCTCATTTGTATTACTGAG	23-1	TTTGTATCATTCATTTTGTGTGTA
	AGAACCTTTTGAAACCAAGAGTG		AAAAACACGGTTCTATGTGAAAAG
9a (br)	TCCGCTGTGGCTCAGAACAC	23-2	CTTAATGTCTGTATAAGAGTCTC
	AGTAGAAGAGGATGCACAGCC		ACTTTAGATTAATAATGGTAATCTC
10a	ACGTAATTTTGTACTTTTTCTTCC	23a	AGCCAGAAATAGTATACATGATTGGGT
	CAATAGAAAGGAGGTGAGATTC		CTATTTTCTGCCAGAATTAGTAGA
10b	AACTATTGAGTGTTCTACTATACC	24	TTGAACTCTTTGTTTTCATGTCTT
	TCTTGGCGATTCAGCTAAACC		GGAATTTAAGATAGCTAGATTATC
10c	CTTGGTACCCTTTAGCAGTCAC	25	AATATAATAATTATATTTGGGAAGGT
	CCTTCTTTCTCCATGGAG		GAAAATATTTGATTCAAACAGAGC
11	GTACTCCAGTGTTATGTTTACC	26	GCTTTGTCTAATGTCAAGTCAC
	TAAAGTTGAAATTTAAAAATTAAAGTAC		TTAAACGGAGAGTGTTCACTATC
12a	AAACCTTACAAGAAAAACTAAGCT	27a*	GTTACAAGTTAAAGAAATGTGTAG
	ATTACCATTCCAAATATTCTTCCA		CTAACAAGTGGCCTGGTGGCAAAC
12b	TTTCTAGTGAATCTCCTTCAAGT	27b*	TTTATTGTTTATCCAATTATAGACTT
	ATGAAATTTACCAAATTTCATTCAG		TCCTGTTAAGTCAACTGGGAAAAAC
13	CACAGTTTATTGCATTGTTAGAT		
	GCCATGTGCTTTGAGGCAGAA		

Note. Primer pairs marked by an asterisk for exons 8, 9, 15, 21, 27a, and 27b amplify from chromosome 17 and the homologous loci. Primer pairs for exons 7 and 8 have been combined and amplify an ~700-bp PCR product, which amplifies preferentially from chromosome 17, but also amplifies from the homologous loci on chromosomes 18 and 21. Primer pairs for exon 9a (identical to exon 9br—Danglot *et al.,* 1995) were derived from sequence submitted to GenBank.

Of note, none of the clones from *NF1*-related loci cross-hybridize to chromosome 17. Furthermore, all of the *NF1* clones hybridized only to 17q11.2. These observations suggest that FISH is likely specified by the intron sequences. This may simply reflect long stretches of unique DNA within the introns, which would imply a higher degree of divergence in intronic versus exonic sequences in each of the *NF1*-related loci. Alternatively, these intron sequences may have a higher efficiency of hybridization in FISH analysis, due to repetitive, lower complexity intron sequences in the respective loci. Some insight to this observation of FISH specificity may be gained by direct comparison of intron sequences between *NF1* and *NF1*-related loci and/or the performance of FISH analysis under different hybridization conditions.

NF1-related sequences have been previously reported on chromosomes 2, 12, 14, 15, 20, 21, and 22 (Legius *et al.,* 1992; Marchuk *et al.,* 1991; Cummings *et al.,* 1993; Gasparini *et al.,* 1993; Suzuki *et al.,* 1994). Our evidence independently confirms the finding of previously reported loci, and it demonstrates a second locus on chromosome 2 and a locus on chromosome 18, neither of which have been described previously. The application of FISH in this study also provides an approximate band position for each of the related loci on chromosomes 2, 14, 15, 18, 21, and 22 (Table 1). It is interesting to note that the location of P1-15 on chromosome 22 maps to band q11.2, which is the breakpoint for a balanced t(17;22) translocation that was instrumental in physically mapping the *NF1* gene (Ledbetter *et al.,* 1989). Additional loci on chromosomes 12 and 15

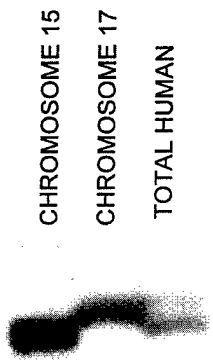

FIG. 3. Denaturing gel electrophoresis of a PCR product for exon 27a from total human genomic DNA and DNA from monochromosomal somatic cell hybrids for chromosomes 15 and 17. The product using total human genomic DNA as a template shows coamplification from the locus on chromosome 15 and chromosome 17. The product from the chromosome 15 locus shows the presence of a deletion, indicated by the shorter length of the product in comparison with the locus on chromosome 17, which on sequencing was shown to be a single base deletion of guanine (position 4451 in the *NF1* cDNA). The primer pair used is I27aUP and I27aRP (Li *et al.,* 1995). There was no amplification of rodent DNA using this primer set.

have been identified by PCR of somatic cell hybrids; neither locus is represented in our set of FISH-mapped genomic clones.

The most extensively characterized *NF1*-homologous locus is the *NF1*-related locus on chromosome 15 (Legius *et al.,* 1992). In addition, a separate locus on chromosome 15 (NF1-HHS at 15q24–qter), which differs from that described by Legius *et al.* (1992), has been reported by Gasparini *et al.* (1993) based on sequence divergence of a single PCR product amplified by *NF1* primers derived from sequences in a segment encompassing exon 24. By FISH analysis we demonstrate a chromosome 15 locus that maps to 15q11.2 using both P1-4 and P1-10 clones as probes. Comparison of the *NF1*-homologous locus on 15q11.2, represented by sequence from the two clones P1-4 and P1-10, to the *NF1*-related locus on chromosome 15 showed complete identity for exons 20, 21, and 27a, which supports the localization of the *NF1*-related locus (Legius *et al.,* 1992) to 15q11.2. However, the sequence from the *NF1*-related locus cDNA diverges remarkably from the sequence represented by P1-4 for exon 24. We hypothesize either that this may represent a third locus on chromosome 15 or that the exon 24 sequence depicted from the *NF1*-related locus may not represent the genomic sequence. The sequence reported by Legius *et al.* (1992) is a PCR product from cDNA synthesized by reverse transcription of total RNA isolated from cultured human/rodent somatic cell hybrid cells containing chromosome 15 as the human complement. It is possible that the primary transcript from this homologous locus is processed differently and exon 24 is aberrantly spliced. Furthermore, the *NF1*-related locus sequence contains only 12 bases of exon 24, and only 9 of those 12 are identical with *bona fide NF1* cDNA sequence. This raises the possibility that this sequence may not truly represent exon 24 sequence from the *NF1*-related locus at the genomic level. We have also independently confirmed the existence of homologous loci on chromosomes 14 and 22 (Marchuk *et al.,* 1991) and chromosome 21 at 21q11.2 (Suzuki *et al.,* 1994) by FISH and PCR of somatic cell hybrids.

Genetic variation within pseudogenes may be important reservoirs that cause mutations by homologous recombination between pseudogenes and genomic segments encoding functional domains. Conversions between gene and pseudogene have been previously reported for a number of genes (Braun *et al.,* 1990; Sorge *et al.,* 1990; Urabe *et al.,* 1990; Matsuno *et al.,* 1992; Collier *et al.,* 1993; He and Grabowski, 1993), all of which represent linked loci. The only example of gene conversion for unlinked loci was reported for the von Willebrand factor gene on chromosome 12 and its pseudogene on chromosome 22 (Eikenboom *et al.,* 1994). This raises the hypothesis that homologous recombination involving intragenic segments between *NF1* and *NF1*-homologous loci could be the etiology of some *NF1*-disease causing mutations (Cummings *et al.,* 1993). Mutation by gene conversion predicts that some *NF1* mutations would correspond to sequences from *NF1*-homologous loci. We have examined 21 known *NF1* mutations (NNFF Mutation Analysis Consortium Newsletter, June 1995) that lie in exons for which we have detected *NF1*-homologous segments. Only one mutation, R1513X in exon 27a, corresponds to a base change in an *NF1*-homologous locus on 15q11.2; however, this mutation occurs at a highly mutable CpG site. Thus, this limited analysis provides no direct evidence of *NF1* gene conversion.

NF1-homologous loci complicate mutation analysis of the *NF1* gene. We have detected regions homologous to exons 7, 8, 9, 11, 13, 15, 16, 17, 18, 19a, 19b, 20, 21, 22, 23-1, 24, 27a, and 27b on chromosomes 2, 12, 14, 15, 18, 21, and 22. To design *NF1*-specific primers, we sequenced intronic segments from PCR products from both genomic clones and monochromosomal somatic cell hybrids representing *NF1*-related loci and compared them with *bona fide NF1* sequence. New primers were designed to have natural mismatches with the homologous sequences at the 3′ end of the oligonucleotides. When only a single naturally occurring mismatch was available, we created an additional mismatch to increase primer specificity, whereby multiple mismatches would lead to preferential hybridization of the primer to the *NF1* locus. Thus, we have compiled a set of oligonucleotide primer pairs that amplify uncloned human DNA template specifically from the *NF1* locus (Table 3); only primer pairs for exons 8, 9, 15, 21, 27a, and 27b are nonspecific. PCR amplification using these *NF1*-primer pairs has simplified the DNA-based

screening protocol for detection of mutations within the *NF1* gene.

ACKNOWLEDGMENTS

We acknowledge Margaret Robertson for various aspects of DNA sequencing, Edward Meenan for oligonucleotide synthesis, Jeff Stevens, Robert Weiss, and Diane Dunn for various aspects of P1-bacteriophage library screening, and the Molecular Cytogenetics Core facility of the Huntsman Cancer Institute, University of Utah Health Sciences Center. We thank Mark Leppert for the monochromosomal somatic cell hybrid DNA, and Aron Branscomb for useful discussions. R.C. was supported by the Howard Hughes Medical Institute, the National Neurofibromatosis Foundation, the National Cancer Institute (R55CA57511-01), and the U.S. Department of the Army (DAMD 17-93-J-3044). D.V. was supported by the National Institute of Neurological Disorders and Stroke (K08 NS01492) and the U.S. Department of the Army (DAMD 17-93-J-3070).

REFERENCES

Albertsen, H. M., Smith, S. A., Mazoyer, S., Fujimoto, E., Stevens, J., Williams, B., Rodriguez, P., Cropp, C. S., Slijepcevic, P., Carlson, M., Robertson, M., Bradley, P., Lawrence, E., Sheng, Z. M., Hoopes, R., Sternberg, N., Brothman, A. R., Callahan, R., Ponder, B. A. J., and White, R. (1994). A physical map and candidate genes in the BRCA1 region. *Nature Genet.* **7:** 472–479.

Andersen, L. B., Fountain, J. W., Gutmann, D. H., Tarle, S. A., Glover, T. W., Dracopoli, N. C., Housmann, D. E., and Collins, F. S. (1993). Mutations in the neurofibromatosis 1 gene in sporadic melanoma cell lines. *Nature Genet.* **3:** 118–121.

Ballester, R., Marchuk, D., Boguski, M., Saulino, A., Letcher, R., Wigler, M., and Collins, F. (1990). The NF-1 locus encodes a protein functionally related to mammalian GAP and yeast IRA proteins. *Cell* **63:** 851–859.

Barker, D., Wright, E., Nguyen, K., Cannon, L., Fain, P., Goldgar, D., Bishop, D. T., Carey, J., Baty, B., Kivlin, J., Willard, H., Waye, J. S., Greig, G., Leinwald, L., Nakamura, Y., O'Connell, P., Leppert, M., Lalouel, J. M., White, R., and Skolnick, M. (1987). Gene for Von recklinghausen neurofibromatosis is in the pericentromeric region on chromosome 17. *Science* **236:** 1100–1102.

Basu, T. N., Gutmann, D. H., Fletcher, J., Glover, T. W., Collins, F. S., and Downward, J. (1992). Aberrant regulation of ras proteins in malignant tumour cells from type-1 neurofibromatosis patients. *Nature* **356:** 713–715.

Braun, L., Schneider, P. M., Giles, C. M., Bertrams, J., and Rittner, C. (1990). Null alleles of human C4. *J. Exp. Med.* **171:** 129–140.

Cawthon, R. M., Weiss, R., Xu, G., Viskochil, D., Culver, M., Stevens, J., Robertson, M., Dunn, D., Gesteland, R., O'Connell, P., and White, R. (1990). A major segment of the neurofibromatosis type 1 gene: cDNA sequence, genomic structure and point mutations. *Cell* **62:** 193–201.

Collier, S., Tassabehji, M., and Strachan, T. (1993). A *de novo* pathological point mutation at the 21-hydroxylase locus: Implications for gene conversion in the human genome. *Nature Genet.* **3:** 260–265.

Crowe, F. W., Schull, W. J., and Nell, J. V. (1956). "A Clinical, Pathological, and Genetic Study of Multiple Neurofibromatosis," Charles C. Thomas, Springfield, IL.

Cummings, L. M., Glatefeller, A., and Marchuk, D. A. (1993). NF-1 related loci on chromosomes 2, 12, 14, 15, 20, 21, and 22: A potential role for gene conversion in the high spontaneous mutation rate of NF-1? *Am. J. Hum. Genet.* **53**(Suppl. 3): A672.

Danglot, G., Regnier, V., Fauvet, D., Vassal, G., Kujas, M., and Bernheim, A. (1995). Neurofibromatosis 1 (*NF1*) mRNAs expressed in the central nervous system are differentially spliced in the 5′ part of the gene. *Hum. Mol. Genet.* **4:** 915–920.

DeClue, J. E., Papageorge, A. G., Fletcher, J. A., Diehl, S. R., Ratner, N., Vass, W. C., and Lowy, R. D. (1992). Abnormal regulation of mammalian p21ras contributes to malignant tumour growth in Von Recklinghausen (Type1) neurofibromatosis. *Cell* **69:** 265–273.

Eikenboom, J. C., Vink, T., Briet, E., Sixma, J. J., and Reitsma, P. H. (1994). Multiple substitutions in the von Willebrand factor gene that mimic the pseudogene sequence. *Proc. Natl. Acad. Sci. USA* **91:** 2221–2224.

Gasparini, P., Grifa, A., Origone, P., Coviello, D., Antonacci, R., and Rocchi, M. (1993). Detection of a neurofibromatosis type 1 (NF-1) sequence by PCR: Implications for the diagnosis and screening of genetic diseases. *Mol. Cell. Probes* **7:** 415–418.

Hajra, A., Martin-Gallardo, A., Tarle, S., Freedman, M., Wilson-Gunn, S., Bernards, A., and Collins, F. (1994). DNA sequences in the promoter region of the NF-1 gene are highly conserved between human and mouse. *Genomics* **21:** 649–652.

He, G. S., and Grabowski, G. A. (1993). Gaucher disease: A G + 1 → A + 1 IVS2 splice donor site mutation causing exon 2 skipping in the acid β-glucosidase mRNA *Am. J. Hum. Genet.* **51:** 810–820.

Johnson, M. R., Look, A. T., DeClue, J. E., Valentine, M. B., and Lowy, D. R. (1993). Inactivation of the NF-1 gene in human melanoma and neuroblastoma cell lines without impaired regulation of GTP-ras. *Proc. Natl. Acad. Sci. USA* **90:** 5539–5542.

Ledbetter, D. H., Rich, D. C., O'Connell, P., Leppert, M., and Carey, J. (1989). Precise localization of NF1 to 17q11.2 by a balanced translocation. *Am. J. Hum. Genet.* **44:** 20–24.

Legius, E., Marchuk, D., Hall, B. K., Andersen, L. B., Wallace, M. R., Collins, F. S., and Glover, T. W. (1992). NF-1 related locus on chromosome 15. *Genomics* **13:** 1316–1318.

Legius, E., Marchuk, D. A., Collins, F. S., and Glover, T. W. (1993). Somatic deletion of the neurofibromatosis type 1 gene in a neurofibrosarcoma supports a tumour suppressor gene hypothesis. *Nature Genet.* **3:** 122–126.

Li, Y., Bollag, G., Clark, R., Stevens, J., Conroy, L., Fults, D., Ward, K., Friedman, E., Samowitz, W., Robertson, M., Bradley, P., McCormick, F., White, R., and Cawthon, R. (1992). Somatic mutations in the neurofibromatosis gene in human tumors. *Cell* **69:** 275–281.

Li, Y., O'Connell, P., Breidenbach, H. H., Cawthon, R., Stevens, J., Xu, G., Neil, S., Robertson, M., White, R., and Viskochil, D. (1995). Genomic organization of the neurofibromatosis 1 gene (*NF1*). *Genomics* **25:** 9–18.

Marchuk, D. A., Saulino, A. M., Tavakkol, R., Swaroop, M., Wallace, M. R., Andersen, L. B., Mitchell, A. L., Gutmann, D. H., and Collins, F. S. (1991). cDNA cloning of the type 1 neurofibromatosis gene: Complete sequence of the *NF1* gene product. *Genomics* **11:** 931–940.

Martin, G. A., Viskochil, D., Bollag, G., McCabe, P. C., Crosier, W. J., Haubruck, H., Conroy, L., Clark, R., O'Connell, P., Cawthon, R. M., Innis, M. A., and McCormick, F. (1990). The GAP related domain of the neurofibromatosis type 1 gene product interacts with ras p21. *Cell* **63:** 843–849.

Matsuno, Y., Yamashiro, Y., Yamamoto, K., Hattori, Y., Yamamoto, K., Ohba, Y., and Miyaji, Y. (1992). A possible example of gene conversion with a common β-thalassaemia mutation and Chi sequence present in the β-globin gene. *Hum. Genet.* **88:** 357–358.

Orita, M., Suzuki, Y., Sekiya, T., and Hayashi, K. (1989). Rapid and sensitive detection of point mutations and DNA polymorphisms using the polymerase chain reaction. *Genomics* **5:** 874–879.

Riccardi, V. M. (1992). Neurofibromatosis Phenotype, Natural History and Pathogenesis," 2nd ed., pp. 1–8, Johns Hopkins Univ. Press, Baltimore, MD.

Shannon, K. M., O'Connell, P., Martin, G. A., Paderanga, D., Olson, K., Dinndorf, P., and McCormick, F. (1994). Loss of the normal

NF1 allele from the bone marrow of children with type 1 neurofibromatosis and malignant myeloid disorders. *N. Engl. J. Med.* **330:** 597–601.

Sorge, J., Gross, E., West, C., and Beutler, E. (1990). High level transcription of the glucocerebrosidase gene in normal subjects and patients with Gaucher disease. *J. Clin. Invest.* **86:** 1137–1141.

Suzuki, H., Ozawa, N., Taga, C., Kano, T., Hattori, M., and Sakkai, Y. (1994). Genomic analysis of a *NF1*-related pseudogene on human chromosome 21. *Gene* **147:** 277–280.

The, I., Murthy, A. E., Hannigan, G. E., Jacoby, L. B., Menon, A. G., Gusella, J. F., and Bernards, A. (1993). Neurofibromatosis type 1 gene mutations in neuroblastoma. *Nature Genet.* **3:** 362–366.

Urabe, K., Kimura, A., Harada, F., Iwanga, T., and Sasazuki, T. (1990). Gene conversion in 21-hydroxylase genes. *Am. J. Hum. Genet.* **46:** 1178–1186.

Viskochil, D., Buchberg, A. M., Xu, G., Cawthon, R. M., Stevens, J., Wolff, R. K., Culver, M., Carey, J. C., Copeland, N. G., Jenkins, N. A., White, R., and O'Connell, P. (1990). Deletions and translocations interrupt a cloned gene at the neurofibromatosis type 1 locus. *Cell* **62:** 187–192.

Wallace, M. R., Marchuk, D. A., Andersen, L. B., Letcher, R., Odeh, H. M., Saulino, A. M., Fountain, J. W., Breeton, A., Nicholson, J., Mitchell, A. L., Brownstein, B. H., and Collins, F. S. (1990). Type 1 neurofibromatosis gene: Identification of a large transcript disrupted in 3 NF-1 patients. *Science* **249:** 181–186.

Xu, G., O'Connell, P., Viskochil, D., Cawthon, R., Robertson, M., Culver, M., Dunn, D., Stevens, J., Gesteland, R., White, R., and Weiss, R. (1990a). The neurofibromatosis type 1 gene encodes a protein related to GAP. *Cell* **62:** 599–608.

Xu, G., Lin, B., Tanaka, K., Dunn, D., Wood, D., Gesteland, R., White, R., Weiss, R., and Tamanoi, F. (1990b). The catalytic domain of the neurofibromatosis type I gene product stimulates rasGTPase and complements ira mutants of S. cerevisae. *Cell* **63:** 835–841.

Xu, P., Zhu, X. L., Hueckstead, T. P., Brothman, A. R., and Hoidal, J. R. (1994). Assignment of human xanthine dehydrogenase gene to chromosome 2p22. *Genomics* **23:** 289–291.

Xu, W., Mulligan, L. M., Ponder, M. A., Liu, L., Smith, B. A., Mathew, C. P. G., and Ponder, B. A. J. (1992). Loss of NF-1 alleles in phaeochromocytomas from patients with type-1 neurofibromatosis. *Genes Chrom. Cancer* **4:** 337–342.

日皮会誌：105（9），1187—1196，1995（平7）

神経線維腫症1の遺伝子解析

澤田俊一[1)2)] David H. Viskochil[2)]

要旨

10名のNeurofibromatosis 1（NF1）患者の末梢血白血球分画より抽出したconstitutional DNAを被験対象として*NF1*遺伝子変異の解析を行った．*NF1*遺伝子には現在59のエクソンが確認されているが，今回我々はそのうちエクソン40から49までの11エクソンについて，13の領域を増幅する*NF1*エクソン特異的プライマーを設定しpolymerase chain reaction（PCR）法を行い，さらに21M13, M13RP1ユニバーサルプライマーを用いて，size-shift assay，single strand conformation polymorphism（SSCP）法，magnetic beadsを利用したdirect sequence法で遺伝子変異の解析を行った．結果は1症例で，エクソン44においてNF1 disease causingと思われる*NF1*遺伝子の変異を確認した．この変異はcDNAポジション7712から7720までの9bpの欠失と，あわせて同部位に2bpが挿入された結果，7bpのフレームシフトを起こしコードする蛋白が異なり，32コドン下流でストップコドンの出現をみている．また我々は，イントロン40においてポリモルフィズムを検出した．今回の結果より，我々が確立したこの実験系が，*NF1*遺伝子変異の解析について有用であることが証明された．また21M13，M13RP1ユニバーサルプライマーならびにmagnetic beadsを利用したこの実験系は*NF1*遺伝子変異の解析のみならず，他の遺伝性疾患のDNA診断，感染症のDNA診断等にも有力な実験系であると考え報告した．

緒言

NF1は皮膚および神経の多発性神経線維腫，カフェ・オ・レ斑，虹彩小結節を主徴とし，骨病変，神経腫瘍，その他多彩な症候を呈する常染色体優性の遺伝性疾患である．DNAマーカーを利用したrestriction fragment length polymorphisms（RFLPs）解析により*NF1*遺伝子は17q11.2に座位することが明らかにされ，さらに1990年にクローン化され[2)3)]，その構造も次第に明らかにされてきている[1)4)~10)]．

また*NF1*-homologous lociの存在が近年報告されている[11)~15)]．*NF1*遺伝子蛋白はニューロファイブロミンと呼ばれ，その機能の解析も解析されつつある[5)16)~20)]．ニューロファイブロミンはチューブリンへの局在が最近報告されている[21)22)]．

また*NF1*遺伝子について，特に変異のホットスポットは認められていない[2)4)15)23)~41)]．*NF1*遺伝子が巨大遺伝子であり，その全てのエクソンについて検討されていないことが，検索された症例の20%以下にしか変異が見つかっていない原因と考えられる．我々は当初49と報告されたエクソンが，59に分けられることを報告し（Table 1），それぞれのエクソンを特異的に増幅するプライマーを作製した[1)]．今回パイロットスタディーとしてエクソン40から49までを解析し，遺伝子変異検出の実験系を確立し，さらに興味ある変異を検出したので報告する．

対象と方法

1）対象

米国ユタ大学小児科NF外来を受診した10名のNF1患者より，採血によって得た末梢血白血球分画より抽出したDNAを解析の対象とした．いずれも父親か母親にNF1の家族歴を認める患者である．

2）方法

a）*NF1*遺伝子増幅PCRプライマー

*NF1*遺伝子解析のためのPCRプライマーはMarchukらの*NF1*遺伝子配列の報告[6)]に基づき設定した．今回我々はエクソン40から49までの11エクソンのプライマーペアを用いて解析した．Table 2にその塩基配列を示す．エクソン40から48までの9エクソンについては，Wallaceの設定したオリゴヌクレオチドプライマーを改良し用いた[42)]．またエクソン48aのプライマーは独自に設定し，エクソン49についてはWeissらの塩基配列の報告[43)]に基づき設定し，ストップコドンを含む468base pair（bp）を増幅する49.1と，CpG

1）東京慈恵会医科大学皮膚科学教室（主任　新村眞人教授）
2）Division of Medical Genetics, Department of Pediatrics University of Utah (Director Prof. Jhon C. Carey)
平成7年1月30日受付，平成7年4月6日掲載決定
別刷請求先：（〒105）東京都港区西新橋3—19—18
東京慈恵会医科大学皮膚科学教室　澤田　俊一

Table 1 Coding exons of *NF1*

Coding *NF1* exons showing cDNA position of exon boundary (column 2), size of exon (column 3), and intron size between two adjacent exons (column 4). Question marks denote an inability to PCR amplify across the intron, which suggests that it is over 2.5kb in length. (Ying-Li *et al.*, 1995 *Genomics* appended)

Exon #	cDNA position	Size (bp)	Introns (kb)
1	1	60	40—120
2	61	144	?
3	205	84	?
4a	289	195	?
4b	484	103	2.0
4c	587	68	0.22
5	655	76	0.80
6	731	158	?
7	889	174	0.40
8	1,063	123	?
9	1,186	75	4.0
10a	1,261	142	?
10b	1,393	135	4.0
10c	1,528	114	2.5
11	1,642	80	0.54
12a	1,722	124	?
12b	1,846	156	1.2
13	2,002	250	0.49
14	2,252	74	0.23
15	2,326	84	1.3
16	2,410	441	0.38
17	2,851	140	0.28
18	2,991	123	0.26
19a	3,114	84	1.2
19b	3,198	117	0.55
20	3,315	182	0.12
21	3,497	212	2.2
22	3,709	162	0.14
23-1	3,871	104	?
23-2	3,975	136	4.0
(23a	4,111	63	6.0)
24	4,111	159	0.53
25	4,270	98	1.25
26	4,368	147	1.27
27a	4,515	147	?
27b	4,662	111	45—50
28	4,773	433	1.3
29	5,206	341	2.7
30	5,547	203	4.3
31	5,750	194	1.55
32	5,944	141	0.15
33	6,085	280	0.40
34	6,365	215	0.24
35	6,580	62	0.15
36	6,642	115	0.57
37	6,757	102	1.7
38	6,859	141	2.4
39	7,000	127	6.0
40	7,127	132	0.93
41	7,259	136	2.0
42	7,395	158	4.0
43	7,553	123	0.35
44	7,676	131	0.18
45	7,807	101	1.1
46	7,908	143	0.35
47	8,051	47	1.4
48	8,098	217	6.5
(48a	8,315	54	6.7)
49	8,315	153	
——— 3′ Non-coding ———			

Table 2 Intron-based primers used to amplify *NF1* exons

We have used intron-based exon-specific primer pairs to get sequence spanning exons 40 to 49. Oligonucleotide primers are synthesized from genomic DNA sequence. In order to use in subsequent analysis, primers are tagged with an additional 18 bases, to generate 21M13 (5′ TGAAAAACGACGGCCAGT 3″) site for upstream primers, and M13RP1 (5′ GAGCAAACAGCTATGACC 3″) site for downstream primers. The 3′-UTR cDNA sequence is represented in the contiguous genomic sequence downstream of the stop codon, which, is base 8455 in the genomic sequence (Weiss et al., 1992).

EXON(bp)	SEQUENCE (5′ → 3′)
40	TGTAAAACGACGGCCAGT-TCAGGGAAGAAGACCTCAGCAGATGC
(328)	CAGGAAACAGCTATGACC-TGAACTTTCTGCTCTGCCACGCAACC
41	TGTAAAACGACGGCCAGT-TTATGTAGTCTTCCAAAATATGTG
(339)	CAGGAAACAGCTATGACC-TTGCCTCCATTAGTTGGAAAATTG
42	TGTAAAACGACGGCCAGT-CTTGGAAGGAGCAAACGATGGTTG
(356)	CAGGAAACAGCTATGACC-CAAAAACTTTGCTACACTGACATGG
43	TGTAAAACGACGGCCAGT-GCTCCAGGGATGTATTAGAGCTTTC
(318)	CAGGAAACAGCTATGACC-CATGTACTCTCCCACCTTATTTTC
44	TGTAAAACGACGGCCAGT-ATACAGCATTGTAAATAGGTAGCC
(355)	CAGGAAACAGCTATGACC-AAAATTTGAGGGTGGGGGACTC
45	TGTAAAACGACGGCCAGT-TCCCCTTTTTGAGTCCCCCACC
(341)	CAGGAAACAGCTATGACC-CACATTACTGGGTAAGCATTTAAC
46	TGTAAAACGACGGCCAGT-ATTTGGAAAATGAAGAAATGCCCC
(347)	CAGGAAACAGCTATGACC-ATGTTAGCAAGTTCATCAACCATC
47	TGTAAAACGACGGCCAGT-TCTCAACTGTATGTCCAATGTAAC
(337)	CAGGAAACAGCTATGACC-TGTGTGTTCTTAAAGCAGGCATAC
48	TGTAAAACGACGGCCAGT-TAATATTTTTGGCTTCAGATGGGG
(360)	CAGGAAACAGCTATGACC-CACAAGGGAATTCCTAATGTTGGTG
48a	TGTAAAACGACGGCCAGT-ATCTAGTATCTAATTGTATTTCACC
(245)	CAGGAAACAGCTATGACC-GCAGACTGAGCTTACAGGGAC
49.1	TGTAAAACGACGGCCAGT-CAGAACAACTGCAAAGAAAGTG
(468)	CAGGAAACAGCTATGACC-CCCACTTTCTTTGCAGTTGTTCTG
49.2	TGTAAAACGACGGCCAGT-TTCTGGGGTAAGTTTCACAGTTTC
(326)	CAGGAAACAGCTATGACC-TTTCAAACTCCTAGGATGTACTTAC
49.3	TGTAAAACGACGGCCAGT-GTAAAGCAGTTAGTTGCTGCAC
(435)	CAGGAAACAGCTATGACC-GGGAAGAAAACAGAGCCGATAC

含有が多い49.2の領域，エクソン49の3′end を増幅する49.3の３つの領域について検索した．プライマーはそれぞれのエクソンを特異的に増幅するよう隣接するイントロン20bp から24bp の塩基配列を求め，245から468bp の DNA 断片を増幅するように設定した．5′側プライマーには18bp の21M13 (5′TGTAAAACGACGGCCAGT 3′) site を，3′側プライマーにも18bp の M13RP1 (5′CAGGAAACAGCTATGACC 3′) site を付加している．プライマーは各25pM として保存し，最終的には2.5pM を使用した．

b) PCR (Polymerase chain reaction) 法

PCR 反応後は75ng から100ng の DNA を鋳型として dNTPs (最終濃度；0.12mM)，各プライマー (2.5 pM)，$MgCl_2$ (2.5mM)，Spermidine (0.25mM)，2.5 μl の10XPCRbuffer；Tris (10mM, PH=8.3)，KCl (50mM)，ならびに Taq polymerase (0.5U) で全量を25μl として，94°C45秒，60°C45秒，72°C90秒の反応条件で，35サイクルの反応を DNA thermal cycler (Perkin Elmer Cetus) を用いて行った．PCR 終了後は PCR 反応液10μl を１％アガロースゲルで電気泳動し，DNA 断片の増幅を確認した．

c) Size-shift assay

アガロースゲル電動泳動では検出できない10bp 以下の欠失，挿入といった微細な遺伝子変異を検出するため本法を開発した．T4ポリヌクレオチドキナーゼを用いて21M13ユニバーサルプライマーの3′末端を〔γ-^{32}

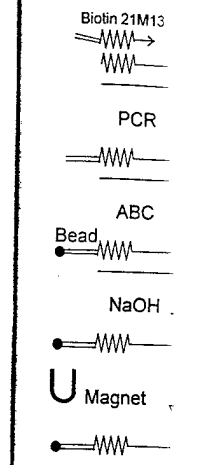

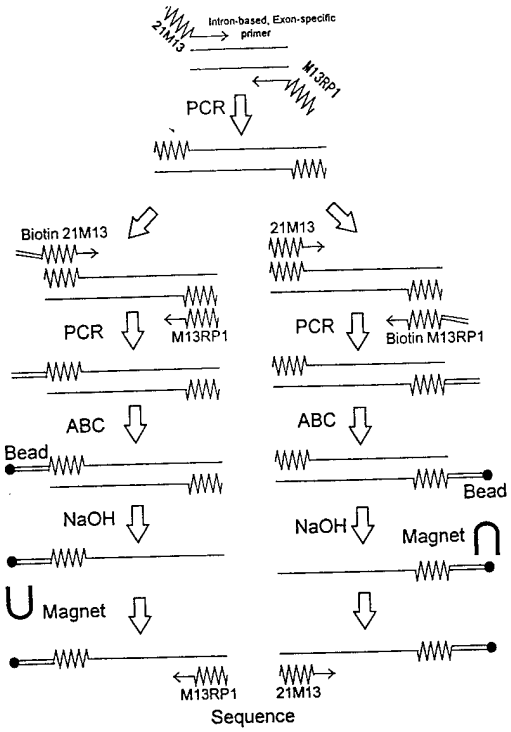

Fig. 1 Diagram of the method
Genomic DNA is amplified using a intron-based exon-specific primer pair. A separate second PCR amplification using two sets of primers, one biotinylated and the other one non-biotinylated (Biotin21M13 and M13RP1, 21M13 and Biotin M13 RP1), is performed under standard conditions. In our protocols, magnetic beads are used to collect immobilized single-stranded DNA for the subsequencing reaction. The second PCR products are bound to magnetic beads by the ABC (avidin-biotin complex). DNA strands are separated by adding 0.1N NaOH, and immobilized ssDNA is collected by using a magnet. Collected immobilized ssDNA are directly sequenced by using 0.5pM of either upstream primer (21M13) or downstream primer (M13RP1).

P] ATP (3,000Ci/mM, 1mCi/ml) で標識し[44]，アイソトープ未標識の21M13プライマーと1：6で混合し5′側プライマーとして用いた．3′側プライマーはアイソトープ未標識のM13RP1ユニバーサルプライマーを使用した．それぞれのプライマーは6pMを使用し，上記一次PCR反応産物を1：100に希釈したものを鋳型として1μlを用いて，全量を20μlとして再度PCRを行った．反応条件は95°C30秒，50°C30秒，72°C60秒で，25サイクルの反応を行った．これで得た二次PCR反応産物をホルムアミド色素溶液（20mM EDTA, 0.05% bromophenol blue, 0.05% xylene cyanol）で12倍に希釈し，95°Cで5分加熱変性させた後，1.5μlを通常のシークエンシングに使用する6%ポリアクリルアミド（49：1 acrylamide to methylene-bisacrylamide）8.3M尿素ゲル（0.1M Trisborate, 2mM EDTA）（6%PAGE-Urea ゲル）にて，90Wで5時間泳動した．PCR反応で増幅されるDNA断片の大きさが異なる試料を用いた場合には数検体同時に電気泳動できるため，我々は各患者検体について6つの異なるエクソンのPCR産物を混合し，同じレーンに添加している．

d) SSCP（Single strand conformation polymorphism）法

本法は我々が既に報告した方法[4)45)]に従い，PCR施行時に0.4μlの〔d-^{32}P〕dCTP (3,000Ci/mM, 10mCi/ml)を加えラベルする方法を用いた．一次PCR反応産物を1：100に希釈したものを鋳型として1μlを用いて，全量を20μlとして，6pMの21M13プライマーとM13RP1プライマーを用いて二次PCR反応を行った．反応条件は95°C30秒，50°C30秒，72°C60秒で，25サイクルの反応を行った．二次PCR反応で得られた増幅DNA断片をホルムアミド色素溶液で60倍に希釈し，95°Cで5分加熱変性させた後，2μlを5%グリセロールを添加した10%ポリアクリルアミドゲル(0.1M Tris-borate, 2mM EDTA）にて，40W，4°C（cold room）で6時間泳動した．

e) Direct sequence 法

我々はMagnetic beads（Dynabeads™ M-280 Streptavidin）を使用しsingle-stranded DNA（ssDNA）を得，それをdideoxy chain termination法を用いてダイレクトシークエンシングする方法を用いた．Fig. 1にその概要を示す．一次PCR反応産物をDNA回収用フィルター付遠心チューブ（Centricon™-100 microconcentrator)を用いて精製し，蒸留水にて1：100に希釈したものを二次PCR反応の鋳型として1μl使用した．二次PCR反応は2組のプライマーの組み合わせで行った．5pMのBiotin付加21M13と15pMのM13RP1とのペアならびに15pMの21M13と5pMのBiotin付加M13RP1とのペアである．反応後はdNTPs (0.2mM), $MgCl_2$ (2.5mM), 5μlの10 XPCRbufferならびにTaq polymerase (2U) で全量を50μlとして，size-shift assayの二次PCR反応と同

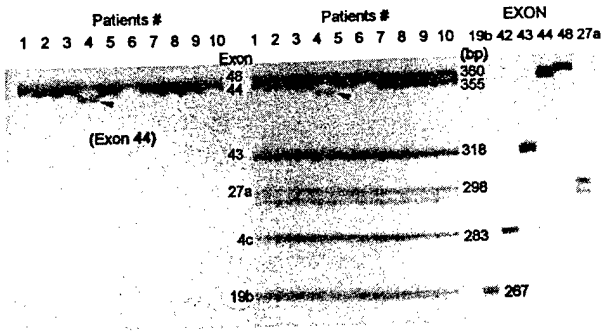

Fig. 2 Screen 10 NF1 patients by size-shift assay
Autoradiograph of the size-shift assay of radioactive PCR products synthesized from genomic DNA as template from 10 NF1 patients with facing primers specific for their respective exon. The UP primer is end-labeled by the kinase reaction prior to amplification and the products are denatured with 47.5% formamide and heating to 85°C prior to loading on a 6% polyacrylamide, 8.3M Urea denaturation gel. This autoradiograph identifies only the sense strand of the PCR products. The far right shows each exon product from one individual loaded separately (approximate sizes are in parentheses). The doublet for exon 27a probably represents amplification from an *NF1*-homologous locus, and its product deviates from the length of the *NF1* product by 3 to 8 bases. The middle portion of the autoradiograph displays individuals who have had all exons pooled prior to loading. Patient 4 shows a smaller band in the upper doublet band that represents exons 44 and 48. By loading exons 44 and 48 separately, we identified the size-shift for patient 4 to be in exon 44.

様の反応条件で行った．この二次PCR反応で得たPCR産物に室温でavidin-biotin complexとしてMagnetic beadsを付着させ，次いで0.1Nの水酸化ナトリウムで二本鎖DNAを解離させ，Magnetic beadsの付着する側のssDNAをmagnet (Dynal MPC™)で回収した[46]．回収されたBiotin21M13側のssDNAにはM13RP1プライマーを用いて（アンチセンス方向；RP direction），BiotinM13RP1側のssDNAには21M13プライマーを用いて（センス方向；UP direction）アニールし，T7 DNA polymerase (Sequenase version 2.0) ならびに0.5μlの〔α-^{35}S〕dATP (3,000 Ci/mM, 1mCi/ml)を用いて，dideoxy chain termination法にてシークエンスを行った．6%PAGE-Ureaゲルにて，90Wで1.5時間ならびに3時間の電気泳動を行い，塩基配列を決定した．また，*NF1*遺伝子に変異を認めたものについては蛍光式自動DNAシークエンサー（Applied Biosystems）にて再度その変異を確認した．

結　果

10名の米国人NF1患者の末梢血白血球分画より抽出したconstitutional DNAを被験対象としてsize-shift assay，SSCP法，ならびにdirect sequence法を用いて*NF1*遺伝子変異の解析を行った．*NF1*遺伝子には59のエクソンが現在確認されているが，そのうちエクソン40から49までの11エクソンについて，13の領域を増幅する特異的プライマー(Table 2)を用いて検討した．結果は1例 (patient #4) で，エクソン44においてNF1 disease causingと思われる*NF1*遺伝子変異が確認された．Fig. 2にそのsize-shift assayの結果を示す．我々は今後*NF1*の59全てのエクソンについて解析を予定しており，データにはエクソン40から49以外のエクソンも含まれている．ここでは10症例について*NF1*の6つのエクソンからのPCR産物の大きさを検討している．すなわちエクソン4c，19b，27a，43，44ならびに48で，それぞれ期待されるPCR産物の大きさは283，267，298，318，355ならびに360bpである．矢印の示すごとく，patient #4のエクソン44において期待されるPCR産物の大きさの355bpより5から10bpほど小さいPCR産物を認めている．図の左側はエクソン44のみを泳動したもので，右側は正常コントロールについてそれぞれ6つのエクソンを分けて泳動し，目的とされるPCR産物の大きさを示している．

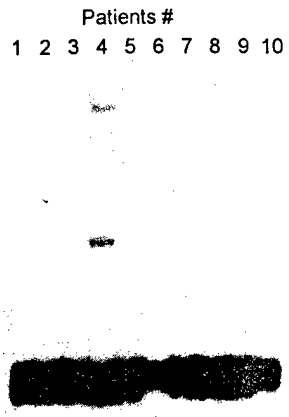

Fig. 3 Screen of 10 NF1 patients by SSCP method at exon 44
Screen 10 NF1 patients at exon 44 using SSCP analysis. I labeled UP and RP universal primers by [γ-32P] dATP and amplified the first PCR products. PCR products were diluted 60-fold in a buffer consisting of 20mM EDTA, 0.05% bromophenol blue, and 0.05% xylene cyanol and then heated to 85°C for 5 minutes to denature the DNA. Samples were applied on a 10% neutral polyacrylamide gel with 5% glycerol. Electrophresis was carried out at 40W at 4°C for 6 hours. Arrow shows the shifted bands of patient 4.

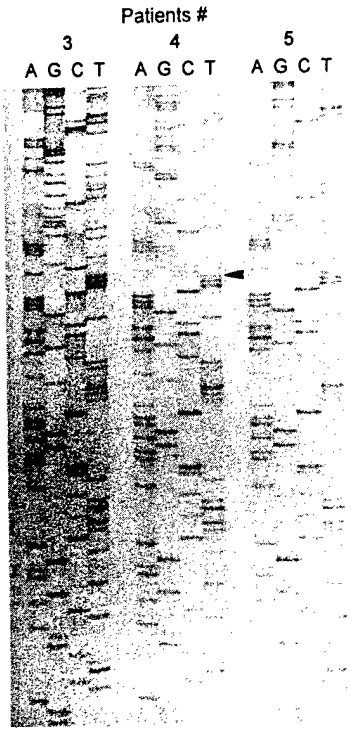

Fig. 4 DNA sequence analysis at exon 44 from three patients
DNA sequence analysis of the PCR products from exon 44 from three patients (3, 4, and 5). The technique of direct sequencing using magnetic beads was used. This gel autoradiograph displays the sequence from the RP direction (anti-sense strand). The arrow marks where the DNA sequence diverges in patient 4; above the arrow there are two separate representations of two alleles. The DNA sequence is readable from both alleles.

Fig. 3 にエクソン44において10症例を SSCP 法で解析した結果を示す．正常アレルから得られるバンドとは別に矢印の示すごとく patient #4においてシフトしたバンドを認める．以上の結果より patient #4ではエクソン44において小さな欠失が起きている可能性が考えられシークエンスを行った．3症例(patient #3，4，5)のエクソン44についてダイレクトシークエンシングした結果 Fig. 4 に示す．アンチセンスストランドのシークエンスで，矢印は *NF1* における cDNA ポジション7712を示す．patient #4においては正常アレルからのシークエンスバンドと変異アレルからのバンドが混在するため，矢印より上は二重バンドとなっているが，バンドが明瞭であるため読みとりは容易であった．その解読結果を Fig. 5 に示す．変異アレルにおいては，cDNA ポジション7712から7720までの9bp (ATTTA CGT A) が欠失しており，あわせて同部位に2bp (GC) が挿入した結果，7bp のフレームシフトを起こしている．この結果によりコードする蛋白が異なり，32コドン下流のエクソン45との境界部で TAG のストップコドンが出現している．さらに我々はシークエンス結果に間違いがないことを再度蛍光式自動 DNA シークエンサーを用いて，センスならびにアンチセンスストランド両方より確認している．

また我々はイントロン40においてポリモルフィズムを検出している．エクソン40を増幅するイントロンプライマー (Table 2) を用いて，20人の NF1患者 DNA ならびに5人の正常コントロール DNA を検索したところ，Fig. 6 の矢印に示すようにエクソン40の3′ end より10bp 下流のイントロン40において CG ポリモルフィズムを認めている．図ではこのポリモルフィズムが分かり易いように25試料について全てグアノシン

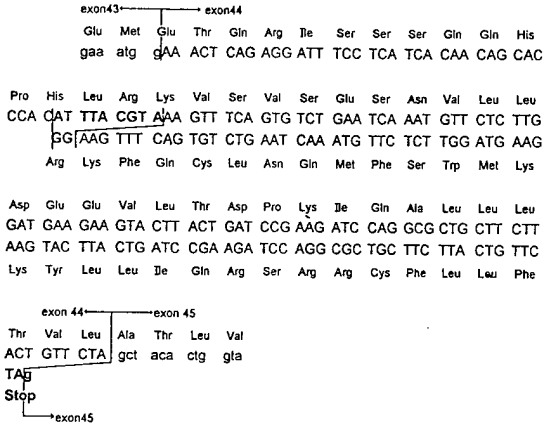

Fig. 5 Sequence divergence at exon 44 from patient 4
Sequence divergence begins at base 7712 in the cDNA sequence. It is a complex sequence variant which has 9-base pair deletion and a 2-base pair insertion that results in a frame shift. It encodes a peptide that would prematurely stop translation 32 codons downstream; the stop codon, TAG, lies in exon 45. The sequence show above compares the coding sequence between the normal *NF1* allele and the variant allele from patient 4 from end of the exon 43 through the beginning of exon 45.

(G) のみを並べて電気泳動している．25試料中20試料で本来シトシン (C) のみられる位置にグアノシンのバンドを検出している．

考　按

NF1 遺伝子の構造ならびにニューロファイブロミンについて：

NF1 遺伝子はゲノムマッピングアプローチにより1990年にクローニングされ[2)3)]，そのcDNAの塩基配列が決定された[3)~6)]．ゲノムDNAでの *NF1* 遺伝子の大きさは350kbにわたる巨大な遺伝子であり，cDNAの大きさは8,457bpで[6)]，23aと48aの二つのalternative splice formを持ち[4)7)8)]，現在までに59のエクソンが確認されている (Table 1)[1)]．*NF1* 遺伝子蛋白はニューロファイブロミンと呼ばれ，2,818アミノ酸残基よりなる分子量約220～280kDの不溶性蛋白である．ニューロファイブロミンにはyeast *IRA* (inhibitory regulator of *ras*) *1*, *IRA2* ならびにmammalian p120 GAPとの相同性を持つドメインを認める (NF1-GAP related domain: NF1-GRD)[5)16)17)]．NF1-GRDが

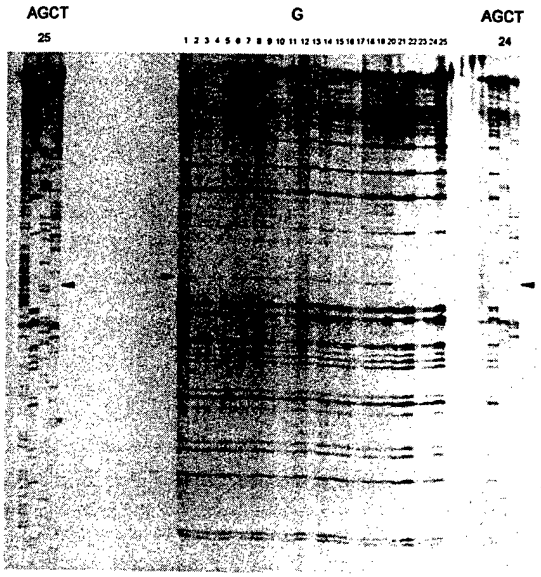

Fig. 6 Sequence variant at intron 40
Screen of 20 NF1 patients and 5 controls at exon 40. In this data, I applied all G samples together on the gel. Arrow shows sequence variant+10bps downstream of the 3'end of exon 40; there is an unexpected guanosine in 20 of 25 individuals.

IRA1, *IRA2* の変異を相補でき，ニューロファイブロミンは正常型 *ras* のGTPase活性を活性化することが知られている[17)~19)]．またニューロファイブロミンはチューブリンに局在し[21)]，チューブリンの量を減らすとニューロファイブロミンのGAP活性が減少することが報告されている[22)]．以上より *NF1* 遺伝子は *ras* のネガティブレギュレーターであり，癌抑制遺伝子の一つであると考えられている[20)]．

NF1 遺伝子変異について：

NF1 遺伝子の変異は現在までに約70例が報告されている (NNFF Consortium)[2)4)15)23)~41)]．相互転座[3)23)24)]，大きな欠失[2)25)~28)]，小さな欠失[28)~34)]，大きな挿入[26)35)]，小さな挿入[15)26)30)36)37)]，点突然変異[4)15)26)28)37)~41)]の報告があり，主にNF1-GRDでの変異が初期には注目されたが，その後の検索で *NF1* 遺伝子変異のホットスポットはないとされている．また，検索された本症の約20%以下にしか *NF1* 遺伝子の変異はみつかっていない．これは *NF1* 遺伝子の今てのエクソンについて検索された報告がないことに起因するものと考えられる．当初49のエクソンが *NF1* 遺伝子に確認されていたが (NNFF International Consor-

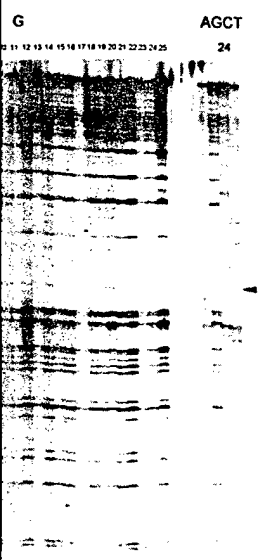

ariant at intron 40
and 5 controls at exon 40.
G samples together on the
ce variant+10bps down-
xon 40; there is an un-
of 25 individuals.

できる，ニューロファイブロ
se 活性を活性化すること
ニューロファイブロミンは
チューブリンの量を減らす
のGAP活性が減少するこ
により *NF1* 遺伝子は *ras* の
であり，癌抑制遺伝子の一
[20].

て：
在までに約70例が報告され
tium)[2)4)15)23)~41)]．相互転
，小さな欠失[28)~34)]，大きな
[15)26)30)36)37)]，点突然変
り，主にNF1-GRDでの変
，その後の検索で *NF1* 遺
はないとされている．また，
下にしか *NF1* 遺伝子の変
れは *NF1* 遺伝子の今ての
た報告がないことに起因す
49のエクソンが *NF1* 遺伝
NFF International Consor-

tium on Gene Cloning and Gene Function for NF1 and NF2, Oxford, UK, 1992)，我々の研究室では *NF1* 遺伝子の構造を詳しく解析し，エクソン4は4a，4bならびに4cに，エクソン10は10a，10bならびに10cに，エクソン12は12aと12bに，エクソン23では既にalternative splice exon 23aがあるため23-1と23-2に，イントロンの存在で分けられていることを報告した[1)]．また，エクソン19は19aと19bに[9)]，エクソン27は27aと27bに[10)]分けられ，合計59のエクソンが *NF1* 遺伝子に現在確認されている．我々はすでにこの59のエクソンをそれぞれ特異的に増幅するプライマーを作製している[1)]．今回はエクソン40から49までの11エクソンについて検討し，10症例中1症例で *NF1* 遺伝子の変異を検出した．今後はこれらプライマーを用いて残りのエクソンを解析することで，ほとんどの症例より *NF1* 遺伝子の変異を検出できるのではないかと予想している．

変異検出の方法について：

NF1 遺伝子変異の検出方法としてSouthern blotting法，pulse field gel法，SSCP法，STS(Sequence Target Site)-Linkage法，hydrolink gel法，heteroduplex法，direct sequence法，protein truncation法，chemical mismatch cleavage法等の手技が用いられている．我々は高率に *NF1* 遺伝子変異を検出する方法として，*NF1* エクソン特異的プライマーを設定しPCR法を行い，さらにsizeshift assay，SSCP法，magnetic beadsを利用したdirect sequence法を用いて変異の検出を行う実験系を確立した．*NF1* エクソン特異的プライマーの5′側プライマーには21M13 siteを3′側プライマーにはM13RP1 siteを付加しておき，これらを用いて一次PCR反応を行った．21M13，M13 RP1ユニバーサルプライマーを利用して二次PCR反応を行うことにより，以降のsize-shift assay，SSCP法，magnetic beadsを利用したdirect sequence法を簡便に伝えるのがこの実験系の長所である．magnetic beadsを利用したdirect sequence法は，サブクローニングの手間を省き，また非対称PCRの必要もなくセンスならびにアンチセンスストランド両方の塩基配列を決定出来る[46)]．今回の結果よりこの実験系が *NF1* 遺伝子変異の解析手段として有用であることが証明され，これを用いて *NF1* 遺伝子のすべてのエクソンを検索した場合には，高率に変異が検出されるものと思われる．*NF1* 遺伝子が巨大な遺伝子であり，遺伝子変異のホットスポットがないことにも起因するが，59のエクソンについて特異的プライマーを設定しそれぞれを分けて検索するため，大変な手間がかかるのがこの実験系の最大の短所である．しかしながらこの実験系は *NF1* 遺伝子変異の解析のみならず，他の遺伝性疾患のDNA診断，感染症のDNA診断等にも有力な実験系であると考える．

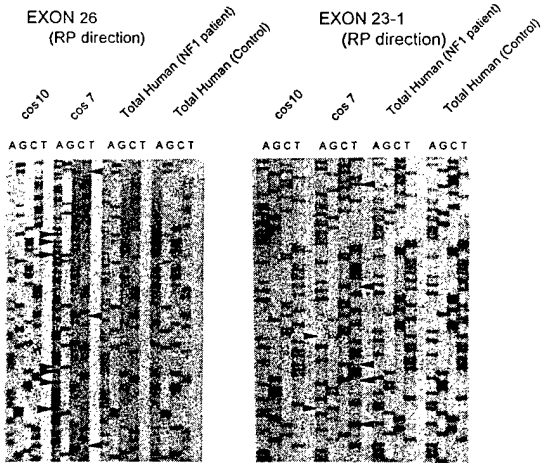

Fig. 7 Sequence difference with Cos 10 sequence and Cos 7.
DNA sequence analysis of the PCR products from cos 10, cos 7, total human DNA from a NF1 patient, and total human DNA from a non-NF1 control, which were amplified by the intron-based, exon-specific primer pair. Arrows show the differences between con 10 sequence (chromosome 17) and cos 7 sequence (chromosome 15) at exon 23-1 and exon 26.

***NF1*-homologous lociについて：**

NF1 遺伝子のエクソン1から27bには *NF1*-homologous lociが存在し，現在までに染色体2[12)14)]，12[12)]，14[12)14)]，15[11)13)~15)]，20[12)]，21[12)14)]，22[12)]に存在することが報告されている．*NF1*-homologous lociの存在が今後の *NF1* 遺伝子の検索を困難にする可能性が考えられる．Fig. 2のsize-shift assayの結果で，エクソン27aのPCR産物は二重バンドになっている．多少わかりにくいがエクソン19bのPCR産物も二重バンドである．これは明らかに17番染色体以外の *NF1*-homologous lociがPCR反応で増幅された結果と考えられる．Fig. 7にはエクソン26とエクソン23-1におけるシークエンス結果を示す．Cos10 (chromosome 17) とcos7 (chromosome15) を．比較しているが，矢印に示す部位が一致しない塩基配列で，それ以外は

全く同様の塩基配列を呈している．ここではゲノムDNAからのシークエンスはcos10と一致していた．今後，他のエクソンの検索で*NF1*-homologous lociの存在がシークエンスを困難にする可能性があり，その場合は17番染色体上の*NF1*遺伝子のみを特異的に増幅するようにプライマーを変更する必要がある．

現在我々は今回解析した11のエクソン以外の残りのエクソンについても解析を続けており，*NF1*遺伝子のDNA診断を確立することを目標に，この実験系をさらに改良，発展させたいと考えている．

本論文の要旨は1994年7月10日～14日 FASEB Conference on Neurofibromatosis meeting (Santa Cruz, CA, U.S.A.)において発表した．稿を終えるにあたり，本研究に御協力を頂いたRichard Cawthon, MD, PhDをはじめ米国ユタ大学Human Gentetics部門の各諸兄ならびに，論文の御指導を頂いた東京慈恵会医科大学皮膚科学教室の新村眞人教授，本田まりこ先生に深謝いたします．

文献

1) Li Y, O'Connell P, Breidenbach H, et al: Genomic organization of the neurofibromatosis 1 gene, *Genomics,* (in press).
2) Viskochi DH, Buchberg AM, Xu G, et al: Deletions and a translocation interrupt a cloned gene at the neurofibromatosis type 1 locus, *Cell,* 62：187-192, 1990.
3) Wallace MR, Marchuk DA, Anderson LB, et al: Type 1 neurofibromatosis gene: Identification of a large transcript disrupted in three patients, *Science,*249：182-186, 1990.
4) Cawthon RM, Weiss R, Xu G, et al: A major segment of the neurofibromatosis 1 gene: cDNA sequence, genomic structure. and point mutations, *Cell,* 62：193-201, 1990.
5) Xu G, O'Connell P, Viskochil DH, et al: The neurofibromatosis 1 gene encodes a protein related to GAP, *Cell,* 62, 599-608, 1990.
6) Marchuk D, Saulino A, Tavakkol R, et al: cDNA cloning of the type 1 neurofibromatosis gene: Complete sequence of the *NF1* gene product, *Genomics,* 11：931-940, 1991.
7) Nishi T, Lee P, Oka K, et al: Differential expression of two types of the neurofibromatosis type 1 (NF1) gene transcripts related to neuronal differentiation, *Oncogene,* 6：1555-1559, 1991.
8) Suzuki Y, Suzuki H, Kayama T, Yoshimoto T, Shibahara S: Brain tumors predominantly express the neurofibromatosis type 1 gene transcripts containing the 63 base insert in the region coding for GTPase activating protein-related domain, *Biochem Biophys Res Comm,* 181, 955-961, 1991.
9) Witkowski R: Institute of Medical Genetics, Humbolt University, Berlin, personal communication.
10) Martin GA, Viskochil D, Bollag G, et al: Sequencing and analysis of genomic fragments from the NF1 locus, *DNA Sequence,* 3：237-243, 1992.
11) Legius E, Marchuk D, Hall BK, et al: NF-1 related locus on chromosome 15, *Genomics,* 13：1316-1318, 1992.
12) Cummings R, Glatfelter A, Marchuk D: NF1-related loci on chromosomes 2,12,14,15,20,21, and 22：A potential role for gene conversion in the high spontaneous mutation rate in NF1? *Am J Hum Genet,* 53：672A, 1993.
13) Gasparini P, Grifa A, Origone P, et al: Detection of a neurofibromatosis type 1 (NF-1) sequence by PCR：Implications for the diagnosis and screening of genetic disease. *Mol Cell Probes,* 7：415-418, 1993.
14) Viskochil D, Breidenbach HH, Cawthon R, Zhu XL, Brothman A: A mapping neurofibromatosis 1 homologus loci by fluorescence in situ hybridization, *Am J Hum Genet,* 55：A375, 1994.
15) Purandare SM, Lanyon WG, Connor JM: Characterization of inherited and sporadic mutations in neurofibromatosis type-1, *Hum Mol Genet,* 3, 1109-1115, 1994.
16) Buchberg AM, Cleveland LS, Jenkins NA, Copeland NG: Sequence homology shared by neurofibromatosis type-1 gene and *IRA-1* and *IRA-2* negative regulators of the *RAS* cyclic AMP pathway, *Nature,* 347：291-294, 1990.
17) Xu G, Lin B, Tanaka K, Dunn D, Wood D: The catalytic domain of the NF1 gene product stimulates ras GTPase and complements IRA mutants of *S. Cerevisiae, Cell,* 63：835-841, 1990.
18) Martin GA, Viskochil D, Bollag G, et al: The GAP-related domain of the NF1 gene product interacts with ras p21, *Cell,* 63：843-849, 1990.
19) Ballester R, Marchuk D, Boguski M, et al: The *NF1* locus encodes a protein functionally related to mammalian GAP and yeast IRA proteins, *Cell,* 63：851-859, 1990.
20) 本田まりこ，新村眞人：神経線維腫症／neurofibromatosis type I, type II,実験医学，12：739-745, 1
21) Gutmann toward un von Reck: *Neurol,* 31
22) Bollag G, ' zation of inhibits Ra 1927, 1993.
23) Ledbetter M, Carey J 11.2 by ba *Genet,* 44：
24) Menon AG Characteriz von Reckli of chromos
25) Upadhyaya al: A 90 neurofibrom -741, 1990.
26) Upadhyaya Analysis of 1 (NF-1) lo 1992.
27) Kayes LM, I Stephens K: patient with tal retardati 29：686-690,
28) Weiming X, analysis of N *Hum Mut,* 1
29) Stark M, As tion and an a tial stem loc *Genet,* 87：68
30) Zhong J, Spe Two novel n in the NF-1 *Hum Mol G*
31) Shun MH, U mutation in type 1 (NF1) 1993.
32) Shun MH, Neurofibroma for mutations Hydrolink ge 1993.
33) Colman SD, C terization of

739-745, 1994.
21) Gutmann DH, Collins FS: Recent progress toward understanding the molecular biology of von Reckinghausen neurofibromatosis, *Annu Neurol,* 31: 555-561, 1992.
22) Bollag G, McCormick G, Clark R: Characterization of full-length neurofibromin: tubulin inhibits Ras GAP activity, *EMBO J,* 12: 1923-1927, 1993.
23) Ledbetter DH, Rich DC, O'Connell P, Leppert M, Carey JC: Precise localization of NF1 to 11.2 by balanced translocation, *Am J Hum Genet,* 44: 20-24, 1989.
24) Menon AG, Ledbetter DH, Rich DC, et al: Characterization of a translocation within the von Recklinghausen neurofibromatosis region of chromosome 17, *Genetics,* 5: 245-249, 1989.
25) Upadhyaya M, Cherryson A, Broadhead W, et al: A 90 kb deletion associated with neurofibromatosis type-1, *J Med Genet,* 27: 738-741, 1990.
26) Upadhyaya M, Shen M, Cherryson A, et al: Analysis of mutations at the neurofibromatosis-1 (NF-1) locus, *Hum Mol Genet,* 1: 735-740, 1992.
27) Kayes LM, Riccardi VM, Burke W, Bennet RL, Stephens K: Large de novo DNA deletion in a patient with sporadic neurofibromatosis 1, mental retardation and dysmorphism, *J Med Genet,* 29: 686-690, 1992.
28) Weiming X, Yu, Q, Lihzi L, et al: Molecular analysis of Neurofibromatosis type 1 mutations, *Hum Mut,* 1: 474-477, 1992.
29) Stark M, Assum G, Krone W: A small deletion and an adjacent base exchange in a potential stem loop region of the NF-1 gene, *Hum Genet,* 87: 685-687, 1991.
30) Zhong J, Speigel R, Boltshauser E, Schmid W: Two novel mutations 5108delAG and 5816insG in the NF-1 gene detected by SSCP analysis, *Hum Mol Genet,* 2: 1491-1492, 1991.
31) Shun MH, Upadhyaya M: A de novo nonsense mutation in exon 28 of the neurofibromatosis type 1 (NF1) gene, *Hum Genet,* 92: 410-412, 1993.
32) Shun MH, Harper PS, Upadhyaya M: Neurofibromatosis type 1 (NF-1):The search for mutations by PCR heteroduplex analysis on Hydrolink gels, *Hum Mol Genet,* 2: 1861-1684, 1993.
33) Colman SD, Collins FS, Wallace MR: Characterization of a single base pair deletion in neurofibromatosis type-1, *Hum Mol Genet,* 2: 1709-1711, 1993.
34) Wallace MR: Personal comunication. *NNFF Comsortium Newsletter,* 2(1), Jan. 1994.
35) Wallace MR, Andersen LB, Saulino AM, Gregory PE, Glover TW, Collins FS: A de novo *Alu* insertion results in neurofibromatosis type 1, *Nature,* 353: 864-866, 1993.
36) Purandare SM, Davidson HR, Lanyon WG, Connor JM: A novel insertional mutation of a single base in exon 34 of the neurofibromatosis-1 gene, *Hum Mut,* 3: 76-78, 1994.
37) Ainsworth PJ, Rodenheiser DI,Costa MT: Identification and characterization of inherited and sporadic mutations in exon 31 of the neurofibromatosis (NF-1) gene, *Hum Genet,* 91: 151-156, 1993.
38) Li Y, Bollag G, Clark R, et al: Somatic mutations in the neurofibromatosis 1 gene in human tumors, *Cell,* 69: 275-281, 1992.
39) Estivill X, Lazaro C, Casals T, Ravella A: Reccurence of a nonsense mutation in the NF-1 gene causing classical neurofibromatosis-1, *Hum Genet,* 88: 185-188, 1991.
40) Horiuchi T, Hatta N, Matsumoto M, et al: Nonsense mutations at Arg-1947 in two cases of familial neurofibromatosis type 1 in Japanese, *Hum Genet,* 93: 81-83, 1994.
41) Breidenbach H, Cawthon RM: Identification of NF1 mutations by a protein truncation assay. 1994 FASEB summer research conference, Senta Cruz, CA, U.S.A.
42) Wallace P: *NF1* exon DNA PCR primers (NNFF Consortium).
43) Weiss R, Dunn D, DiSera L, Wheatley W, Kimball A, Rote C, et al: The human neurofibromatosis type 1 locus: Genomic sequence of the 3′ region, 1-100849, Genbank Accession Number L05367, 1992.
44) 中村祐輔：末端標識法，堀　雅明，中村祐輔 編：ラボマニュアル ヒトゲノムマッピング，丸善株式会社，東京，1991, 40.
45) Sawada S, Honda M, Niimura M: Molecular genetic analysis of the von Recklinghausen neurofibromatosis (NF1) gene using polymerase chain reaction—single strand conformation polymorphism (PCR-SSCP) method, *J Dermatol (Tokyo),* 21: 294-300, 1994.
46) Hultman T, Stahale S, Hornes E, Uhlen M: Direct solid phase sequencing of genomic and plasmid DNA using beads as solid support, *Nucleic Acid Research,* 17: 4937-4946, 1989.

GENOMICS 25, 9–18 (1995)

Genomic Organization of the Neurofibromatosis 1 Gene (*NF1*)

YING LI,* PETER O'CONNELL,*,[1] HEIDI HUNTSMAN BREIDENBACH,* RICHARD CAWTHON,* JEFF STEVENS,* GANGFENG XU,*,[2] SHANNON NEIL,† MARGARET ROBERTSON,* RAY WHITE,* AND DAVID VISKOCHIL†,[3]

*Department of Human Genetics, Eccles Institute of Human Genetics, University of Utah, Salt Lake City, Utah 84112; and †Department of Pediatrics, University of Utah, Salt Lake City, Utah 84112

Received June 22, 1994; revised September 23, 1994

Neurofibromatosis 1 maps to chromosome band 17q11.2, and the *NF1* locus has been partially characterized. Even though the full-length *NF1* cDNA has been sequenced, the complete genomic structure of the *NF1* gene has not been elucidated. The 5′ end of *NF1* is embedded in a CpG island containing a *Not*I restriction site, and the remainder of the gene lies in the adjacent 350-kb *Not*I fragment. In our efforts to develop a comprehensive screen for *NF1* mutations, we have isolated genomic DNA clones that together harbor the entire *NF1* cDNA sequence. We have identified all intron–exon boundaries of the coding region and established that it is composed of 59 exons. Furthermore, we have defined the 3′-untranslated region (3′-UTR) of the *NF1* gene; it spans approximately 3.5 kb of genomic DNA sequence and is continuous with the stop codon. Oligonucleotide primer pairs synthesized from exon-flanking DNA sequences were used in the polymerase chain reaction with cloned, chromosome 17-specific genomic DNA as template to amplify *NF1* exons 1 through 27b and the exon containing the 3′-UTR separately. This information should be useful for implementing a comprehensive *NF1* mutation screen using genomic DNA as template.

INTRODUCTION

Neurofibromatosis type 1 (NF1) afflicts approximately 1 in 3500 individuals worldwide. This autosomal dominant condition typically manifests café-au-lait macules in the first decade of life and cutaneous neurofibromas during adolescence. Approximately $\frac{1}{3}$ of afflicted individuals display assorted medical complications involving many organ systems, and they carry a small but increased risk for the development of malignancy. In addition to the highly pleiotropic nature of NF1, the clinical manifestations are quite variable, even among family members who carry the same disease allele. The *NF1* gene was cloned by the mapping approach (Cawthon *et al.*, 1990a; Viskochil *et al.*, 1990; Wallace *et al.*, 1990), and its cDNA has been sequenced (Cawthon *et al.*, 1990a; Wallace *et al.*, 1990; Xu *et al.*, 1990a; Marchuk *et al.*, 1991). The coding segment of *NF1* spans approximately 350 kb of genomic DNA, and the cDNA is 8454 bp long (Marchuk *et al.*, 1991), exclusive of two alternative splice forms that contain insertion exons of 54 (Cawthon *et al.*, 1990a) and 63 (Nishi *et al.*, 1991; Suzuki *et al.*, 1991) bp. *NF1* encodes neurofibromin, a 2818-amino-acid polypeptide with domains of homology to yeast IRA1 and IRA2 and to mammalian p120GAP (p21ras GTPase-activating Protein) (Buchberg *et al.*, 1990; Xu *et al.*, 1990a). The domain demonstrating homology to the catalytic domain of p120GAP activates the intrinsic GTPase of p21ras *in vitro* (Ballester *et al.*, 1990; Martin *et al.*, 1990; Xu *et al.*, 1990b). Other functions of neurofibromin have not been conclusively demonstrated.

A detailed understanding of gene structure at the *NF1* locus is paramount in evaluating the molecular basis of the high mutation rate of NF1, estimated to be one of the highest among human genetic disorders (approximately 1/10,000 gametes per generation) (Carey *et al.*, 1986). Even though the *NF1* cDNA sequence is known, precise identification of *NF1* mutations in patients has not been very fruitful; mutations have been defined in fewer than 20% of screened *NF1* patients (NNFF International NF1 Genetic Analysis Consortium, Fax: (617) 277-5933) and include translocations, deletions, insertions, and point mutations that are generally "inactivating." The identification of exon boundaries and determination of intronic sequences flanking these boundaries would enable investigators to adopt additional screening approaches to facilitate the further evaluation of mutations in the *NF1* gene.

The availability of cloned genomic DNA from the cosmid contig containing a portion of the *NF1* cDNA (Viskochil *et al.*, 1990) enabled Cawthon *et al.* (1990a)

Variable lengths of intronic sequence on both sides of *NF1* exons 2 through 27b have been deposited with GenBank under Accession Nos. U17656–U17690. Continuous DNA sequence spanning exons 28 through 49 have been deposited under Accession No. L05367.

[1] Present address: University of Texas Health Sciences Center-San Antonio, Department of Pathology, San Antonio, TX 78284.

[2] Present address: Dana-Farber Cancer Institute, Harvard Medical School, Boston, MA 02114.

[3] To whom correspondence should be addressed at the Division of Medical Genetics, 413 MREB, University of Utah, Salt Lake City, UT 84112. Telephone: (801) 581-8943. Fax: (801) 585-5241.

0888-7543/95 $6.00

initially to identify nine exon boundaries with flanking intronic sequence. Subsequently, we used the same clones to define the boundaries of downstream exons (this report), and these have been confirmed by DNA sequence generated by Weiss *et al.* (1992). Finally, *NF1* cDNAs mapping further 5′ and extending centromeric of the cosmid contig were used to isolate genomic clones to generate exon boundaries in the 5′ portion of the gene. Based on preliminary results, an exon numbering system was adopted by consensus at the NNFF International Consortium on Gene Cloning and Gene Function for NF1 and NF2 (Oxford, UK, 1992), which redesignated exon 1 reported by Cawthon *et al.* (1990a) as exon 28; the exon containing the stop codon was designated exon 49. We report here the genomic organization of all *NF1* exons, and we present exon boundaries with flanking intronic sequences.

To complete the structural analysis of the *NF1* gene, we characterized the 3′ end of *NF1* cDNAs. None of the cDNA clones used originally to identify the *NF1* gene included polyadenylation tracts that typically mark the 3′ end of mRNA transcripts. Furthermore, the 11- to 13-kb size of human *NF1* mRNA on Northern analysis (Buchberg *et al.,* 1990; Viskochil *et al.,* 1990; Wallace *et al.,* 1990; Suzuki *et al.,* 1992) predicts that there is an additional 2.5 to 4 kb of noncoding sequence in the mature *NF1* transcript. One human cDNA clone from an oligo(dT)-primed library made from a basophilic leukemia cell line was reported to contain the 3′ end of *NF1* (Suzuki *et al.,* 1992); however, only a segment of that clone, pHN-2, was sequenced, and the 3′-untranslated region was not reported. Bernards *et al.* (1993) have cloned and sequenced mouse cDNAs that contain up to 3211 bp of DNA beyond the mouse *nf1* stop codon and have shown that the mouse 3′-UTR cDNA sequence is highly homologous to the human genomic sequence lying immediately downstream of its *NF1* stop codon. In this report we define the 3′ end of human *NF1,* and we demonstrate that the 3′-untranslated region of *NF1* mRNA from four different tissues is continuous with the stop codon in exon 49.

MATERIALS AND METHODS

Isolation of genomic clones. *NF1*-specific genomic clones were selected from a cosmid library that was constructed with DNA prepared from human peripheral blood leukocytes and inserted into the *Bam*HI restriction site of the pWE15 vector (Stratagene, La Jolla, CA). A premade P1-bacteriophage human genomic library (The DuPont–Merck Pharmaceutical Co., Wilmington, DE, DMPC-HFF#1 Series B) cloned into the *Bam*HI site in the pAd10sacBII vector (Pierce and Sternberg, 1992) provided a second source of genomic clones. High-density P1-bacteriophage libraries were screened as previously described (O'Connell *et al.,* 1990) using radioactive probes representing different *NF1* cDNA sequences. Hybridization on nylon membranes was carried out in 50% formamide, 5× SSC, 50 m*M* sodium phosphate (pH 6.5), 2× Denhardt's solution, 1% dextran sulfate, 0.1% SDS, and 100 μg of denatured total human DNA per milliliter for 14–16 h at 42°C. Filters were sequentially washed under increasingly stringent conditions, with the final wash in 0.1× SSC, 0.1% SDS at 55°C for 5 min for P1 bacteriophage libraries and at room temperature for 5 min for cosmid libraries. Positive clones were identified by autoradiography and purified by subsequent screenings using similar methodology. Isolated colonies were prepared by $CsCl_2$/ethidium bromide buoyant density centrifugation using standard protocols (Pierce and Sternberg, 1992; Sambrook *et al.,* 1989). Genomic clones were sized by agarose gel electrophoresis of *Eco*RI- and *Bam*HI-digested fragments both under standard conditions (Sambrook *et al.,* 1989) and using field-inversion methodology (Carle *et al.,* 1986). The overlapping ends of selected cosmid clones were mapped by Southern analysis using T7 and T3 polymerase-generated RNA probes synthesized from the ends of the clones.

cDNA screening. Premade Lambda ZAP cDNA libraries (Stratagene) were screened with PCR-labeled probes as previously described (Xu *et al.,* 1990a). Libraries constructed from four different tissue sources were screened: fetal brain (random and oligo(dT) primed, Stratagene, 936206), fetal retina from pooled tissue (oligo(dT) primed, Stratagene, 937202), muscle from an adult female (oligo(dT) primed, Stratagene, 936215), and adult heart (random and oligo(dT) primed, Stratagene, 936207). Isolated clones were excised according to the manufacturer's recommendations (Stratagene Protocol 200253), and the resultant *NF1* cDNA inserts in pBluescript SK(−) vectors were sized and sequenced by standard techniques.

Probe synthesis. PCR probes were synthesized by incorporating [α-^{32}P]dCTP into a PCR product (Saiki *et al.,* 1988). Template DNA was obtained from clones representing *NF1* cDNA between exons 2 and 27b. PCR conditions for probe synthesis were as follows: 1–10 ng template DNA, 1.2 m*M* dATP/dTTP/dGTP, 2.5 μ*M* dCTP, 10–15 μl of [α-^{32}P]dCTP (Amersham, Arlington Heights, IL; sp act, >6000 Ci/mmol), 4 m*M* $MgCl_2$, 10 m*M* Tris (pH 8.3), 50 m*M* KCl, 0.5 m*M* primers, and 2.5 units *Taq* polymerase, in a total volume of 50 μl. Routine thermal cycling included denaturation at 93°C, variable annealing temperatures, and extension at 72°C for 1 min for 20 cycles. The final step included heat denaturation at 93°C for 3 min, and the probe was placed on ice for at least 5 min before being added (40 μl) to the hybridization solution.

RNA probes from the ends of cosmid inserts were synthesized according to the manufacturer's instructions accompanying the T7 and T3 RNA polymerase transcription kit (Ambion, Austin, TX; No. 1326). Cosmid DNA (1–2 mg) digested with *Rsa*I served as template for probe synthesis using [α-^{32}P]UTP (Amersham, sp act, 800 Ci/mmol). The probes were routinely used directly in Southern analysis at template concentrations of 10 ng/ml hybridization solution.

Identification of intron–exon boundaries. Initial characterization of exon boundaries and flanking intronic sequences was performed in an empiric fashion by a PCR approach. Facing *NF1* cDNA oligonucleotides, tagged with universal primer sequence at the 5′ ends (universal (21m13)—GTAAAACGACGGCCAGT; reverse (m13RP1)—AACAGCTATGACCATG), were synthesized approximately 150 bp apart according to the cDNA sequence. These primers were used to amplify DNA isolated from genomic clones. PCR conditions varied for each primer pair; however, the routine reaction was based on the manufacturer's recommendations for the respective *Taq* polymerase, and the annealing temperature was set at approximately 5°C below the estimated T_m for 35 cycles. PCR products larger than the size predicted on the basis of cDNA sequence presumably carried an intron, and each PCR product was sequenced from both directions to identify divergence points from cDNA sequence. The presence of consensus splice junctions at sites where the sequence of a PCR product diverged from known *NF1* cDNA sequence identified the intron–exon boundaries. Initially, for those "introns" that did not amplify, boundaries were obtained by direct DNA sequencing of subclones. In this case, DNA from genomic clones was digested with *Sau*3A, subcloned in the *Bam*HI site of pBluescript, and selected with *NF1* cDNA probes. Plasmid DNA from positive clones was directly sequenced using either the universal or the reverse primer and T7 DNA polymerase (Sequenase Version 2.0, U.S. Biochemicals (USB), Cleveland, OH). Later in the project other techniques replaced the subcloning protocols. Those regions that could not be amplified by primer pairs 150 bp apart were subjected to either anchored PCR (Roux and Dhanarajan, 1990) or inverse PCR (Ochman *et al.,* 1988) techniques to obtain exon boundaries and flanking intronic se-

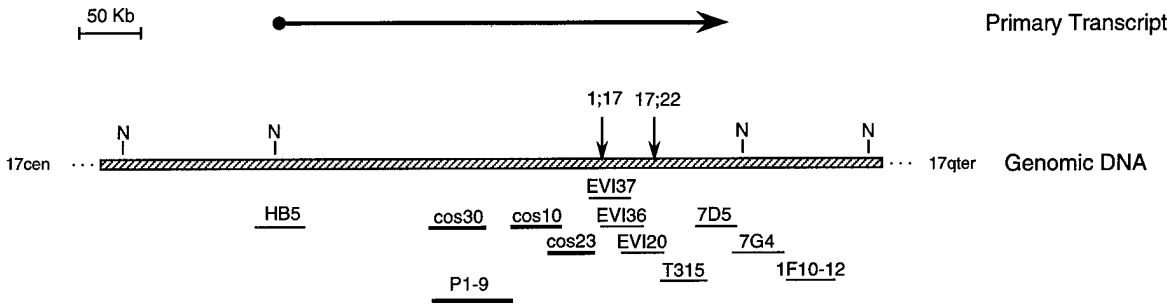

FIG. 1. The *NF1* locus. Genomic DNA is represented as a hatched bar; the length and transcriptional direction of *NF1* is depicted by the arrow above the region of genomic DNA that it spans. N denotes *Not*I restriction endonuclease cleavage sites (Fountain *et al.,* 1989; O'Connell *et al.,* 1989). Cosmid and P1 clones that cover all *NF1* exons are shown below the map. Clones not previously reported are indicated by thick bars. Breakpoints of two previously characterized chromosomal rearrangements, t(1;17) and t(17;22) (O'Connell *et al.,* 1990), are indicated by downward arrows above the genomic fragment.

quences. The PCR products were sequenced according to established methods of automated dideoxy sequencing using fluorescently labeled primers and either T7 or *Taq* polymerase.

DNA sequencing. Purified genomic DNAs from cosmid and P1 clones served as templates in routine PCR using *NF1*-specific primers tagged with 21m13 (upstream primer) and m13RP1 (downstream primer). The resulting PCR products were purified by Centricon-100 ultrafiltration (Amicon, Beverly, MA) and sequenced using a test-site protocol provided by Applied Biosystems, Inc. (Foster City, CA). This procedure involved performing dideoxy sequencing reactions with *Taq* polymerase in a thermal cycler, using fluorescently tagged M13 universal (UP) or reverse (RP) sequencing primers, for analysis on an Applied Biosystems Model 373A automated sequencer.

Subcloned genomic DNA in pBluescript was sequenced by the dideoxy method using either [α-^{32}P]dATP or [^{35}S]dATP (Amersham, Arlington Heights, IL) and a Sequenase II kit with UP and RP sequencing primers (USB). cDNA inserts in pBluescript vectors were sequenced with T7 polymerase (Sequenase Version 2.0, USB) using fluorescently tagged UP and RP sequencing primers in an ABI protocol (Cawthon *et al.,* 1990a). Internal sequence was obtained manually using *NF1*-specific primers with a sequencing kit (Sequenase Version 2.0, USB) and [α-^{32}P]dATP.

RESULTS

Physical map of the 5′ end of the NF1 locus. We had previously generated a cosmid contig now known to cover the portion of the *NF1* locus harboring exons 28 through 49 (O'Connell *et al.,* 1990; Viskochil *et al.,* 1990). The contig bounded by cosmids EVI36 and 7D5 is approximately 101 kb (Weiss *et al.,* 1992). The telomeric end of 7D5 maps 2.5 kb upstream of the telomeric *Not*I site of the approximate-size 350-kb *Not*I fragment (R. Weiss, University of Utah, pers. comm., 1994). To characterize the 5′ end of the *NF1* gene further, we used *NF1* cDNAs as probes under stringent hybridization conditions to isolate genomic clones mapping upstream of exon 28. As shown in Fig. 1, the newly defined genomic contig consists of cosmids 30, 10, and 23 and the P1-bacteriophage clone P1-9. An overlap of approximately 7.5 kb between the two contigs was established by Southern blot analysis using RNA probes from the T7 end of cosmid EVI37 and the T3 end of cos23 (data not shown). On the basis of Southern blot analysis, we estimate that the contig consisting of cos30, P1-9, cos10, and cos23 is approximately 100 kb long. Cosmid HB5 (Jorde *et al.,* 1993) maps to the centromeric end of the 350-kb *Not*I fragment, and it extends approximately 20 kb telomeric of the *Not*I site (Fig. 1). The difference between the estimated size of the *Not*I fragment and the amount of genomic DNA contained in clones mapping between the *Not*I sites is about 115 kb; this gap lies between clones HB5 and cos30.

Even though the cloned contig does not cover the entire gene, all of the *NF1* exons are represented in genomic clones. Exon 1 maps just 5′ to the centromeric *Not*I site (Marchuk *et al.,* 1992) and is contained in cosmid HB5 (data not shown). Exon 2 maps to cos30 and P1-9 by Southern analysis and by sequence identity of PCR amplification products. Thus, uncloned genomic DNA lying in the gap between HB5 and cos30 is contained within intron 1.

NF1 exon boundaries. The cloning of genomic DNA encompassing all known *NF1* exons provided substrate for the delineation of exon boundaries and flanking intronic sequences. Using genomic clones from the contig, four approaches enabled us to generate exon-selected template for sequencing: (1) direct PCR using facing exon-based oligonucleotides as primers; (2) subcloning of *Sau*3A-digested DNA; (3) inverse PCR with tail-to-tail, exon-based primer pairs (Ochman *et al.,* 1988); and (4) "anchored PCR" using *NF1* cDNA-specific primers with a universal primer to amplify DNA fragments that have been ligated to a restriction site-specific, universal anchor adapter primer (Roux and Dhanarajan, 1990). The exon boundaries depicted in Fig. 2 designate sites where *NF1* cDNA sequence diverged from genomic DNA sequence. Around these sites of divergence, the sequences were typical of splice junctions.

In the course of this work several introns were identified after the adoption of the *NF1* exon numbering system (NNFF International Consortium on Gene Cloning and Gene Function for NF1 and NF2). We have found that exon 4 is actually divided into 4a, 4b, and 4c; exon 10 is divided into 10a, 10b, and 10c; and exon 12 is divided into 12a and 12b. Exon 23 is also interrupted by an intron, but because the previous designation of the alternatively spliced insertion exon 23a was al-

FIG. 2. Locations of exon boundaries in relation to the *NF1*-encoded amino acid sequence (initiating methionine is 1). Downward arrowheads indicate exon boundaries, and the exon number is marked to the right of each arrowhead at the 5′ end of its respective exon. The exon boundaries between 27a and 27b and between 19a and 19b have also been determined by others (Martin-Gallardo *et al.,* 1992; P. Robinson, pers. comm., 1994).

ready firmly established, we elected to designate the two exons derived from exon 23 as 23-1 and 23-2. We have confirmed an unpublished report that exon 19 is divided into exon 19a and 19b (P. Robinson *et al.,* Institute of Medical Genetics, Humboldt University, Berlin, pers. comm., 1994). Finally, exon 27 is divided into 27a and 27b (Martin-Gallardo *et al.,* 1992).

NF1 exon-flanking sequences were derived from the following genomic clones (see Fig. 1): exon 1—cosmid HB5; exons 2 through 6—cosmid c30; exons 7 through 10b—bacteriophage P1-9; exons 10c through 23-1—cosmid c10; exons 23-2 through 27b—cosmid c23; and exons 28 through 49—cosmids cEVI36, cEVI20, cT315, and c7D5. Oligonucleotide primers synthesized from intronic sequences were used to PCR-amplify *NF1* exons using DNA from *NF1* genomic clones as template. The sequences of these primer pairs are presented in Table 1 along with the size of each PCR product generated (shown in parentheses under the number of the exon that it contains).

Sizes of the majority of *NF1* introns are shown in Table 2. The exact lengths of all introns from exons 28 through 49 are known from sequence analysis. The lengths of introns between exons upstream of exon 27b have been estimated by agarose gel electrophoresis of PCR amplification products using facing, exon-based primer pairs from adjacent exons with cloned *NF1* genomic DNA as template. Inability to amplify by PCR indicated that the intron was likely to be longer than 4 kb in length. Numerous introns have been fully sequenced and are marked with an asterisk in column 4 of Table 2.

Intron 10c harbors sequence from a cDNA, pHN-3, that was isolated from a human placenta library (Suzuki *et al.,* 1992). We found that the divergence point of pHN-3 with respect to *NF1* cDNA lies at an exon boundary and that the sequence of pHN-3 cDNA downstream of this boundary is continuous genomic sequence that extends 241 residues into intron 10c. Thus, failure to splice exon 10c to exon 11 could lead to alternative processing of the *NF1* message, resulting in a

TABLE 1

Intron Primers Used to Amplify *NF1* Exons

Exon (bp)	Sequence (5′ → 3′)	Exon (bp)	Sequence (5′ → 3′)
1	CAGACCCTCTCCTTGCCTCTT	18	AGAAGTTGTGTACGTTCTTTTCT
(438)	GGATGGAGGGTCGGAGGCTG	(367)	CTCCTTTCTACCAATAACCGC
2	TTTTAAGGATAAACTGTTTACGTG	19a	TCATGTCACTTAGGTTATCTGG
(221)	TCCCCAAAACACAGTAACCC	(267)	TGTAATTAAGTAGTTATAACTCTC
3	TTTCACTTTTCAGATGTGTGTTG	19b	CCTAAAGTTTATATCTGTTAATAAG[a]
(195)	AATTCCAAGCCTCCTACTTAG	(276)	TGGTGGGGGGCTTTATTTGC
4a	TTTGAAAATTTTCATAATAGAAAATGT	20[b]	CCACCCTGGCTGATTATCG
(415)	GAGGTCAAAGCTGCTGTGAG	(402)	TAATTTTTGCTTCTCTTACATGC
4b	CTCCTGGCCTCAAGTGGTC	21	AAATGAAAGTTTCATATAGAAATAC
(339)	TTATAAAATCCAGATTGGTGTTC	(374)	ATTTGCTATGTGCCAGGGAC
4c	TTTCCTAGCAGACAACTATCGA	22[b]	TGCTACTCTTTAGCTTCCTAC
(283)	CATCAAAAAAAAAAATTTTAATACCAG	(331)	CCTTAAAAGAAGACAATCAGCC
5	TGACTTGAGTGATAGTTTCACAT	23-1	TTTGTATCATTCATTTTGTGTGTA
(240)	AAAAAAAAATCAATCGTATCCTTA	(281)	AAAAACACGGTTCTATGTGAAAAG
6	CATGTTTATCTTTTAAAAATGTTGCC	23-2[b]	CTTAATGTCTGTATAAGAGTCTC
(301)	ATAATGGAAATAATTTTGCCCTCC	(268)	ACTTTAGATTAATAATGGTAATCTC
7	TGCTATAATATTAGCTACATCTGG	23a	AGCCAGAAATAGTATACATGATTGGGT
(373)	CCTATGAACTTATCAACGAAGAG	(447)	CTATTTTCTGCCAGAATTAGTAGA
8	TGTGCTGCTTCTGGCAACTG[a]	24[b]	TTGAACTCTTTGTTTTCATGTCTT
(318)	CTAGTCTTTCTGTTTATAAAGGAT[a]	(266)	GGAATTTAAGATAGCTAGATTATC
9	TTTGACCTCATTTGTATTACTGAG	25[b]	AATATAATAATTATATTTGGGAAGGT
(248)	AGAACCTTTTGAAACCAAGAGTG	(338)	GAAAATATTTGATTCAAACAGAGC
10a	ACGTAATTTTGTACTTTTTCTTCC	26	GCTTTGTCTAATGTCAAGTCAC
(232)	CAATAGAAAGGAGGTGAGATTC	(342)	TTAAACGGAGAGTGTTCACTATC
10b	CTTTAAAGTGATAGCTATTACC	27a	GTTACAAGTTAAAGAAATGTGTAG
(267)	TCTTGGCGATTCAGCTAAACC	(298)	CTAACAAGTGGCCTGGTGGCAAAC[c]
10c	CTTGGTACCCTTTAGCAGTCAC	27b	TTTATTGTTTATCCAATTATAGACTT
(379)	CCTTCTTTCTCCATGGAG	(296)	TCCTGTTAAGTCAACTGGGAAAAAC[c]
11	GTACTCCAGTGTTATGTTTACC	48a	ATCTAGTATCTAATTGTATTTCACC
(189)	TAAAGTTGAAATTTAAAAATTAAAGTAC	(246)	GCAGACTGAGCTTACAGGGAC
12a	AAACCTTACAAGAAAAACTAAGCT	49.1	CTGGGAGAAACAGGCTATAC
(303)	ATTACCATTCCAAATATTCTTCCA	(327)	TTTGAAACTGCCAGCGCT
12b	TTTCTAGTGAATCTCCTTCAAGT	49.2	GCAATGAAATTCAGTCCTGGAAGG
(382)	ATGAAATTTACCAAATTTCATTCAG	(449)	CCCACTTTCTTTGCAGTTGTTCTG
13	CACAGTTTATTGCATTGTTAGAT	49.3	AAGAAAGTGGGAGGTCAGGAA
(382)	GCCATGTGCTTTGAGGCAGAA	(678)	ACTTTGTTCACTGATTACCCTGC
14[b]	TCCTTTTGGGTGGAGCTTATC	49.4	AAACTCAGTCATCCAAACTAG
(285)	TATACTTGTAATATGCACGTATC	(776)	GAAACTCCCCTCTCCCCTAG
15	TGTGATCAGGAATAGCTTTTGAA	49.5	GTAGTGCTGTTTCATTAGAGG
(275)	TTAACAGATAAAAGTCAACTTTAC	(888)	ACATTTTAGTTACTTGGAAAGCTAG
16[b]	TGGATAAAGCATAATTTGTCAAGT	49.6	ACCTTGTTTAAAGAACTTCTGAC
(549)	TAGAGAAAGGTGAAAAATAAGAG	(717)	CACAAACTATTTACAGGTGAATATAC
17	CTCTGTGTGTTTAGATCAGTCA	49.7	CAGGTTTGTAGGTTTTAGG
(318)	TTTATCAATTACTACCAGTATCAG	(707)	GGGAAGAAAACAGAGCCGATAC

Note. Oligonucleotides synthesized from intronic sequences were used in routine PCR to amplify the expected size products as noted in parentheses below each exon number. Exon 49 including the 3′-UTR has been amplified in seven overlapping segments.

[a] Sequence derived from clones that map to *NF1*-homologous loci.

[b] Primer pairs that yield *NF1*-specific sequence using uncloned genomic DNA as template.

[c] Primer sequence from Martin-Gallardo *et al.* (1992).

shorter mRNA species that encodes a smaller isoform of neurofibromin.

NF1 3′-untranslated region. The original reports of *NF1* cDNAs failed to identify the 3′ end of the gene. The majority of published *NF1* cDNA sequences were derived from a human fetal-brain library that was oligo(dT) and random-primed for reverse transcription into cDNA (Cawthon *et al.,* 1990a; Xu *et al.,* 1990a; Marchuk *et al.,* 1991). Other 3′-end cDNAs were isolated from various libraries, including cauda equina and B lymphoblasts (Wallace *et al.,* 1990), pre-B lymphocytes (Bernards *et al.,* 1992), basophilic leukemia cells (Suzuki *et al.,* 1992), and fetal muscle, adult brain, and endothelial cells (Marchuk *et al.,* 1991); the longest extended 291 bases downstream of the stop codon (Bernards *et al.,* 1992). None of these *NF1* cDNAs contained a poly(A) tail, multiple clones were chimeric, and no clones terminated at the same site. Subsequently, we isolated two cDNA clones that matched genomic sequence downstream of the stop codon, FB12 and HB4

TABLE 2

Coding Exons of *NF1*

Exon No.	cDNA position	Size (bp)	Introns (kb)	Exon No.	cDNA position	Size (bp)	Introns (kb)
1	1	60	? (20–140)	(23a	4111	63	6.0)
2	61	144	3.10	24	4111	159	0.53*
3	205	84	?	25	4270	98	1.25
4a	289	195	?	26	4368	147	1.27
4b	484	103	2.0	27a	4515	147	?
4c	587	68	0.22*	27b	4662	111	45–50
5	655	76	0.80	28	4773	433	1.3
6	731	158	?	29	5206	341	2.7
7	889	174	0.40	30	5547	203	4.3
8	1063	123	?	31	5750	194	1.55
9	1186	75	4.0	32	5944	141	0.15
10a	1261	142	?	33	6085	280	0.40
10b	1393	135	4.0	34	6365	215	0.24
10c	1528	114	2.5	35	6580	62	0.15
11	1642	80	0.54	36	6642	115	0.57
12a	1722	124	?	37	6757	102	1.7
12b	1846	156	1.2	38	6859	141	2.4
13	2002	250	0.49	39	7000	127	6.0
14	2252	74	0.23*	40	7127	132	0.93
15	2326	84	1.3	41	7259	136	2.0
16	2410	441	0.38*	42	7395	158	4.0
17	2851	140	0.28*	43	7553	123	0.35
18	2991	123	0.46*	44	7676	131	0.18
19a	3114	84	1.2	45	7807	101	1.1
19b	3198	117	0.55	46	7908	143	0.35
20	3315	182	0.12*	47	8051	47	1.4
21	3497	212	2.2	48	8098	217	6.5
22	3709	162	0.14*	(48a	8315	54	6.7)
23-1	3871	104	?	49	8315	153	
23-2	3975	136	4.0	— 3′ Noncoding —			

Note. Intron lengths were determined either by PCR amplification using facing exon primers from adjacent exons or by complete sequence between exons (denoted by an asterisk). Question marks denote inability to amplify by PCR across the intron; such introns are likely to be larger than 4 kb.

(Fig. 3). FB12 was selected with a PCR probe from the 5′ end of exon 49, and H4B was selected with a PCR probe from exon 48a. FB12 ends at base 8749 (cDNA numbering system from Marchuk *et al.,* 1991), which is the same termination site as the cDNA clone designated Nalm6 (Bernards *et al.,* 1992), and H4B terminates at base 8926, respectively, 291 and 474 bases downstream of the stop codon. Based on Northern analysis of mRNA species that are approximately 11 and 13 kb in length (Viskochil *et al.,* 1990; Wallace *et al.,* 1990; Suzuki *et al.,* 1992), one would predict a 3′-UTR of at least 2.5 kb; therefore, it seemed unlikely that H4B and FB12 represented the 3′ end of the gene. The observation that the mouse *nf1* cDNA is highly homologous to human *NF1* genomic DNA downstream of the stop codon (Bernards *et al.,* 1993) suggested that genomic probes downstream of the stop codon could identify cDNAs that harbor 3′-UTR sequences. A PCR probe representing bases 86168 to 87104 in the genomic sequence (Weiss *et al.,* 1992) identified two independent clones from a fetal-retina cDNA library, FR5 and FR11, and one clone, M13, from an adult-muscle cDNA library; furthermore, a probe from bases 88724 through 89159 (Weiss *et al.,* 1992) identified a clone, FB21D, from a fetal-brain cDNA library. The sequences from the ends of the cDNA inserts matched the genomic sequence downstream of the *NF1* stop codon, and the insert sizes were those predicted based on the uninterrupted genomic sequence. The cDNAs that map to the 3′ end of *NF1* are schematically represented in Fig. 3. Clone FR5 is the longest, covering approximately 3.45 kb; it begins with base 8508 (Marchuck *et al.,* 1991), 53 bp downstream from the stop codon (base 8455), and

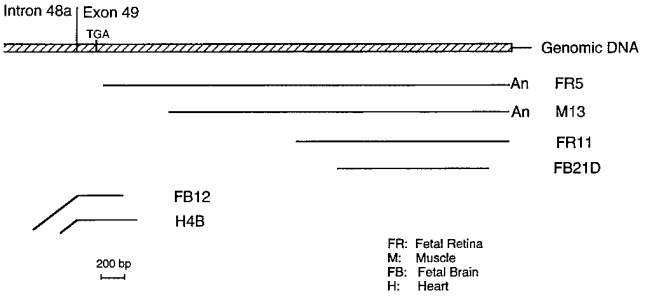

FIG. 3. The 3′-untranslated region of *NF1*. Genomic DNA is represented as a hatched bar, and the boundary between intron 48a and exon 49 is marked. The stop codon 143 bp downstream of the boundary is represented as a TGA above the genomic sequence. Six cDNAs mapping to the 3′-UTR genomic sequence are denoted by horizontal lines; clones FB12 and H4B contain upstream cDNA sequence denoted by an angle at the intron–exon boundary.

terminates in a poly(A) tract at base 11954 in the cDNA sequence, which corresponds to base 89095 in the genomic sequence (Weiss *et al.,* 1992). This clone identifies the *NF1* 3′-UTR as continuous with the stop codon and suggests that splicing does not occur in the 3′-untranslated region.

Both cDNA clones FR5 and M13 terminate at the same base with the addition of poly(A) tails of 18 residues added to an identical site in the genomic sequence. The genomic sequence spanning the polyadenylation site, TTAAGTAAAATGTAAATT**CAA**TCT, contains a potential polyadenylation signal, AGUAAA, an uncommon sequence variant that is only $\frac{1}{3}$ as efficient as AAUAAA in polyadenylation activity (Wickens, 1990). There are two adenosine residues in the genomic sequence at the site of poly(A) addition; therefore, 18 residues could be attached to the boldfaced C in the same sequence shown (position 11954), or 16 residues could be attached to the boldfaced A (position 11956). Clone FR11 extends to base 11957 (additional T residue), but it does not contain a poly(A) tail. Neither does clone FB21D, which covers bases 10603 through 11838. Two sequence differences are notable between the 3′-UTR cDNAs and cosmid 7D5, which served as the template for the genomic sequence. Clones FR5, FR11, and M13 contain a 9-bp insertion (underlined) at base 10408 shown in the following sequence: CAGTGCCAAGGATGCCAAGCTGCCACC. Seven of the nine bases represent a duplication of an immediate upstream sequence. Clone FB21D carries a 7-bp deletion of a tandem duplication at base 11346, underlined in the following sequence derived from the cosmid clone 7D5: CAGTTTTGTTTGGGTTTTTTGTTTTTTTGTTTTTGTTTCTA. The possibility that these sequence variants may represent useful polymorphisms is currently being investigated.

The contig of *NF1* cDNA clones shown in Fig. 3 indicates that the stop codon and the 3.5-kb 3′-untranslated region lie within the same *NF1* exon in genomic DNA. This observation establishes the 3′ end of the gene either at base 11954 or at base 11956 in the cDNA sequence and maps the end of *NF1* approximately 15 kb upstream of the telomeric *Not*I site.

DISCUSSION

The cDNAs described in this report identify the 3′ end of the *NF1* mRNA and establish the telomeric boundary of the *NF1* gene. *NF1* spans all but approximately 15 kb of an estimated 350-kb *Not*I fragment; exons 2 through 47, which includes the stop codon and the 3′-UTR, lie within this single fragment. Exon 1, which contains 5′-untranslated sequence in addition to coding sequence, maps to an adjacent 120-kb *Not*I fragment and lies immediately downstream of a functional promoter of transcription (G. Xu and R. White, unpublished data). The intron between exon 1 and exon 2 could be as large as 140 kb; 20 kb of genomic DNA downstream of exon 1 (represented in cosmid HB5) plus an estimated 115 kb of uncloned genomic DNA (this gap represents the portion of the estimated 350-kb *Not*I fragment not accounted for in the cloned contig) plus a maximum of 5 kb depending on the position of exon 2 within the end fragment of cosmid c30, the most 5′ genomic clone in the contig. Exons 2 through 27b are contained in approximately 100 kb of cloned genomic sequence, and exons 28 through 49 are contained in approximately 52 kb of sequenced genomic DNA. Like intron 1, intron 27b is also relatively large, approximately 45 to 50 kb, and it harbors three embedded genes, *EVI2A* (Cawthon *et al.,* 1990b), *EVI2B* (Cawthon *et al.,* 1991), and *OMGP* (Viskochil *et al.,* 1991). Intron 27b also contains two variable-repeat sites, separated by approximately 31 kb of genomic sequence, which have been adapted by clinical laboratories for linkage analysis (Lazaro *et al.,* 1993; K. Ward, University of Utah, pers. comm., 1994).

The role that the two large introns may play in *NF1* expression is unknown. The genes embedded in intron 27b are likely to place some constraints on the ubiquitous expression of *NF1*, although no transcriptional interference has been demonstrated. Even though an accurate ascertainment of the size of intron 1 will not be possible until the cloned contig is linked to cosmid HB5, its estimated size of 140 kb suggests that intron 1 could harbor regulatory elements that influence *NF1* expression in some way. In view of the presence of genes within intron 27b, the possibility that embedded genes also lie within this relatively large intron should be considered.

Knowledge of *NF1* structure enabled us to locate other landmarks in the gene. Amino acid homology with yeast Ira1 and Ira2 covers encoded exons 16 through 40. The homology with bovine P120GAP extends from exon 21 through 27a. Two known *NF1* translocation breakpoints t(1;17) and t(17;22) map to introns 27b and 31, respectively. The *AK3* pseudogene (Xu *et al.,* 1992) maps to intron 39. Finally, the two known alternative splice exons, 23a (Nishi *et al.,* 1991; Suzuki *et al.,* 1991) and 48a (Cawthon *et al.,* 1990a; Gutmann *et al.,* 1993), respectively, map to the 10-kb intron 23-2 and the 13.2-kb intron 48.

The two *NF1* cDNA clones that end in poly(A) tails define the 3′-UTR and establish the full length of the mRNA transcript as approximately 12 kb. There is evidence that mouse *nf1* cDNAs demonstrate alternative polyadenylation (Bernards *et al.,* 1993). Given that human *NF1* 3′-UTR contains other potential polyadenylation signals—AUUAAA at positions 9919, 10000, and 10086 and AUUAAA at positions 9140 and 9979—we evaluated all isolated cDNA clones for alternative polyadenylation. Although the cluster of polyadenylation signals between bases 9919 and 10086 could explain the approximate 2-kb difference between an 11- and a 13-kb mRNA species identified by Northern blot analysis (Suzuki *et al.,* 1992), we have not identified human *NF1* cDNAs that end within 20 bases downstream of

those motifs. Therefore, the basis of the size difference remains unknown.

Several sequence motifs identified in 3′-UTRs from other genes are known to affect mRNA stability and gene regulation (Jackson, 1993; Rastinejad and Blau, 1993); therefore, we speculate that the *NF1* 3′-UTR may play some role in the variability of clinical expression of NF1 by influencing *NF1* mRNA levels in a stochastic manner. However, there are few motifs present that could provide clues toward understanding its role in mRNA processing. The *NF1* 3′-UTR contains no UA-rich mRNA instability determinants (consensus UUAUUUAU), although several adenylation control elements are present (ACEs—consensus UUUUUUAU or UUUUAAU) (Jackson, 1993), of which the one nearest to the AAGUAA polyadenylation signal lies 460 bases upstream. A search of the nucleic acid sequence databases identified two homologies with 3′-UTRs from other genes; one is a short GT-rich segment in β-actin 3′-UTR, and another is a 100-bp stretch in the α-tropomyosin 3′-UTR. The functional significance of these homologies and motifs has not been tested.

Boundaries and splice junctions have been identified for all of the known *NF1* exons. Examination of the intronic splice sites reveals general adherence to the GT–AG rule (Shapiro and Senapathy, 1987). The 5′-splice sites are invariant for GT, although 7 introns lack the consensus purine residue at the third position. Likewise, the 3′ splice sites are invariant for AG, and only introns 25 and 36 have a purine instead of a pyrimidine in the preceding position. Notably, the 3′ splice junction between exons 10c and 11 lacks a polypyrimidine tract immediately upstream of the fourth position; instead, it has a stretch of 7 adenosine residues preceded by 13 pyrimidine residues. This sequence structure may confer a regulatory function for alternative processing leading to the 2.9-kb mRNA isoform from human placenta that terminates within exon 10c (Suzuki *et al.,* 1992).

Knowledge of the *NF1* exon boundaries and flanking sequence enabled us to design intron-based primer pairs to amplify individual exons from genomic DNA template. Using these specific primers in PCR amplifications, we have been able to determine the exon composition of genomic clones, to order the clones, and to map partially the regions of overlap within the contig. All of the known *NF1* exons are contained in either P1 or cosmid clones of genomic DNA. Sequence analysis of PCR products synthesized from the genomic clones shown in Fig. 1 revealed exon sequences identical to *NF1* cDNA sequence. Several other cosmid and P1 clones originally identified with *NF1* exon-based probes upstream of exon 28 were amplified by PCR using several primer pairs; however, the DNA sequences of exon regions from these PCR products are not identical to *NF1* cDNA sequence (data not shown). These clones map by fluorescence *in situ* hybridization to other chromosomes (D. Viskochil, unpublished data), and we interpret this to mean that they represent distant loci related to *NF1*. *NF1*-homologous loci have been described by others (Legius *et al.,* 1992; Gasparini *et al.,* 1993; Cummings *et al.,* 1993); the best characterized locus maps to chromosome 15. It shares about 90% homology with *NF1* within the intronic regions where sequences are known (Y. Li and R. Cawthon, unpublished data). Although a high degree of sequence homology exists between exons in the *NF1* GAP-related domain and the corresponding portion of the chromosome 15 locus, we have noted some frame-shifting deletions in the latter. Therefore, we conclude that even if it is transcribed, the chromosome 15 homologue does not encode a functional GAP-related protein. The identification of RT-PCR products where sequences are homologous, but not identical, to *NF1* exons (Cummings *et al.,* 1993) suggests that at least some *NF1*-related loci may be transcriptionally active. We have not fully evaluated the possibility that the chromosome 15 locus, or the other *NF1*-homologous loci, is expressed either in various tissues or in a developmentally regulated fashion.

We have synthesized oligonucleotide primers based on flanking intronic sequences for 56 of the 59 *NF1* exons and have demonstrated PCR amplification of a product of the expected size from genomic clones for each of them; primer pairs for exons 37, 38, and 39 remain to be synthesized. However, amplification by PCR of *NF1*-homologous loci when using oligonucleotide primers that are derived from intronic sequence from *bona fide NF1*-specific genomic clones complicates efforts to screen genomic DNA for *NF1* mutations by the direct-sequencing approach. This approach may require knowledge of intronic DNA sequences derived from cloned *NF1*-homologous loci before primer pairs can be designed to amplify *NF1* sequence specifically from genomic DNA. Using this information, we have synthesized seven primer pairs (superscript b in Table 1) that yield *NF1*-specific sequence using uncloned genomic DNA as template. The development of intron-based, exon-specific pairs of primers to amplify each *NF1* exon from genomic DNA is a logical first step toward implementation of a comprehensive, DNA-based screening protocol for *NF1* mutations.

ACKNOWLEDGMENTS

We acknowledge the technical expertise of Melanie Culver, primer synthesis by Edward Meenan, DNA sequencing by Paige Bradley, and Rick Lifton for providing the cosmid library from human peripheral blood leukocytes. We thank Ruth Foltz for her help in preparing the manuscript. R.C. was supported by grant awards from the National Neurofibromatosis Foundation (NNFF) and the National Cancer Institute (R55CA57511-01). P.O.C. was supported by Grant PO1 HG00470 from NIH. D.V. was supported as a clinical investigator by the National Institute of Neurological Disorders and Stroke (K08 NS01492), U.S. Department of Defense (DAMD 17-93-J-3070), Rocky Mountain Center for the Biology of Development under the Childrens Health Research Center, National Institute of Child Health, the NIH (5P30 HD27827), and the NNFF.

APPENDIX B

1. Ota M., Ballard L., Coffin C., Parham D., Shearer P., and Viskochil D. (1996). Genetic Evaluation of Malignant Peripheral Nerve Sheath Tumors from Non-Neurofibromatosis 1 (NF1) Individididuals. *Abstract to US and Canadian Academy of Pathology*, 1997 Meeting.

2. Viskochil D., Sawada S., Florell S., Purandare S., Ota M., and Stephens K. (1996). Identification of *NF1* Mutations in both Alleles of a Dermal Neurofibroma. *Am. J. Hum. Genet.* **62**:Abstract#453.

3. Purandare S., Ota A., Neil S., and Viskochil D. (1996) Identification of *cis*-Regulatory Elements in the Neurofibromatosis 1 Gene. *Am. J. Hum. Genet.* **62**:Abstract#888.

for office use only

ABSTRACT DEADLINE

Abstracts must be **postmarked** as follows:

Mailed within USA - September 18, 1996

International Air Mail (includes Canada) September 13, 1996

International Overnight Express Mail September 18, 1996

Additional abstract forms: (706) 733-7550 or FAX (706) 733-8033

PRESENTATION CHOICE

Poster only _____

Either Poster or Platform ____xxx____

Stowell-Orbison _____ (application form enclosed)

Autopsy Award _____ (application form enclosed)

CATEGORY (see listing on reverse)

Pediatric

ABSTRACT CHECKLIST

(Please Complete)

- _x_ Format corresponds to sample
- _x_ Completed Postcard enclosed
- _x_ Original and 3 photocopies enclosed
- _x_ Presentation choice checked
- _x_ Abstract fits within blue lines
- _x_ Abstract is typed directly on original form

MAIL ORIGINAL AND THREE (3) PHOTOCOPIES TO:

United States and Canadian Academy of Pathology
3643 Walton Way Extension
Augusta, GA 30909 U.S.A.

GENETIC EVALUATION OF MALIGNANT PERIPHERAL NERVE SHEATH TUMORS (MPNSTs) FROM NON-NEUROFIBROMATOSIS 1 (NF1) INDIVIDUALS.

M. Ota, L. Ballard, C. Coffin, D. Parham, P Shearer, D. Viskochil.
University of Utah and Primary Children's Medical Center, Salt Lake City, UT, University of Arkansas for Medical Sciences, Little Rock, AR, and St. Jude Children's Research Hospital, Memphis, TN.

Background: Childhood MPNST is often associated with NF1. Although adult MPNST in NF1 usually have loss of chromosomal 17 material, genetic abnormalities have not been documented in sporadic pediatric MPNST.
Design: Five sporadic, pediatric MPNST were examined. The diagnosis was confirmed by two pathologists using standard techniques and immunohistochemistry. DNA was extracted from microdissected 4-mm paraffin sections and evaluated for *NF1* mutations by PCR-based, exon-specific size shift as determined by denaturing gel electrophoresis. Genotype analysis was also performed using the microsatellite markers UT57 (17p, D175740) and UT290 (just telomeric of *NF1* on 17q, D175966). Patient-matched archival material was used for the extraction of constitutional DNA.
Results: Genotype analysis demonstrated allelic imbalance at UT290 in 3 of 3 informative tumors. Allelic balance at UT57 was preserved in 2 of 2 informative tumors. Mutation analysis on 90% of the coding region of the *NF1* gene identified one size-shift variant in exon 4b of one tumor.
Conclusion: Our results suggest that tumorigenesis of MPNST arising in children and adolescents without clinical manifestations of NF1 involves somatic alteration of the *NF1* locus. However, our inability to identify "second hits" at the *NF1* locus in 4 of 5 tumors suggests that other modifying loci may also play significant roles in MPNST tumorigenesis.

box abstract fold not do

printer's cut lines - do not type on or outside blue lines

This abstract has not been submitted for publication or presentation at another meeting, and there is no conflicting relationship with a commercial enterprise.

SIGNATURE: Cheryl M. Coffin MD

Name and Address of Author for Correspondence:

David H. Viskochil, MD, PhD
Division of Medical Genetics
413 MREB
University of Utah
Salt Lake City, UT 84112

Phone: (801) 581-8943 Fax: (801) 585-5241

Name and address of non-members for mailing meeting registration information:

David Viskochil, MD, PhD
Division of Medical Genetics
413 MREB
University of Utah
Salt Lake City, UT 84112

****

REGISTRATION - Authors presenting the accepted scientific entries will be required to pay the general registration fee for the meeting. Meeting registration information is NOT automatically mailed to non-members. Please indicate above if you wish to receive this information.

448

Validation of Primed In situ hybridization (PRINS) for nuclear in situ (nuc ish) analysis. Comparative studies with fluorescence in situ hybridization (FISH) and chromosome analysis. S. A. Tharapel, G. V. N. Velagaleti and A. T. Tharapel. Veterans Affairs Medical Center and The University of Tennessee, Memphis, Tennessee, USA.

Clinical and prognostic implications of karyotypic changes in human neoplasms have been well documented, particularly in hematological disorders. Karyotypic changes like monosomy 7 and trisomy 8 in myelodysplastic syndromes (MDS) and trisomy 12 in chronic lymphocytic leukemia of B-cell lineage (CLL) have been implicated in diagnosis and prognosis, making cytogenetic diagnosis an important aspect of clinical management. Success of cytogenetic diagnosis depends on the availability of dividing cells in the bone marrow, and also on the quality of the preparations. Introduction of FISH has improved our ability to detect specific chromosomal changes in neoplasia. In an effort to design new alternatives for FISH that are cost effective, easier and accurate, we evaluated the efficacy of PRINS technology for the detection of aneuploidy in the interphase cells of patients with MDS and CLL.

We analyzed fourteen cases with MDS (monosomy 7 in four and trisomy 8 in ten cases) and three cases of CLL with trisomy 12 and six controls using PRINS technique. Single strand primers were used to target the respective pericentromeric alpha satellite region of these chromosomes. PRINS is based on sequence-specific annealing of an unlabeled oligonucleotide primer, followed by primer elongation with Taq polymerase, *in situ* on nuclei and metaphase chromosomes on a slide. Slides were blind coded prior to hybridization and analysis. At least 200 nuclei were analyzed for each sample and scoring was done by two independent and experienced cytogeneticists. The results obtained by PRINS were compared to the cytogenetic and conventional FISH interphase analyses to evaluate the efficacy, accuracy and reliability. Comparison showed that PRINS is in fact as sensitive, accurate and specific as conventional FISH. Based on our experience with PRINS and these results, we conclude that PRINS is a viable, easier and cheaper alternative to conventional FISH in the detection of aneuploidy.

449

Altered expression of hMSH2 and hMLH1 in tumors with microsatellite instability and genetic alterations in mismatch repair genes. S.N. Thibodeau[1], A.J. French[1], P.C. Roche[1], J.M. Cunningham[1], D.J. Tester[1], N.M. Lindor[1], G. Moslein[2], R.M. Liskay[3], S.M. Baker[3], L.J. Burgart[1], R. Honchel[1], and K.C. Halling[1]. [1]Mayo Foundation, Rochester, MN; [2]Univ. of Dusseldorf, Germany; and [3]Oregon Health Science Univ., Portland.

Four genes involved in DNA mismatch repair (MMR), hMSH2, hMLH1, hPMS1, and hPMS2 have been shown to be altered in the germline of patients (pts) with hereditary nonpolyposis colon cancer (HNPCC). Additionally, loss of MMR function has been shown to lead to the phenomenon of microsatellite instability (MIN) in tumors from these pts. Establishing the diagnosis of HNPCC and the subsequent identification of germline mutations, however, has been problematic. The diagnosis is dependent on a pedigree analysis and there is a spectrum of mutations and genetic heterogeneity. Although MIN offers a screening tool for the identification of pts with HNPCC, this phenotype does not necessarily define which MMR gene is involved and MMR gene mutations have not been found in a significant number of pts with MIN+ tumors. In this study, we have examined the protein expression pattern of hMSH2 and hMLH1 by immunohistochemistry in paraffin-embedded tumors from 7 pts with MIN+ sporadic cancer, 13 pts with familial colorectal cancer, and 12 pts meeting the strict Amsterdam criteria for HNPCC. The relationship between the expression of these two gene products, the presence of germline or somatic mutations, and the presence of tumor MIN was examined. Nineteen of the 28 tumors studied demonstrated MIN while mutations in hMLH1 and hMSH2 were detected in 8 pts. Of the 8 MIN+/Mutation+ cases, the absence of protein expression was detected for the corresponding gene product in all but 1 case (missense mutation in hMLH1). However, 7 MIN+/Mutation- cases also showed no expression of either hMLH1 (n=5), hMSH2 (n=1), or both (n=1), while 4 MIN+/Mutation- cases demonstrated normal expression for both. None of the MIN-/Mutation- cases (n=9) demonstrated an altered expression pattern for either protein. These data suggest that examination of protein expression by immunohistochemistry may be a readily available and rapid method for pre-screening of tumors for mutations in the MMR genes.

450

Rb1 mutation mosaicism in a retinoblastoma family. F. Thonney[1,2], F. Munier[1,2,3], A. Balmer[3], E. Heon[3,4], G. Pescia[1], D.F. Schorderet[1,2]. [1]Division of Medical Genetics, [2]Unit of Molecular Genetics, CHUV; [3]Hopital Jules Gonin. University of Lausanne, Switzerland and [4]Department of Ophthalmology, University of Toronto, Canada.

We report a 2 generation retinoblastoma family, consisting of the bilaterally affected proband, her unilaterally affected father, and her 2 paternal healthy half-brothers. Linkage analysis revealed that the presumably mutated intragenic haplotype was shared by the 2 unaffected sibs. Mutation identification was performed in the proband and showed a T to C transition in exon 8 of the RB1 gene leading to a stop codon (R251X) and to the suppression of a TaqI site. Because this mutation was not clearly seen in the affected father, PCR amplicons obtained from white blood cells were subcloned and individual clones analyzed for the presence/absence of the TaqI site. Ten percent of the clones showed the R251X mutation. The two unaffected half-brothers were homozygote for the wild-type allele. These data suggest the existence of two cell populations in the father's somatic and germinal tissues which implies a very early occurrence of the first mutation during embryogenesis.

Because of a possible mosaicism in unilaterally affected founders of retinoblastoma families, diagnosis of non penetrance in allegedly healthy children cannot be established by linkage analysis alone, unless corroborated by the cosegregation of the causal mutation.

This work is supported by the "Recherche suisse contre le cancer" (grant AKT621).

451

Novel hMSH2 gene mutations in African patients with microsatellite unstable colorectal carcinomas. E.J. van Rensburg[1], C.M. Hattingh [1], L. Dreyer[2], M. Hale [3] and I. Segal [4]. [1]Department of Human Genetics and [2]Department of Anatomical Pathology, Univ of Pretoria Medical School, Pretoria, [3]Department of Histopathology and [4]G.I.T. Unit, Baragwanath Hospital, Univ of Witwatersrand, Johannesburg, South Africa.

Colorectal cancer (CRC), one of the commonest neoplasms in the Western world is notably less prevalent in black Africans. In South Africa the majority of black CRC patients present with the non-polypoid type. Recently, four genes involved in DNA mismatch repair (hMSH2, hMLH1, hPMS1 and hPMS2) were implicated in hereditary non-polyposis colorectal carcinoma (HNPCC). A pilot study to determine whether mismatch repair genes are involved in the molecular etiology of CRC in black South African patients is reported.

Normal and tumour tissue from 82 patients was analyzed for the presence of microsatellite instability using a set of ten microsatellite markers. Instability was found in 23 (28 percent) tumours, which were then screened for mutations in the hMSH2 gene. Using exon-by-exon PCR-SSCP analysis six novel hMSH2 mutations (sequence variants, ie N127S, Y103D and I237V ; frameshifts in exon 2, ie 76del AG and 87del5; and exon 5 donor splice site G-A transition)and one previously reported mutation (A-T transversion in exon 5 donor splice site) were detected. Of these, seven were somatically derived and the other (76delAG in exon 2) was a germline mutation which was also present in the germline of an asymptomatic family member. To the best of our knowledge this is the first black African family reported with HNPCC. These results thus implicate the involvement of mismatch repair genes in the etiology of CRC in black Africans.

452 Poster Symposium–Session 30

Genomic changes in microdissected breast tumors detected by CGH. V.S. Venkatraj, S. Bose, H. Hibshoosh and D.Warburton. Columbia University, New York, NY

Comparative genomic hybridization (CGH) has been shown to be a reliable method of surveying genomic gains and losses in tumor tissue without the need for preparing and analyzing metaphase figures from the tumor. However, this technique is sensitive to the admixture of normal cells which is often found in fresh or fixed tumor tissue and may decrease the ability to detect genetic changes in tumor cells. We have used microdissection of 5 to 10 H and E stained slides of 8 micron paraffin sections to isolate areas of breast tumor from surrounding normal tissue. DNA was then extracted from the isolated material for use in CGH. Preliminary results on five invasive ductal breast carcinomas identified multiple clear-cut amplifications and deletions. Consistent changes observed were gains of 1q32-42, 8q, 16p, 17q21-25 and 20q. Other gains and losses were seen in isolated tumors. Data were available on levels of HER2/neu expression in these tumors, and this was correlated with the presence or absence of amplification in 17q. The genetic changes we observed are similar to those previously identified in breast tumors by CGH, but appear to be seen at a higher frequency. Thus the use of microdissected tumor tissue may provide a higher level of resolution, enabling changes to be detected more reliably and facilitating comparisons of genetic changes relevant to tumor type, progression and aggressiveness.

453

Identification of *NF1* mutations in both alleles of a dermal neurofibroma. D. Viskochil[1], S. Sawada[1,2], S. Florell[1], S. M. Purandare[1*], M. Ota[1,2], K. Stephens[3]. [1]University of Utah, Salt Lake City, [2]Jikei University School of Medicine, Tokyo 105, Japan, [3]University of Washington, Seattle, *Present address: Baylor College of Medicine, Houston, TX.

We have identified a somatic mutation in the normal *NF1* allele in a scalp dermal neurofibroma from an NF1 individual who has a large submicroscopic deletion of the *NF1* locus. This constitutional deletion was identified by somatic cell hybridization studies and fluorescence *in situ* hybridization. A PCR product representing *NF1* exon 4b from frozen tumor DNA demonstrated a size-shift by denaturing gel electrophoresis as compared with the constitutional DNA. This observation predicted the presence of a small deletion in exon 4b. Sequence analysis showed a four base-pair deletion of bases 543 through 546 in the *NF1* cDNA sequence in four of six PCR product subclones. This frame-shift mutation leads to the insertion of an ochre codon 9 amino acids downstream of the deletion site. It predicts an inactivation of neurofibromin function. Cells from adjacent skin that were microdissected from paraffin-embedded tissue sections do not harbor the somatic mutation, yet DNA extracted from regions of homogeneous-appearing tissue demonstrated both normal and 4-bp deleted alleles. Thus, NF1-related dermal neurofibromas are not clonal.

This is the first definitive identification of a somatic mutation which is limited to the *NF1* locus in a benign neurofibroma from an NF1 individual in whom the constitutional *NF1* mutation is known. It supports the hypothesis that a "second hit" in the normal allele is important in the development of neurofibromas in NF1.

883

The Machado-Joseph disease gene product, MJD1, is a cytoplasmic protein expressed widely in the central nervous system. H.L.Paulson, S.S.Das, P.B.Crino, M.K.Perez, S.C.Patel, K.H.Fischbeck and R.N.Pittman. Departments of Neurology and Pharmacology University of Pennsylvania, Philadelphia PA 19104

Machado-Joseph disease (MJD) is one of at least five neurodegenerative diseases caused by an expanded CAG/polyglutamine tract within the protein coding region of the disease gene. Using RT-PCR, we isolated six splice variants and full length human MJD1 cDNA from patient lymphoblastoid cells and normal human brain. One splice variant, encoding MJD1 protein with an internal deletion of 15 amino acids, was used to create a fusion protein for generating antiserum. Anti-MJD1 antiserum specifically recognized normal and expanded MJD1 in lymphoblastoid cells and in cells transfected with normal or expanded repeat MJD1 cDNAs. Western blot analysis of human tissue indicated that the full length protein is the major species expressed in brain and elsewhere. Immunohistochemistry of normal brain demonstrated predominantly cytoplasmic staining in neurons thoughout the brain, although in certain regions only a small subpopulation of neurons were positive (for example, the striatum). In tissue from an MJD patient, the expanded repeat protein was expressed in all regions of the brain, including areas preferentially spared in disease, as well as in other organ systems. The widespread expression of MJD1 indicates that in this disease, as in other polyglutamine repeat diseases, cell specific factors likely account for the selective neurodegeneration seen in patients. However, MJD may differ from Huntington's disease and several other polyglutamine repeat diseases in that some brain regions express MJD1 in distinct subpopulations of neurons, a fact which may provide clues to its normal function.

884

Identification and Functional Characterization of a Missense Mutation found in the Leptin Receptor (OB-R) of the *fatty* Zucker Rat.

M.S. Phillips[1], C.I. Rosenblum[2], M. Tota[2], D. Cully[2], P.J. Hey[1], C.T. Caskey[1], and J.W. Hess[1]. 1. Dept. of Human Genetics, Merck Research Laboratories, WP26-354, Merck & Co., Inc., West Point, PA. 19486. 2. Dept. of Genetics and Molecular Biology, Merck Research Laboratories, Merck & Co., Inc., Rahway, NJ, 07065.

We have identified a novel mutation in the leptin receptor (OB-R) of the fatty Zucker rat which is different from the splicing mutation found in the db mouse. Cloning and comparison of the OB-receptor cDNA's from lean (Wt/?) and obese (*fa/fa*) Zucker rats showed that each encodes a protein of 1162 amino acids and revealed a single nucleotide transversion of A^{880} to C in the *fa/fa* rat. The mutation results in the substitution of Gln^{269} to Pro, a conserved amino acid residue, which is present in the extracellular portion of the receptor in a domain characteristic of type I cytokine receptors. The development of a genomic diagnostic restriction endonuclease assay, has allowed us to genotype a number of rats for the mutation. Examination of 20 obese and 29 lean Zucker rats, an outbred strain, and 15 obese and 15 lean ZDF rats, an inbred strain, showed 100% correlation between the obese phenotype and the presence of the A^{880} to C mutation. Two common laboratory strains, Wistar/Kyoto and Sprague/Dawley, were genotyped and found to be identical to the homozygous wild type Zucker rats.

We have established a functional assay for the OB-R using recombinant leptin and the OB-R expressed in GT1-7 cells. As well, we have developed a binding assay measuring ^{125}I-labeled leptin binding to COS-7 cells. Expression of the *fa* OB-R showed that it bound leptin with equal affinity to that of wild-type OB-R. However, receptor abundance was about 7 fold reduced. In the functional assay, the *fa* OB-R showed a significantly reduced amount of STAT response element activation in comparison to the wild-type but this difference is consistent with the reduced receptor number at the cell surface. Thus, the mutation in the *fa* OB-R protein, while not affecting its ability to stimulate the leptin transduction pathway may affect its ability to be correctly folded and trafficked to the cell surface. Therefore, we propose that reduction in abundance of a functional OB-R can lead to obesity.

885

Exon-intron structure and methylation-associated regulation of expression of the GPC3 gene. R. Huber[1], L. Crisponi[1,2], D. Schlessinger[1], and G. Pilia[2]. [1]Department of Molecular Microbiology, Washington University School of Medicine, St. Louis, MO 63110 and [2]Istituto di Ricerca sulle, Talassemie e Anemie Mediterranee, Cagliari, Italy 09121

Mutations in the glypican 3 (GPC3) gene cause the Simpson-Golabi-Behmel syndrome in a number of instances where X-linked inheritance has been shown. The syndrome is very similar to Beckwith-Weidemann syndrome, however, and X-linkage cannot be assessed by family studies in the predominantly sporadic cases of "BWS". The definitive incidence of involvement of GPC3 modifications in BWS could instead be determined by studies of the expression and structural status of GPC3 in patients. Because GPC3 is not expressed in fibroblasts or blood cells, straightforward mutational analyses of the gene must be done at the DNA rather than the RNA level. To facilitate such studies, we have defined the exon-intron borders of the eight exons of GPC3 and developed PCR primer pairs to amplify each exon and its adjacent genomic DNA. As for the regulation of the gene, tissue-specific control is associated with methylation of the promoter region, and the unmethylated promoter is active when transfected into cells that do not express the endogenous gene. Transcription is efficiently driven by a 584 bp high GC region which contains several putative Sp1 and Ap2 transcription factor binding sites 5' to the start site. In preparation for the analysis of patient DNAs, a PCR primer pair has also been developed to permit amplification of this region.

886

DNA methylation represses the murine Xist promoter by an indirect mechanism. N. Pillet[1,2,3], C. Bonny[3], D.F. Schorderet[1,2,3]. [1]Division of Medical Genetics and [2]Unit of Molecular Genetics, [3]CHUV, Lausanne, Switzerland.

The mouse Xist gene is exclusively expressed from the inactive X chromosome and is involved in the initiation of X-chromosome inactivation in females. Previous studies in somatic tissues have shown that the 5' end of the silent Xist allele is methylated while the expressed allele on the inactive X is characterized by a lack of methylation. A role for methylation in the control of Xist expression is further supported by the finding that differential methylation of Xist alleles precedes the onset of Xist expression. We have recently demonstrated that the different transacting factors binding to the Xist promoter are not sex-specific. It seems therefore reasonable to hypothesize that female-specific Xist expression is regulated by methylation.

In a cell culture experiment, treatment of mouse XY fibroblasts with 5-azacytidine resulted in activation of the transcription of the Xist gene, as seen by RT-PCR. To study further the molecular mechanisms involved, a CAT reporter gene construct containing the Xist promoter and part of the first exon (-1157/+917) was methylated in vitro and transfected into murine fibroblasts. Methylation of the construct resulted in complete repression of the Xist promoter. Analysis of different deletions of the promoter showed that methylation of 9 CpG sites within the -132/+20 region is sufficient to block in vitro transcription, suggesting that the extend of the repression is not dependent on the density of methylation. Mobility shift assays indicated that DNA binding of transcription factors to the Xist promoter is not prevented by methylation. In the contrary a new, yet unidentified, nuclear protein was able to bind to the -53/-18 region in a sequence-methyl-CpG-specific manner. This binding was lost when some of the methyl-CpG sites were mutated to TpG. It is possible that the methyl-CpG binding protein (MCPGBP) inhibits all interactions between the nuclear proteins binding at -69/-65 and -30/-25. Methylation could also block transcription by triggering a modification of the chromatin structure which would imply the existence of a synergistic relationship between MCPGBP and the chromatin structure.

Poster Presentations

887

Characterization of the human *SOX1* and *SOX2* genes. H.M.Prior and M.A.Walter. Departments of Ophthalmology and Medical Genetics, University of Alberta. Edmonton, Alberta, Canada.

Human development requires complex genetic regulation. Various families of master control genes code for transcription factors which affect the expression of downstream target genes. Genes in the *SOX* family share a DNA-binding motif called the *SRY* box, a region homologous to the HMG-box sequence of *SRY*. Like *SRY*, the mammalian sex determining gene, *SOX* genes also play important roles in chordate development. About 20 *SOX* genes have been identified and partially characterized. For example, mutations in *SOX*9 have been linked to Campomelic dysplasia and autosomal sex reversal. Studies of murine *Sox*-1 and *Sox*-2 suggest they may play a role in embryonic eye development. We have screened a human fetal brain library using murine probes to identify human *SOX*1 and *SOX*2 cDNA candidates. Five clones have been partially characterized by restriction mapping and sequencing. Expression studies of clones which correspond to *SOX*2 localize it to human fetal brain and to a lesser extent adult brain, with no detectable expression in kidney, pancreas, placenta, or muscle. *SOX2* is known to map to 3q26.3-27. Using primers based on the murine *Sox-1* sequence, PCR experiments have been used to amplify sections of the human *SOX1* gene. The HMG-box region of the human *SOX1* gene has been obtained, sequenced, and found to be 99% identical to the murine sequence. Further mapping and chromosomal localization are underway, and may suggest roles for these genes in hereditary eye disease. Characterizing *SOX*1 and *SOX*2 will give us a better understanding of the process of human eye development and disease.

888

Identification of *cis*-regulatory elements in the neurofibromatosis 1 gene. S.M. Purandare[1,*], A. Ota[1], S. Neil[1], and D. Viskochil[1]. [1]University of Utah, Salt Lake City, [2]Jikei University School of Medicine, Tokyo, Japan, [*]Present address: Baylor College of Medicine, Houston, TX.

The promotor region of *NF1* is embedded in a CpG island, and, similar to other "housekeeping" genes, it does not harbor the typical regulatory TATA or CCAAT boxes. To localize potential *cis*-acting elements important in *NF1* expression, a series of *NF1* promoter constructs were generated in pGL2-Basic *luciferase* reporter vector. Liposome-mediated transfection into COS-1 cells resulted in enhanced *luciferase* expression for a number of *NF1* constructs. A construct harboring sequence 4361 bp upstream and 144 bp downstream of the transcription start site demonstrated a 65-fold increased level of luciferase activity over the basic construct. A series of exonuclease-generated deletion constructs were transfected into COS-1 cells and transient expression of luciferase from cell lysates was determined. There was a 2.5-fold increased level of expression using a construct harboring bases -3305 to +474 over the full-length construct (-4361 to +474). A clone which harbors 72 additional basepairs in the 5'-direction (-3377 to +474) demonstrated a 2.5-fold decreased luciferase activity. One hypothesis generated from this data is that a repressor or silencer is contained in the region between -3377 and -3305. We have utilized PCR products spanning this sequence as probes in mobility shift assays using COS-1 cell lysates as a source of DNA-binding proteins. These studies demonstrate the presence of a low-affinity protein-binding site in a 95-basepair segment lying 3300 bp upstream of the *NF1* transcription start site.

PI: David H. Viskochil, MD, PhD

BIBLIOGRAPHY

PUBLICATIONS

Fuller BB and **Viskochil DH**: The Role of RNA and Protein Synthesis in Mediating the Action of MSH on Mouse Melanoma Cells, Life Sciences 24, 2405-2416, 1979.

Wilson EM, **Viskochil DH**, Bartlett RJ, Lea OA, Noyes CM, Petrusz P, Stafford DW, and French FS: Model Systems for Studies on Androgen-Dependent Genet Expression in the Rat Prostate. The Prostatic Cell: Structure and Function Part A, 351-380, 1981.

Viskochil DH, Perry ST, Lea OA, Stafford DW, Wilson EM, and French FS: Isolation of Two Genomic Sequences encoding the M = 14,000 Subunit of Rat Prostatein, J. Biol. Chem. 258, 861-866, 1983.

Viskochil DH: Cloning and Characterization of the C3 Subunit Gene of Prostatein, the Major Androgen-Dependent Secretary Protein of Rat Ventral Prostate, Dissertation for degree of Doctor of Philosophy in the Department of Biochemistry, University of North Carolina, Chapel Hill, 1983.

Perry ST, **Viskochil DH**, Ho KC, Fong K, Stafford DW, Wilson EM, and French FS: Androgen Receptor Binding to the C3 Subunit Gene of Rat Prostatein in Regulation of Androgen Action, Proceedings of an International Symposium, Montreal, pp. 167-173, 1984.

O'Connell P, Leach R, Cawthon RM, Culver M, Stevens J, **Viskochil D**, Fournier REK, Rich DC, Ledbetter DH and White R: Two NF1 translocations map within a 600-kilobase segment of 17q11.2. Science 244: 1087-1089, 1989.

Christensen RD, Koenig JM, **Viskochil D** and Rothstein G: Down-Modulation of neutrophil production by erythropoietin in human hematopoietic clones. Blood 74: 817-822, 1989.

Viskochil DH, Carey J, Glader B, Rothstein G, and Christensen R: Congenital Hypoplastic (Diamond-Blackfan) Anemia in 17 Members of One Kindred. Am J of Med Genet 34: 251-256, 1990.

O'Connell P, **Viskochil D**, Buchberg A, Fountain J, Cawthon R, Culver M, Stevens J, Rich D, Ledbetter D, Wallace M, Carey J, Jenkins N, Copeland N, Collins F and White R: The Human Homologue of Murine Evi-2 between Two von Recklinghausen Neurofibromatosis Translocations. Genomics 7:547-554, 1990.

Cawthon R, O'Connell P, Buchberg A, **Viskochil D**, Weiss R, Culver M, Stevens J, Jenkins N, Copeland N and White R: Neurofibromatosis 1 Region: The Sequence and Genomic Structure of EVI2 and Mapping of Other Transcripts. Genomics 7:555-565, 1990.

Cawthon R, Weiss R, Xu G, **Viskochil D**, Culver M, Stevens J, Robertson M, Dunn D, Gesteland R, O'Connell P and White R: A major segment of the neurofibromatosis type 1 gene: cDNA sequence, genomic structure, and point mutations. Cell 62:193-201, 1990.

Viskochil D, Buchberg A, Xu G, Cawthon R, Stevens J, Wolff R, Culver M, Carey J, Copeland N, Jenkins N, White R and O'Connell P: Deletions and a translocation interrupt a cloned gene at the neurofibromatosis type 1 locus. Cell 62:187-192, 1990.

Xu G, O'Connell P, **Viskochil D**, Cawthon R, Robertson M, Culver M, Dunn D, Stevens J, Gesteland R, White R and Weiss R: The neurofibromatosis type 1 gene encodes a protein related to GAP. Cell 62:599-608, 1990.

Martin G, **Viskochil D**, Bollag G, McCabe P, Crosier W, Haubruck H, Conroy L, Clark R, O'Connell P, Cawthon R, Innis M and McCormick F: The GAP-Related Domain of the Neurofibromatosis Type 1 Gene Product Interacts with ras p21. Cell 63:843-849, 1990.

Viskochil D, Cawthon R, O'Connell P, Xu G, Stevens J, Culver M, Carey J, and White R: The gene encoding the oligodendrocyte-myelin glycoprotein is embedded within the neurofibromatosis type 1 gene. Mol. Cell. Biol. 11:906-912, 1991.

Viskochil D and Carey JC: Nosological considerations of the neurofibromatoses. J of Dermatology 19:873-880, 1992.

Sharony R, Garber A, **Viskochil D**, Schreck R, Platt LD, Ward R, Buehler B, and Graham J: Preaxial Ray Reduction Defects as Part of Valproic Acid Embryofetopathy. Prenatal Diagnosis 13:909-918, 1993.

Jorde L, Watkins WS, **Viskochil D**, O'Connell P, and Ward K: Linkage Disequilibrium in the Neurofibromatosis 1 Region: Implications for Gene Mapping. Am J Hum Genet 53:1038-1050, 1993.

Bleyl S, Ainsworth P, Nelson L, **Viskochil D**, and World K. An Ancient Ta Subclass L1 Insertion Results in an Intragenic Polymorphism in an Intron of the NF1 Gene. Hum Molec Genet 34:517-518, 1994.

Harris C, Townsend J, Norman M, White V, **Viskochil D**, Pysher T and Klatt E. Atelencephalic Aproscencephaly. J Child Neurol 9:412-416, 1994.

Schell U, Hehr A, Feldman GJ, Robin NH, Zacai EH, de Die-Smulders C, **Viskochil DH**, Stewart JM, Wolff G, Ohashi H, Price RA, Cohen Jr MM, and Muenke M. Mutations in FGFR1 and FGFR2 Cause Familial and Sporadic Pfeiffer Syndrome. Hum Molec Genet 4(3):323-328, 1995.

Li Y, O'Connell P, Breidenbach Huntsman H, Cawthon R, Stevens J, Gangfeng X, Neil S, Robertson M, White R and **Viskochil D**. Genomic Organization of the Neurofibromatosis 1 Gene (*NF1*). Genomics 25:9-18, 1995.

Purandare S, Huntsman-Breidenbach H, Li Y, Zhu X-L, Sawada S, Neil S, Brothman A, White R, Cawthon R and **Viskochil D**. Identification of the Neurofibromatosis 1 (*NF1*) Homologous Loci by Direct Sequencing, Fluorescent In Situ Hybridization and PCR Amplification of Somatic Cell Hybrids. Genomics 30:476-485, 1995.

Schell U, Hehr A, Feldman GJ, Robin NH, Zackai EH, Die-Smulders Cd, **Viskochil DH** et al. Mutations in *FGFR1* and *FGFR2* Cause Familial and Sporadic Pfeiffer Syndrome. Hum Molec Genet 4(3):323-328, 1995.

Leppig K, **Viskochil D**, Neil S, Rubenstein A, Johnson V, Zhu X-L, Brothman A, and Stephens K. The Detection of Contiguous Gene Deletions at the Neurofibromatosis 1 Locus with Fluorescent In Situ Hybridization. Cytogenet and Cell Genet 72:95-98, 1996.

Purandare SM, Cawthon R, Nelson LM, Sawada S, Watkins S, Ward K, Jorde L and **Viskochil DH.** Genotyping of PCR-based Polymorphisms and Linkage-Disequilibrium Analysis at the NF1 Locus. Am J Hum Genet 59:159-166, 1996.

Florell SR, Townsend JJ, Klatt EC, Pysher TJ, Coffin CM, Wittwer CT and **Viskochil DH.** Aprosencephaly and Cerebellar Dysgenesis in Sibs. Am J Med Genet 63:542-548, 1996.
Sawada S, Florell S, Purandare S, Ota M, Stephens K and **Viskochil D.** Identification of *NF1* Mutations in Both Alleles of a Dermal Neurofibroma. Nature Genetics (In Press).

Flejter WL, Finlinson D, Root S, Nguyen W, Brothman AR and **Viskochil D.** Familial Ring (19) Chromosome Mosaicism: A Case Report and Literature Review. Am J Med Genet (In Press).

REVIEWS

White R, **Viskochil D** and O'Connell P: Identification and characterization of the gene for neurofibromatosis type 1. Current Opinion in Neurobiology 1:15-19, 1991.

Viskochil D, Cawthon R and White R: The neurofibromatosis type 1 gene. Annual Rev of Neuroscience 16:183-205, 1993.

Viskochil D and Wolff RK. Neurofibromatosis. In: *Molecular Biology and Biotechnology*: A comprehensive desk reference. Ed: R Meyers, VCH Publishers Inc., 1995.

Viskochil DH. Neurofibromatosis 1. In: *Encyclopedia of Neuroscience.* Elsevier Science (In press).

BOOK CHAPTERS

O'Connell P, Cawthon R and **Viskochil D.** Molecular Genetics of Neurofibromatosis Type I. In: *Molecular Genetic Approach to Neuropsychiatric Diseases.* Ed: Brosius J and Fremeau RT, Academic Press, 1991.

Viskochil D and Carey J: Variant forms of the neurofibromatosis. In: *Neurofibromatosis.* Ed: S Huson and RAC Edwards, Chapman and Hall Ltd, 1994.

Viskochil D: Identification and characterization of the neurofibromatosis type 1 gene. In: *Molecular Genetics of Human Inherited Disease.* Ed: D Shaw, John Wiley and Sons, Ltd, 1995.

Carey JC and **Viskochil DH.** Current Status of the Human Malformation Map. Birth Defects Original Article Series 30: 13-34, 1996.

ABSTRACTS

Viskochil D, Sawada S, Florell S, Purandare S, Ota M and Stephens K. Identification of NF1 Mutations in Both Alleles of a Dermal Neurofibroma. Abstract, Am Soc Hum Genet Mtg, 1996.

Purandare SM, Ota A, Neil S and **Viskochil D.** Identification of *cis*-regulatory Elements in the Neurofibromatosis 1 Gene. Abstract, Am Soc Hum Genet Mtg, 1996.

Cvijanovich NZ, **Viskochil D** and Leonard C. Carbohydrate Deficient Glycoprotein Syndrome: A New Variant? Abstract J Invest Med 44(1):145A, 1996.

Purandare S, Breidenbach GH, Li Y, Zhu XL, Sawada S, Neil S, Brothman A, White R, Cawthon and **Viskochil D**. Characterization of Neurofibromatosis 1-homologous loci. Abstract, Am J Hum Genet 57:1828 , 1995.

Viskochil D, Purandare S, Breidenbach HH, Cawthon R, Sawada S, Watkins S and Jorde L. Genotyping of 3 Exon-Based Polymorphisms and Linkage Disequilibrium Analysis at the NF1 Locus. Abstract, Am J Hum Genet 57:1175, 1995.

Viskochil D and Carey JC. Orbitotemporal Plexiform Neurofibroma and Sphenoid Wing Dysplasia: An Unproven Association. Abstract, Proceedings of the Greenwood Genetics Center, Vol 14:117, 1995.

Leppig KA, **Viskochil D**, Kaplan P and Stephens KG. Is NF-1 Gene Deletion the Molecular Mechanism of Neurofibromatosis Type 1 with Distinctive Facies? Abstract, Am J Hum Genet 55:1334, 1994.

Viskochil D, Breidenbach HH, Cawthon R, Zhu XL and Brothman AR. Mapping Neurofibromatosis 1 Homologous Loci by Fluorescence *In Situ* Hybridization. Abstract, Am J Hum Genet 55:2201, 1994.

Carey JC, Baty BJ, Byrne J, Craven C, McDonald J, Miller C, Palumbos J, Pysher T, Varner M and **Viskochil D**. Iniencephaly: A Review of the Pathogenetic, Nosologic, Genetic and Prenatal Diagnostic Aspects of an Interesting Developmental Defect. Abstract, Proceedings of the Greenwood Genetics Center, Vol 12:56, 1993.

Viskochil D, Sivak L, and Carey, JC. Bilateral Presentation of Encephalocraniocutaneous Lipomatosis. Abstract, Proceedings of the Greenwood Genetics Center, Vol 12:71, 1993.

Viskochil D, Ward R, and Carey JC. Radial Aplasia as a Manifestation of Valproate Embryofetopathy. Abstract, Proceedings of the Greenwood Genetics Center, Vol 12:115, 1993.

Jorde L, Watkins S, Stevens J. **Viskochil D** and O'Connell P. Linkage Disequilibrium in the Neurofibromatosis 1 Region. Abstract, Am J Hum Genet 51:A137, 1992.

Viskochil D, Bollag G, Clark R, Li Y, McCormick F and White R. Analysis of the NF1 Gene Encompasses an Alterative Splice Form in the GAP-related Domain. Abstract, Am J Hum Genet 51:A137, 1992.

Viskochil D, Cawthon R, Carey J and White R. Mutation Analysis of the NF1 Gene in Segmental Neurofibromatosis. Abstract, Proceedings of the Greenwood Genetics Center, 1991.

Viskochil D, Cawthon R, O'Connell P, Carey JC and White R. Cloning and Characterization of Contiguous Genes at the Neurofibromatosis Type 1 Locus. Abstract, Proceedings of the Greenwood Genetics Center, Vol. 10: 140, 1990.

ORAL PRESENTATIONS

David W. Smith Workshop on Malformation and Morphogenesis (Los Angeles, CA 1996). The NF1 Mouse as a Model for Neurofibromatosis 1.

Fifth Congress of the European Society for Pediatric Dermatology (Rotterdam, The Netherlands, September 1996). The Newest Developments of Neurofibromatosis Type 1 Mutation Analysis and Update on the Molecular Developments of NF1.

Twenty-first Annual Meeting of the Japanese Society for Investigative Dermatology (Tokyo, Japan, July, 1996). Genomic Organization and Mutation Analysis of the NF1 Gene.

Twenty-seventh Annual March of Dimes Clinical Genetics Conference (San Antonio, TX, March 1996). Neurofibromatosis.

Western Society of Pediatric Research Meetings (Carmel, CA, January 1996). Kaufman-McKusick Syndrome: Case Report and Review.

Update in Pediatric Neurosurgery. (Park City, UT, June 1995). Cloning the NF1 Gene: Historical Perspectives and Current Affairs.

International NF Symposium (Hong Kong, April 2, 1994). Towards the Development of a Comprehensive DNA-Sequencing Approach to NF1 Mutation Analysis.

Pediatric Pathology Meetings (Salt Lake City, UT, September 1994). NF1.

Neurofibromatosis Consortium Meeting on NF1 and NF2 (Ann Arbor, MI, April 23 & 24, 1993). Mapping the 3'-end of the NF1 gene.

LINK (Let's Increase Neurofibromatosis Knowledge - UK NF Foundation; Oxford, UK, October 1992) - Platform presentation on "The Exacerbation of Features of NF1 during Pregnancy."

David W. Smith Workshop on Malformation and Morphogenesis (Winston, Salem, NC 1992). Bilateral Presentation of Encephalocraniocutaneous Lipomatosis.

Neurofibromatosis Consortium Meeting on NF1 and NF2 (Oxford, UK, Sept. 1992) - Platform presentation on the physical structure of the NF1 locus.

Japanese Dermatological Society Meetings (Tokyo, April, 1992) - Platform presentation on "Nosological Considerations of the Neurofibromatoses."

Western Society for Pediatric Research (Carmel, CA, Feb, 1992) - Platform presentation on the neurofibromin-GRD isoforms.

National Neurofibromatosis Foundation sponsored consortium on NF1 and NF2 (Salt Lake City, UT, January 1992) - The alternative splice form of the GAP-related domain of neurofibromatosis and peptide antibody results.

March of Dimes Symposium (Vancouver, BC, July, 1991) - invited presentation - Neurofibromatosis Type 1.

List of all personnel receiving pay from negotiated effort.

No non-salaried personnel received direct pay.

Indirect pay to personnel affiliated with the following:

Huntsman Core Sequencing Laboratory - Margaret Robertson, Director
Huntsman Core Genotyping Laboratory - Mark Leppert, Director
U. of Utah Core FISH Facility - Arthur Brothman, Director
U. of Utah, Dept. of Pathology, Specimen Preparation Laboratory